T.C.
BOLU ABANT İZZET BAYSAL ÜNİVERSİTESİ
INSTITUTE OF GRADUATE STUDIES
DEPARTMENT OF CHEMISTRY

NOVEL THIAZOLE-CARBOHYDRAZONE DERIVATIVES: SYNTHESIS, CHARACTERIZATION AND MULTIMODAL EVALUATION AS ACHE INHIBITORS

MASTER OF SCIENCE, CHEMISTRY

SONER ÖZDEMİR

THESIS SUPERVISOR
Prof. Dr. Cevher ALTUĞ

BOLU, 7/28/2025

ACCEPTANCE AND APPROVAL PAGE

The thesis entitled "**NOVEL THIAZOLE-CARBOHYDRAZONE DERIVATIVES: SYNTHESIS, CHARACTERIZATION AND MULTIMODAL EVALUATION AS ACHE INHIBITORS**'' prepared and submitted by **SONER ÖZDEMİR** in partial fulfillment of the requirements for the degree of **Master of Science** in Department of **CHEMISTRY** with unanimity is hereby approved. 7/28/2025

Jury Members	**Signature**
Supervisor Prof. Dr. Cevher ALTUĞ BOLU Abant İzzet Baysal University	.....
Member Prof. Dr. Mustafa ARSLAN Sakarya University	.....
Member Assist. Prof. Dr. Cem GÖL BOLU Abant İzzet Baysal University	.....

Institute of Graduate Studies Approval

Prof. Dr. İbrahim KÜRTÜL

Director of Institute of Graduate Studies

ETHICAL DECLARATION

In this thesis study, which I have prepared in accordance with Bolu Abant İzzet Baysal University, Institute of Graduate Studies' Thesis Writing Guide and Template;

- I have obtained the data, information and documents presented in the thesis within the framework of academic and ethical rules,
- I have presented all information, documents, evaluations, and results in accordance with the rules of scientific ethics and morality,
- I have cited and referenced all the works I have benefited from in the thesis study,
- I have not made any changes to the data used,
- I declare that the work I have presented in this thesis is original, and in any other case, I declare that I accept all loss of rights that may arise against me.

According to the similarity report obtained by applying the filters determined by the directorate of the institute in the Turnitin program related to the thesis, the similarity index of the thesis does not exceed 30%.

.....

Soner ÖZDEMİR

ABSTRACT

NOVEL THIAZOLE-CARBOHYDRAZONE DERIVATIVES: SYNTHESIS, CHARACTERIZATION AND MULTIMODAL EVALUATION AS ACHE INHIBITORS
MSC THESİS
SONER ÖZDEMİR
BOLU ABANT IZZET BAYSAL ÜNİVERSİTESİ
INSTITUTE OF GRADUATE STUDIES
DEPARTMENT OF CHEMISTRY
(SUPERVISOR: PROF. DR. CEVHER ALTUĞ)
BOLU, 28 JULY 2025
XV + 83

The progression of Alzheimer's disease underscores the urgent need for novel acetylcholinesterase (AChE) inhibitors capable of modulating cholinergic signaling with high specificity and low side effects. In this study, a series of ten 3-methyl-2-(phenylimino)-2,3-dihydrothiazole-4-carbohydrazone derivatives **24 a–j** were designed to integrate the thiazole core and carbohydrazone pharmacophore known for dual-site engagement of AChE. These novel compounds were fully characterized by FT-IR, ^{1}H and ^{13}C NMR, LC-QTOF-MS and LC-MS, confirming their structures and high purity. In vitro enzyme assays revealed submicromolar AChE inhibition for **21** ($IC_{50} = 0.105$ μM), **23** (0.233 μM), and notably **24b** (0.052 μM), **24d** (0.066 μM), **24f** (0.076 μM), and **24h** (0.114 μM), with negligible BChE activity ($IC_{50} > 1$ mM). Selected derivatives (**24b** and **24f**) also inhibited MAO-A ($IC_{50} = 0.072$ and 0.091 μM) and MAO-B (0.064 and 0.081 μM), demonstrating a promising multi-target profile. Molecular docking against human AChE corroborated these findings, predicting strong binding (–9.0 to -9.7 kcal/mol) at both catalytic and peripheral anionic sites. These results establish the thiazole-carbohydrazone scaffold as compelling leads for further optimization and *in vivo* evaluation in Alzheimer's disease.

KEYWORDS: Thiazole. Molecular Docking. Acetylcholinesterase. Hantzsch Thiazole Synthesis

ÖZET

YENİ TİYAZOL-KARBOHİDRAZON TÜREVLERİ: SENTEZİ, KARAKTERİZASYONU VE ACHE İNHİBİTÖRLERİ OLARAK ÇOK YÖNLÜ DEĞERLENDİRİLMESİ
YÜKSEK LİSANS TEZİ
SONER ÖZDEMİR
BOLU ABANT IZZET BAYSAL ÜNİVERSİTESİ
LİSANSÜSTÜ EĞİTİM ENSTİTÜSÜ
KİMLYA ANA BİLİM DALI
(TEZ DANIŞMANI: PROF. DR. CEVHER ALTUĞ))
BOLU, 28 TEMMUZ 2025
XV + 83

Alzheimer hastalığının ilerleyici ve tedaviye dirençli doğası, yüksek özgüllüğe sahip ve yan etkisi düşük yeni asetilkolinesteraz (AChE) inhibitörlerine olan ihtiyacı giderek artırmaktadır. Bu tez kapsamında, tiyazol çekirdeği ve karbohidrazon farmakoforunu bir arada içeren on adet yeni 3-metil-2-(fenilimino)-2,3-dihidrotiyazol-4-karbohidrazon türevi (**24 a–j**) tasarlanmış ve sentezlenmiştir. Tüm bileşiklerin yapısal doğrulamaları FT-IR, ^{1}H NMR, ^{13}C NMR, LC-QTOF-MS ve LC-MS teknikleriyle gerçekleştirilmiş, saflıkları ve kimyasal yapıları teyit edilmiştir. İn vitro enzim testleri, ara ürünler **21** (IC_{50} = 0.105 μM) ve **23** (0.233 μM) ile birlikte özellikle **24b** (0.052 μM), 24d (0.066 μM), **24f** (0.076 μM) ve **24h** (0.114 μM) bileşiklerinin submikromolar düzeyde AChE inhibisyonu gösterdiğini ortaya koymuştur. Tüm bileşikler, BChE üzerinde anlamlı bir etki göstermemiştir (IC_{50} > 1 mM). Ayrıca seçilen türevler (**24b** ve **24f**), MAO-A (IC_{50} = 0.072 ve 0.091 μM) ve MAO-B (0.064 ve 0.081 μM) enzimlerini de inhibe ederek çoklu hedefli inhibitör profiline sahip olduklarını göstermiştir. Moleküler docking çalışmaları, sentezlenen karbohidrazon türevlerinin (**24a–j**), katalitik ve periferik anyonik bölgelerle güçlü etkileşimler kurarak AChE'ye yüksek bağlanma afinitesi sergilediğini doğrulamıştır. Bu bulgular, tiyazol-karbohidrazon iskeletinin asetilkolinesteraz inhibitör tasarımında umut vadeden adaylar sunduğunu ve Alzheimer tedavisine yönelik daha ileri farmakokinetik ve biyolojik çalışmalar için güçlü bir temel oluşturduğunu göstermektedir.

ANAHTAR KELİMELER: Tiyazol. Moleküler Docking. Asetilkolinesteraz. Hantzsch Tiyazol Sentezi

FORMULAE

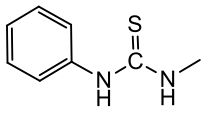

19

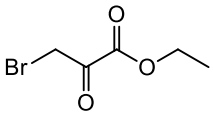

20

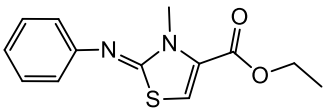

21

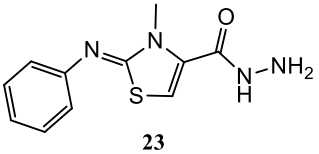

23

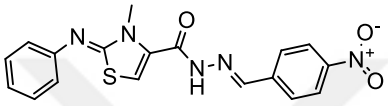

24a

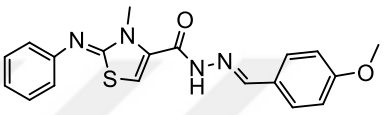

24b

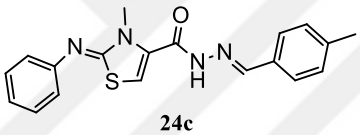

24c

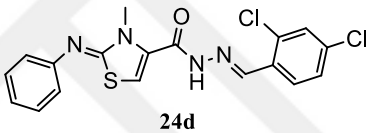

24d

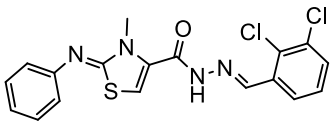

24e

24f

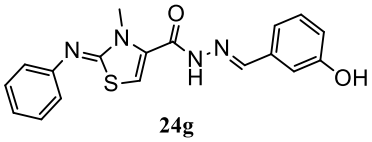

24g

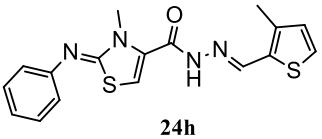

24h

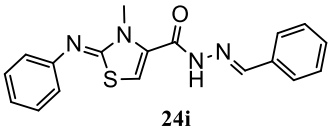

24i

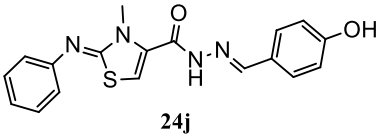

24j

TABLE OF CONTENTS

Page

LIST OF FIGURES

Page

LIST OF TABLES

Page

LIST OF PHOTOS

Page

LIST OF ABBREVIATIONS AND SYMBOLS

Ar : Aryl or aromatic group

α : Alpha

Å : Angström

Asym : Asymmetric

AChE : Acetylcholinesteraze

Broad s : Broad singlet (NMR)

CS_2 : Carbon disulfide

$CDCI_3$: Deuterated Chloroform

^{13}C NMR : Carbon nuclear magnetic resonance

^{o}C : Celsius

D : Doublet (NMR)

Dd : Doublets of doublet (NMR)

DMSO-d_6 : Deuterated dimethyl sulfoxide

EBP : Ethyl Bromopyruvate

EtOAc : Ethyl acetate

EtOH : Ethanol

eq. : Equivalent

ESI^+ : Positive Electrospray Ionization mode

FTIR : Fourier Transform Infrared Spectroscopy

G : Gram

^1H NMR : Proton nuclear magnetic resonance

H : hour

Hz : Hertz

HCl : Hydrochloric acid

H_2O : Water

Hex : Hexane

HTS : Hantzsch Thiazole Synthesis

J : Coupling constants

mL : Milliliter

m.p : Melting point

m : Multiplet (NMR)

MeCN : Acetonitrile

Mg : Milligram

NH_2NH_2 : Hydrazine

NMR : Nuclear magnetic resonance

Na_2CO_3 : Sodium Carbonate

QTOF-MS : Quadrupole Time Of Flight Mass Spectrometry

ppm : Parts per million

q : Quartet (NMR)

R : Any group

r.t. : Room temperature

Rf : Retardation factor

S : Singlet (NMR)

sym. : Symmetric

t : Triplet (NMR)

TLC : Thin layer chromatography

δ : Chemical shift

ACKNOWLEDGEMENT

I wish to express my gratitude and respect to my supervisor, Prof. Dr. Cevher Altuğ, for sharing his extensive knowledge and most importantly, for believing in me and treating me both as a mentor and a friend throughout this research. His guidance and dedication have been invaluable.

I am eternally grateful to my family, especially my father and mother, for their unconditional love and support, which I have always felt. I will forever remain in their debt.

I would like to express my heartfelt thanks to my fiancée, Büşra, for her assistance with the graphic design of this thesis and for being my constant source of motivation.

I would like to thank Associate Professor Dr. Begüm Nur Pelin Sağlık and her team members from Eskişehir Osmangazi University for conducting the in vivo experiments for this study.

Finally, I extend my gratitude to Özkimsan Kimya for their support in providing research materials and financial assistance throughout the course of this thesis. Their contributions have played a significant role in the successful completion of this work.

1. INTRODUCTION

1.1 Thiazole

Thiazole is a distinctive heterocyclic ring system characterized by the presence of both sulfur and nitrogen atoms. This makes it highly versatile in various chemical reactions (**Figure 1.1**). While unsubstituted thiazole does not typically occur in nature, its ring structure is found in natural compounds, including alkaloids cyclopeptides and metabolites (Parthasarathy et al., 2021). The nonbonding pair of electrons on the sulfur in the thiazole is displaced, meeting the requirements of Hückel's rule for a minimum of six pi electrons, which is essential for its stability and reactivity (Alajarín et al., 2006). Thiazole can undergo a wide range of reactions, such as donor–acceptor interactions (Breitung et al., 2000), intramolecular nucleophilic substitutions (Shen et al., 2009), photochemical reactions (D'Auria et al. 2009), arylation (Sadigova et al., 2004), cycloaddition (Shen et al., 2009), oxidation (Y. Huang et al., 2010), transformation (Obushak et al., 2004), and dimerization (Arduengo et al., 1997). These diverse reactivity pathways contribute to thiazole's importance in both synthetic and natural chemistry.

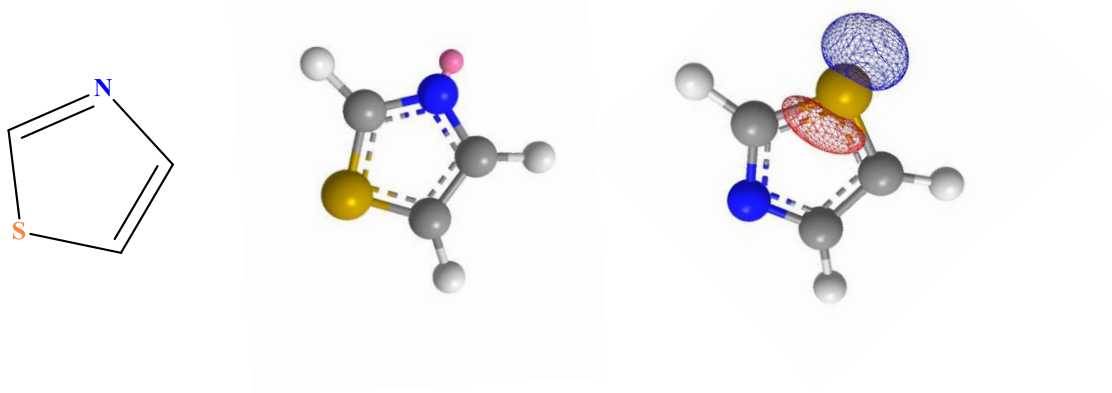

Figure 1.1 2D-3D Representation of thiazole ring

The acidic proton of thiazole at the c-2 position of the thiazole ring significantly increases its chemical reactivity making this heterocycle a versatile and attractive scaffold for the synthesis of structurally diverse compounds. This structural feature enables thiazoles to undergo a variety of chemical transformations

giving rise to numerous derivatives of interest in both medicinal and synthetic chemistry owing to their broad spectrum of chemical, physical, and pharmacodynamic characteristics thiazole-based molecules have been extensively studied structural modifications at different positions. On the thiazole ring have yielded compounds exhibiting a wide range of biological activities covering antioxidant, anti-tubercular, antibacterial, antifungal, diuretic, anticancer, and anti-inflammatory effects these versatile bioactivities highlight the essential role of thiazole derivatives in the identification and development of new therapeutic agents. (Reyadh et al., 2021).

1.2 Hantzsch Thiazole Synthesis (HTS) Definition and History

The HTS is a well-established method in organic chemistry designed for the preparation of thiazole derivatives. This reaction includes α-haloketones with thioureas or thioamides, leading to the formation of thiazole rings. The reaction was first reported by Arthur Hantzsch in 1881, and it has since become a cornerstone in the synthesis of thiazole derivatives due to its simplicity and efficiency (Tomassetti et al., 2021).

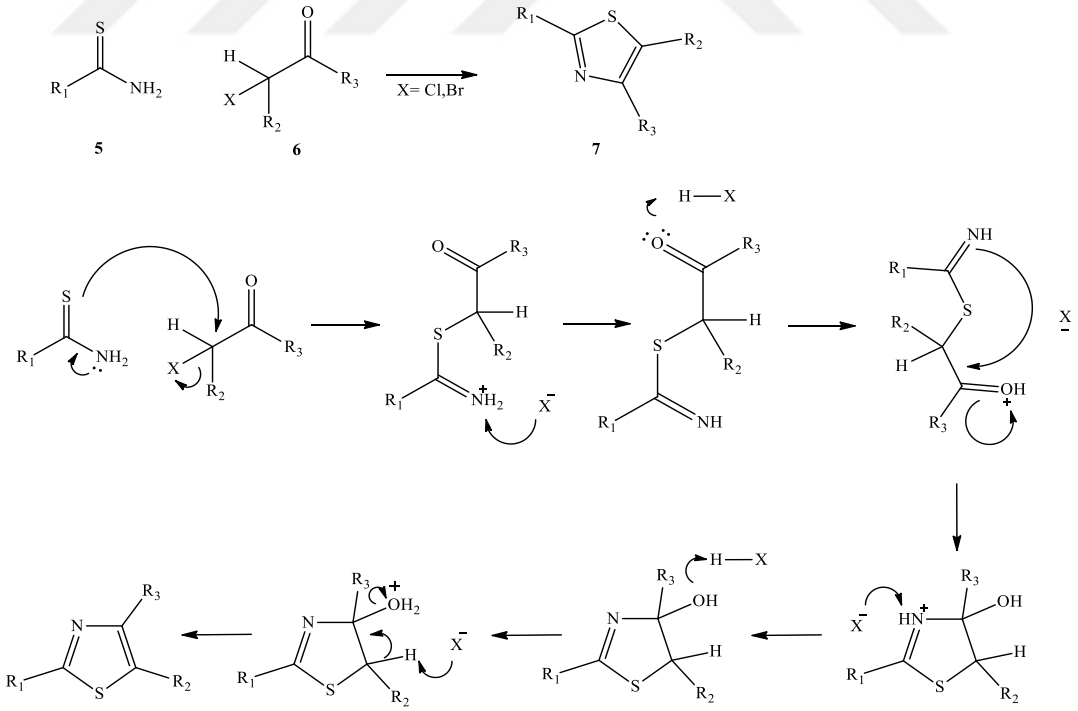

Photo 1.1 HTS and Mechanism

The classical HTS typically employs α-haloketones (6) and thioureas (5) as the primary reactants to yield thiazole (7) **(Photo 1.1)**. The reaction starts through the attack by the nucleophile of sulfur atom in thiourea on the carbon atom of the α-haloketone, then cyclization and elimination of a halide ion by S_N2 process. This mechanism highlights the strong nucleophilicity of sulfur, which is a key feature that facilitates the formation of the thiazole ring (Zhao et al., 2022). The versatility of this reaction has allowed for the incorporation of various substituents on the thiazole ring, leading to a diverse array of thiazole derivatives with potential biological applications (Tomassetti et al., 2021; Zhao et al., 2022). Over the years, numerous modifications and improvements to the Hantzsch thiazole synthesis have been reported. For instance, the use of ionic liquids and deep eutectic solvents, has been explored to enhance reaction efficiency and reduce environmental impact (Zhao et al., 2022). Additionally, microwave-assisted synthesis has been employed to accelerate the reaction and improve yields, demonstrating the adaptability of the HTS to modern synthetic techniques (Kamila et al., 2012).

In conclusion, the HTS is a pivotal reaction in organic chemistry that has significantly contributed to the field of medicinal chemistry. It's historical significance, coupled with its continued relevance in the synthesis of medicinally active scaffolds, underscores the importance of this reaction in the development of new therapeutic agents.

1.3 Some Synthesis Strategies of Thiazoles

The synthesis of thiazoles has been a focal aspect in organic chemistry because of the biological significance of these compounds. Various synthetic strategies have been developed over the years, with the HTS being one of the most prominent methods (**Photo 1.1**).

1.3.1 Cook–Heilbron Thiazole Synthesis

The Cook–Heilbron thiazole synthesis provides an efficient route to 5-aminothiazoles by condensing α-aminonitriles (**8**) with sulfur donors such as carbon disulfide (**9**) or isothiocyanates typically carried out at ambient temperature in aqueous or mixed solvent systems this transformation proceeds under mild conditions and delivers thiazole products in good yields its operational simplicity broad substrate tolerance and ability to introduce diverse substituents

make the cook-heilbron protocol a valuable tool for both academic and industrial applications in heterocycle synthesis and drug discovery (J. J. Li, 2003).

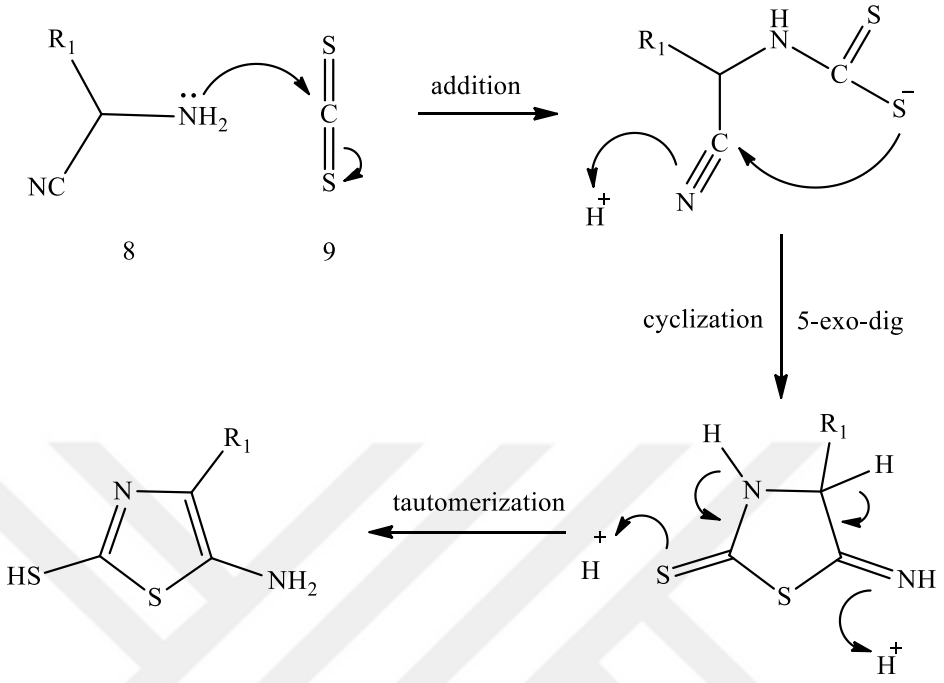

Photo 1.2 Reaction mechanism of Cook–Heilbron thiazole synthesis

1.3.2 Gabriel Thiazole Synthesis

The Gabriel synthesis, as applied to thiazoles, is another method for producing aryl, alkoxy or alkyl substituted thiazoles at the 5,2 or both positions. This reaction specifically involves the treatment of α-acylaminoketones (**10**) with phosphorus pentasulfide (P_2S_5) under controlled conditions (C. B. Mishra et al., 2015).

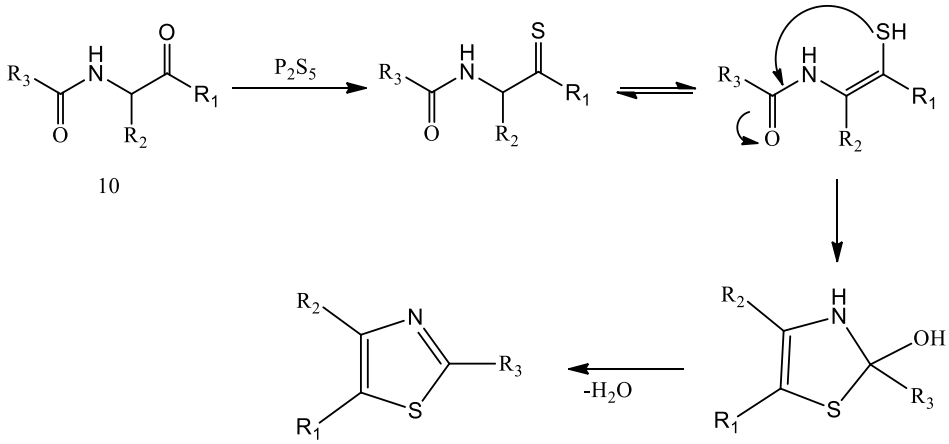

Photo 1.3 Reaction mechanism of Gabriel thiazole synthesis

1.3.3 Recent Advances in Thiazole Synthesis

Tang et al. devised a copper-catalyzed cyclization method to synthesize thiazoles, beginning with oximes (**11**), anhydrides (**12**), and potassium thiocyanate (**13**). After investigating different reaction conditions, the authors identified optimal conditions, which involved using toluene as the solvent with copper (I) iodide as the catalyst, and 2 eq. of potassium thiocyanate as the sulfur source (Tang et al., 2016).

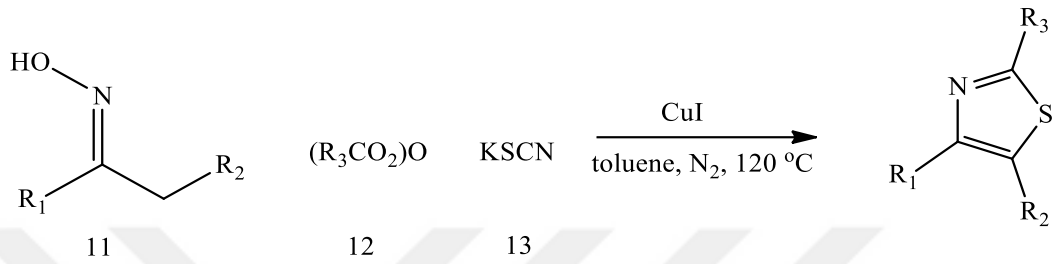

11 12 13

Photo 1.4 Thiazoles from oximes

Wang et al. synthesized a range of thiazole derivatives by reacting amines (**14**), aromatic aldehydes (**15**), and elemental sulfur (**16**) via an oxidation reaction, which was catalyzed by copper salts and facilitated by molecular oxygen (Wang et al., 2018).

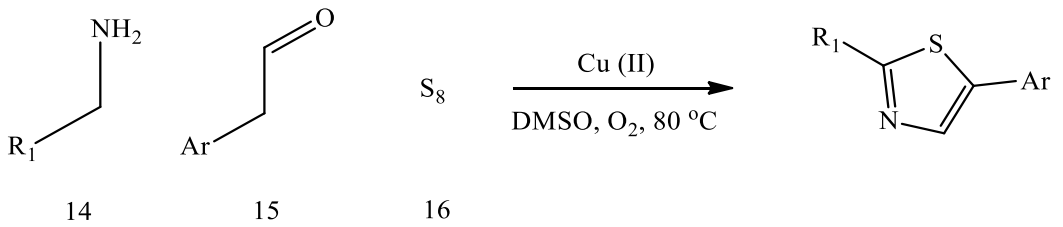

14 15 16

Photo 1.5 Thiazoles from aldehydes and amines

1.4 Important Drugs Synthesized by HTS

The thiazole ring is found in a diverse array of both natural and synthetic molecules, exhibiting a spectrum of biological effects and can be synthesized via HTS. An example of a thiazole-containing natural compound is thiamine. This vital nutrient is fundamentally involved in maintaining the normal functioning related to the nervous system. It achieves this by facilitating the synthesis of acetylcholine, a

key neurotransmitter involved in nerve signal transmission and various cognitive processes (Siddiqui et al., 2009). Sulfathiazole is a thiazole containing synthetic compound and member of the sulfa drug family, widely recognized for its antimicrobial properties and can be made via HTS. It is specifically prescribed for short durations to effectively combat microbial infections by inhibiting bacterial growth and interfering with essential metabolic processes in microorganisms (Meşeli et al., 2021). Clomethiazole is a pharmaceutical drug commonly prescribed for managing sleep disturbances. It is particularly effective in promoting restful sleep by exerting a sedative effect on the central nervous system, making it a valuable option for individuals experiencing insomnia or other related sleep disorders (Gann et al., 2005). Amiphenazole is a drug utilized in the treatment of barbiturate or opiate poisoning. It works by stimulating the respiratory center in the brain, helping to counteract the depressive effects these substances have on the central nervous system, thereby supporting recovery and improving breathing in affected individuals (Dotevall & Herner, 1957). Thiabendazole is an antifungal drug and mold control agent that works by inhibiting a helminth-specific mitochondrial enzyme, disrupting the tricarboxylic acid (TCA) cycle. This interference halts the production of adenosine triphosphate (ATP), depriving the helminths of energy, which leads to their death. Additionally, it is effective in controlling mold growth due to its ability to inhibit fungal cell metabolism (Schaffel et al., 2000). Acotiamide is a selective acetylcholinesterase inhibitor also used in the treatment of functional dyspepsia (Modrić et al., 2022). As a derivative of thiazole, it has inspired the synthesis of biologically effective thiazole based compounds aimed at cholinesterase inhibition (**Figure 1.2)**

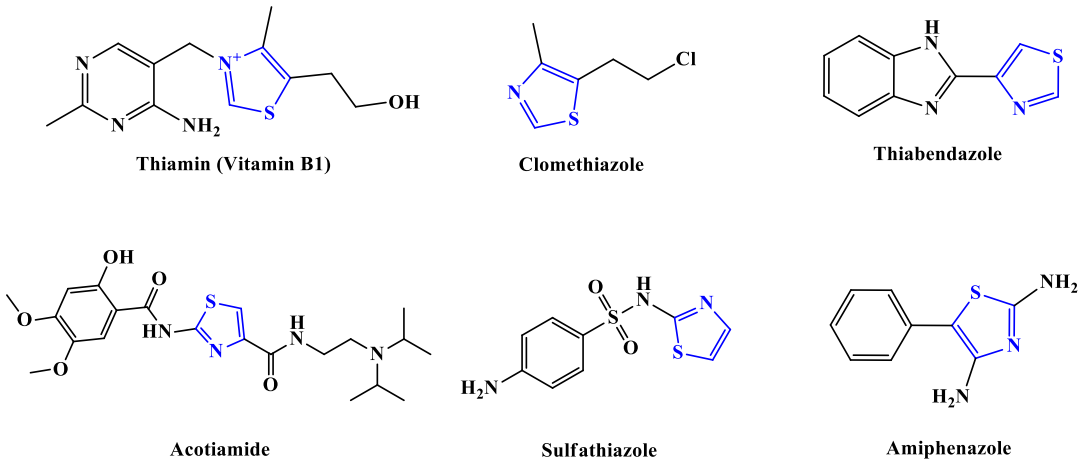

Figure 1.2 Thiazole based some important drugs

1.5 Some Applications of 2,4-Disubstituted Thiazoles

2,4-Disubstituted thiazoles have received considerable attention in medicinal chemistry because the nature and positioning of the substituents at the 2- and 4-positions of the thiazole ring critically influence their pharmacological profiles, yielding a broad array of biological activities and therapeutic potentials. (Davis et al., 2012).

2,4-Disubstituted thiazoles are particularly renowned for their antimicrobial potential, with extensive research confirming their robust activity against both fungal and bacterial pathogens. For instance, Copper (II) complexes of Schiff bases incorporating 2,4-disubstituted thiazoles were synthesized by Bharti et al. and assessed for their antimicrobial properties (**Figure 1.3**), finding promising results against various microbial strains (Bharti et al., 2010). Similarly, According to Chimenti et al., newly synthesized 2,4-disubstituted thiazoles exhibited promising activity against Candida species, highlighting their potential as antifungal drugs (Chimenti et al., 2011).

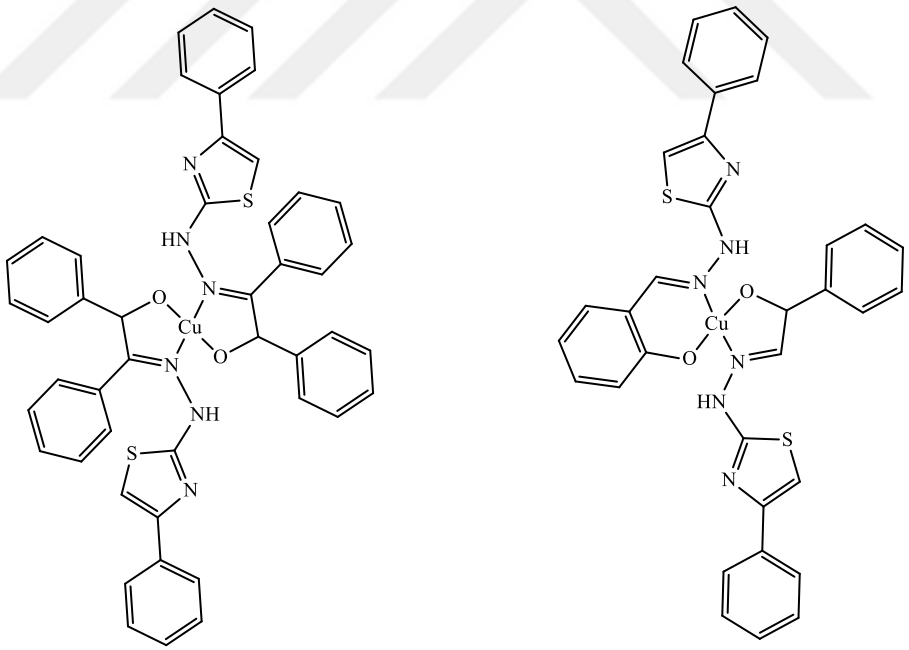

Figure 1.3 Copper (ll) complexes synthesized by Bharti et al.

2,4-Disubstituted thiazoles have also been investigated for their anticancer properties. Gomha et al. reported the synthesis of novel thiazole derivatives incorporating the thiazole moiety, which showed potent anticancer activity in vitro

(Gomha & Khalil, 2012). This underscores the potential of 2,4-disubstituted thiazoles as candidates for cancer therapy.

The inhibition of protein kinases is another important application of 2,4-disubstituted thiazoles. These compounds have been identified as potential inhibitors of various kinases, which play crucial roles in cell signaling and cancer progression. For example, research by Walter et al. focused on identifying CLK1 inhibitors based on a 2,4-disubstituted thiazole scaffold (**Figure 1.4**), suggesting that optimized derivatives could serve as potent and selective kinase inhibitors (Walter et al., 2017). This highlights the relevance of thiazole derivatives in targeting specific pathways involved in cancer and other diseases.

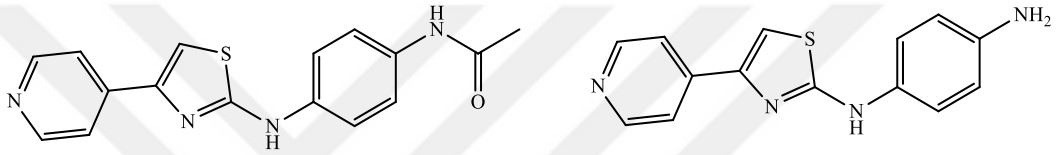

Figure 1.4 CLK1 inhibitors based on thiazole moiety

In addition to their antimicrobial and anticancer properties, 2,4-disubstituted thiazoles have been studied for their antioxidant activities. Čačić and Molnar synthesized novel thiazolidine derivatives and evaluated their antioxidant potential, finding that certain thiazole derivatives exhibited significant free radical scavenging activity (Čačić & Molnar, 2011). This suggests that these compounds could be beneficial in preventing oxidative stress-related diseases.

The antiviral potential of 2,4-disubstituted thiazoles has also been explored. Research indicates that these compounds may possess activity against various viral infections, including those caused by HIV and other viruses (**Figure 1.5**). Pendiukh highlighted the diverse biological activities of thiazoles, including their antiviral properties, suggesting that further investigation could lead to the development of new antiviral agents (Pendiukh et al., 2024). This area of research is particularly relevant given the ongoing need for effective antiviral therapies.

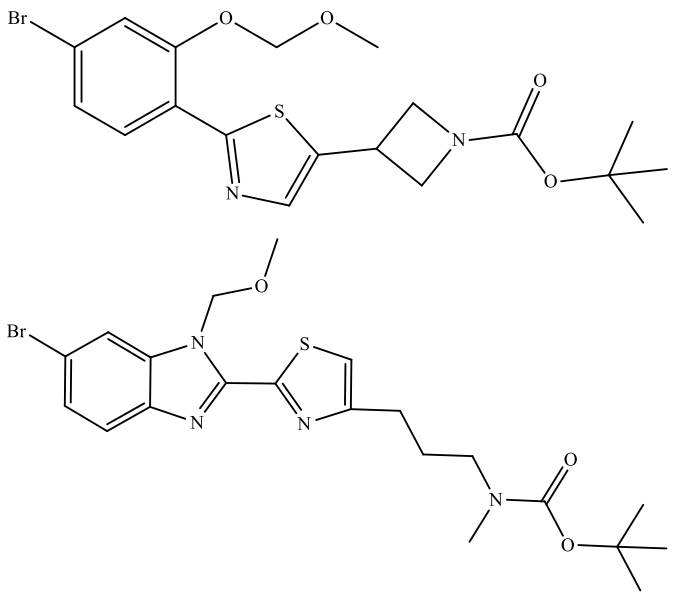

Figure 1.5 2,4-disubstituted thiazoles with possible antiviral potential

The structural diversity of 2,4-disubstituted thiazoles makes them valuable scaffolds in drug design. Their potential to bind to diverse biological sites allows for the development of novel therapeutic agents. For instance, the work by Mishra and Sachan emphasized the importance of thiazole derivatives in medicinal chemistry, noting their potential as bioactive agents in various therapeutic areas (I. Mishra & Sachan, 2022). The thiazole moiety has been identified as an essential component in several clinically approved drugs, further underscoring its significance in drug discovery.

2,4-Disubstituted thiazoles can also serve as bioisosteres for other pharmacophores, such as imidazoles and oxazoles. This property allows medicinal chemists to modify existing drug candidates to improve their efficacy and reduce side effects. For example, the review by Sharma et al. discussed the potential of thiazole derivatives as bioisosteres, highlighting their applications in the design of new therapeutic agents (Sharma et al., 2022). This versatility in drug design is a key advantage of incorporating thiazole motifs into pharmaceutical compounds.

The antiparasitic activity of 2,4-disubstituted thiazoles has also been documented. Research indicates that these compounds may exhibit efficacy against various parasitic infections, including those caused by protozoa and helminths. The work by Borcea et al. emphasized the importance of thiazole derivatives in the

development of antiparasitic agents, suggesting that further studies could lead to the discovery of new treatments for parasitic diseases (Borcea et al., 2021).

Beyond their biological applications, 2,4-disubstituted thiazoles have found utility in material science. Their unique structural properties allow them to be incorporated into various materials, including liquid crystals and polymers. The review by Sadashiva highlighted the potential of thiazole derivatives (**Figure 1.6**) in creating advanced materials engineered for specific functional uses (Singh et al., 2024). This interdisciplinary approach broadens the scope of thiazole research beyond traditional medicinal chemistry.

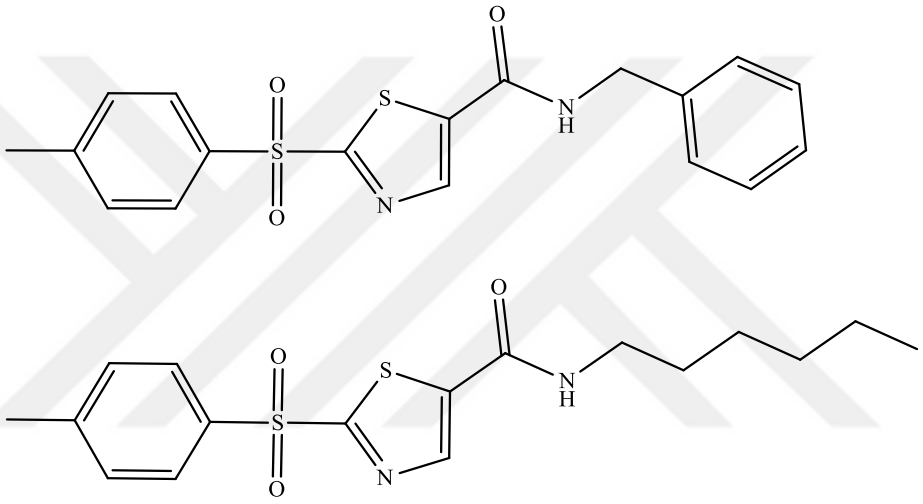

Figure 1.6 2,4-disubstituted thiazoles reported by Singh et al.

1.6 Definition Of Hydrazides and Carbohydrazones

Hydrazide and carbohydrazones are two important classes of organic compounds that play significant roles in medicinal chemistry and organic synthesis. Hydrazides are nitrogen-containing compounds that consist of a hydrazine functional group.

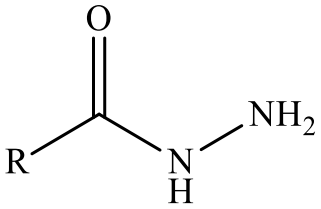

Figure 1.7 Structure of Hydrazide

They are known for their versatility in organic synthesis, serving as key precursors used in the synthesis of diverse nitrogen-based heterocyclic compounds, including pyrazoles and triazoles (Natarajan et al., 2024). The chemical versatility of hydrazides largely stems from the presence of the N–N linkage, allowing them to undergo various types of reactions, such as cycloaddition and condensation reactions with carbonyl compounds (N. Huang et al., 2024). For instance, the condensation of hydrazides with carbonyl compounds leads to the formation of pyrazolines, which are valuable bioactive molecules with diverse pharmacological properties (Y. Li et al., 2020; Natarajan et al., 2024). Additionally, hydrazides have been utilized in the synthesis of agrochemicals and pharmaceuticals, highlighting their importance in drug discovery and development (Chen et al., 2022; N. Huang et al., 2024).

Carbohydrazones possess a carbonyl-linked azomethine group, which contributes to their notable activities, such as anticancer, antimicrobial and anti-inflammatory properties (Easwaran potti et al., 2007; Y. Li et al., 2020; Şener et al., 2017).

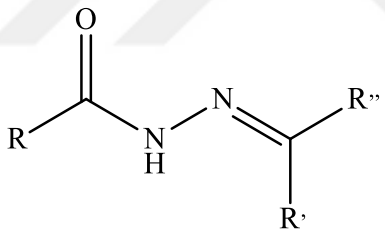

Figure 1.8 Structure of Carbohydrazone

The formation of Carbohydrazones is often facilitated by the condensation reaction of hydrazides with various aldehydes, leading to compounds that exhibit significant pharmacological effects (Y. Li et al., 2020). For example, carbohydrazones have been explored as potential inhibitors of tyrosine phosphatase protein which is a target for obesity (Y. Li et al., 2020). The incorporation of different substituents on the hydrazide or carbonyl moieties can enhance their potency and selectivity against specific biological targets (Easwaran potti et al., 2007; Y. Li et al., 2020). This versatility makes carbohydrazones attractive candidates for further research in medicinal chemistry.

1.7 Definition Of AChE and Monoamine Oxidase

AChE is an enzyme that plays a critical role in the control of cholinergic activity neurotransmission through the hydrolysis of the neurotransmitter acetylcholine. This enzyme is primarily located at cholinergic synapses across the central and peripheral nervous systems, functioning as a key regulatory component in synaptic signaling. By catalyzing the breakdown of acetylcholine into acetic acid and choline, AChE terminates synaptic transmission, thus allowing for the efficient recycling of choline and the modulation of neurotransmitter dynamics at the synapse (Ariantari & Putri, 2023; Nkpaa et al., 2021; Pérez-Sánchez et al., 2021). The activity of this enzyme is essential for proper neurotransmission and is implicated in various physiological and medical conditions, such as neurodegenerative diseases including Alzheimer's disease (Doroszkiewicz & Mroczko, 2022). The therapeutic potential of targeting AChE has been extensively studied. Inhibitors of AChE, namely rivastigmine, donepezil and galantamine are commonly employed in clinical settings to manage symptoms of Alzheimer's disease by prolonging the action of acetylcholine in the synaptic cleft (Ye et al., 2020). In terms of active binding sites, AChE possesses a unique catalytic triad consisting of serine, histidine, and glutamate residues located in the enzyme's active site (**Figure 1.9**).

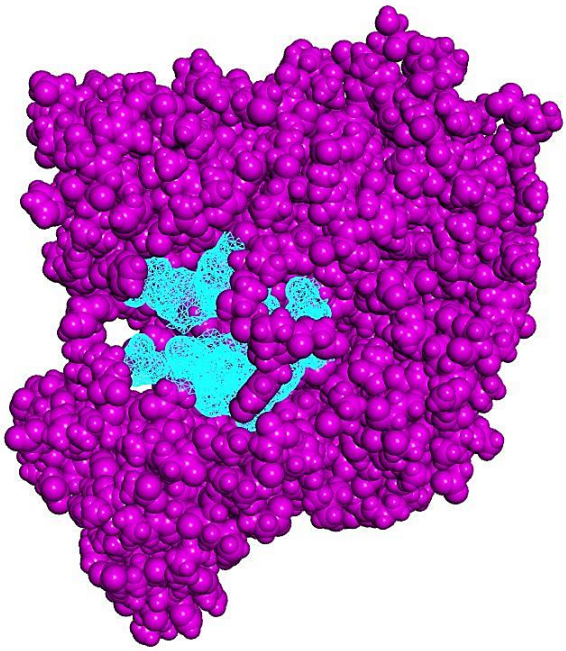

Figure 1.9 Crystal Structure of AChE (Purple) and ligand binding cavity (Turquoise)

These are fundamental to the enzyme's function, facilitating the hydrolysis reaction that breaks down acetylcholine into acetic acid and choline (Jacquet et al., 2021). Its enzymatic function is facilitated by essential structural features, including distinct ligand binding cavity: the catalytic anionic site and the peripheral anionic site. The catalytic anionic site is located at the lower part of a 20 Å deep gorge and plays an essential role in substrate binding and catalysis. The catalysis is executed by a catalytic triad consisting of three critical amino acid residues, glutamate (Glu334), histidine (His447), and serine (Ser203). These residues are involved in the nucleophilic attack on the acetylcholine substrate, facilitating its hydrolysis (Grodner et al., 2024; Kumawat et al., 2021). The peripheral anion-binding site is positioned at the entrance of the active site gorge and consists of several aromatic amino acids, including Tyr70, Asp72, Tyr124, Trp286, and Tyr341. This site serves a dual purpose: firstly, it binds cationic ligands like acetylcholine or inhibitors, providing a pre-catalytic assembly stage that increases the likelihood of enzymatic activity (Grodner et al., 2024; Kumawat et al., 2021). Secondly, it functions in an allosteric capacity to modulate the enzymatic activity of AChE. The binding of

ligands to the peripheral anionic site can induce conformational changes that may either inhibit or activate enzyme activity (Karunakaran et al., 2022).

Monoamine oxidase A (MAO-A) and B (MAO-B) are enzymes located in the brain that are responsible for the breakdown of key neurotransmitters such as serotonin, dopamine, and norepinephrine (Watkins & Jane, 2006). MAO-A predominantly metabolizes serotonin and norepinephrine, whereas MAO-B is more selective for dopamine(Shih et al., 1999). Both isoforms are considered important therapeutic targets in the treatment of neurological disorders such as depression, Parkinson's disease, and Alzheimer's disease.

1.8 Definition Of Molecular Docking

Molecular docking is a sophisticated computational technique that has gained prominence in the fields of biochemistry, molecular biology, and pharmacology, primarily due to its ability to predict the interactions between biomolecules, particularly proteins and small molecules, such as ligands. This technique is integral to the drug discovery process, as it provides insights into how potential therapeutic agents can bind to their target proteins, thereby influencing biological activity. The significance of molecular docking lies in its capacity to simulate and visualize the binding interactions, which are crucial for understanding the mechanisms of action of drugs and for the rational design of new pharmacological agents (B. Billones & T. Bangalan, 2019; Pinzi & Rastelli, 2019). The definition of molecular docking can be articulated as an optimization problem that seeks to determine the most favorable orientation and conformation of a ligand when it binds to a specific protein target. This process entails assessing multiple binding modes and conformations to determine the most energetically favorable interactions between the ligand and the protein. Molecular docking encompasses a variety of methodologies that can differ significantly based on the chemical and biochemical characteristics of the ligands and receptors involved (Murugesan & kaleeswaran, 2024; Umar et al., 2019). It is important to note that molecular docking is not merely a single technique but rather a collection of approaches that utilize different algorithms and scoring functions to predict binding affinities and orientations (Bag et al., 2023). The docking process typically begins with the preparation of three-dimensional models of both the ligand and the protein. This preparation may involve the optimization of the ligand's geometry, the assignment

of partial charges, and the identification of rotatable bonds. The protein structure is often obtained from experimental sources, methods such as X-ray crystallography and nuclear magnetic resonance (NMR) spectroscopy, and may require refinement to ensure that it is suitable for docking studies (Burle et al., 2023). Once the structures are prepared, the docking software generates a series of possible ligand conformations and orientations within the protein's binding site. These conformations are then scored using various scoring functions that estimate the binding energy, allowing researchers to rank the potential binding modes based on their predicted affinities (Gentile et al., 2020; Taghizadeh et al., 2022). In practical applications, molecular docking serves as a foundational tool in structure-based drug design, allowing facilitating the screening of large compound libraries by researchers to identify potential drug candidates that exhibit high binding affinity for their target proteins. The ability to perform virtual screening of compound libraries significantly accelerates the drug discovery process, as it enables researchers to prioritize compounds for experimental validation based on their predicted binding affinities (Ferreira et al., 2015; Fikes & Srougi, 2023). This computational approach is particularly valuable in the early stages of drug development, where it can help to identify lead compounds that warrant further investigation (John Oluwafemi Teibo et al., 2021). The evolution of molecular docking has been marked by the development of advanced algorithms and software tools, such as AutoDock, Vina, and Glide, which facilitate the efficient exploration of ligand conformational space and the prediction of binding poses (Maheswari & Kalaiselvi, 2024; Pinzi & Rastelli, 2019).

In summary, molecular docking is a computational technique that provides invaluable insights into the interactions between proteins and ligands, facilitating the identification and optimization of potential drug candidates. Its application in drug design underscores its importance in modern biomedical research, enabling the development of targeted therapies that can effectively combat various diseases. As the field continues to evolve, molecular docking will undoubtedly remain a critical tool in the quest for new and effective therapeutic agents (Meng et al., 2011).

2. MATERIALS and METHOD

2.1 Experimental

The commercial chemicals and reagents used in this study were obtained from Sigma-Aldrich. Thin-layer chromatography (TLC) was carried out on Merck silica gel F-254 plates, and visualization of the spots was achieved using a potassium permanganate solution. Melting points (Mp) were determined using an uncorrected MELTEMP apparatus with open glass capillaries. FT-IR spectra were recorded using a Perkin Elmer Spectrum FTIR-ATR spectrophotometer. Nuclear magnetic resonance (NMR) spectra of all synthesized compounds were measured at room temperature using a Bruker Avance Neo 500 MHz NMR spectrometer in DMSO-d_6 and $CDCI_3$. The coupling constants (J) are reported in Hertz (Hz), and chemical shifts are expressed in parts per million (ppm). The splitting patterns are designated as follows: singlet (s), doublet (d), multiplet (m), doublet of doublets (dd), and triplet of doublets (td). LC-MS measurements were obtained from ZQ micromass ESI (+). The HRMS measurements were obtained from Agilent 6530 Accurate-Mass Q-TOF LC/MS.

2.2 General Synthesis Procedures

2.2.1 Synthesis Of 1-Methyl-3-Phenyl Thiourea (19)

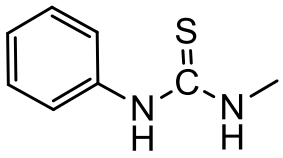

19

To a round-bottomed flask, phenylisothiocyanate (**17**) (40 mmol, 5.408 g, 1.0 equiv) was dissolved in 20 mL of dry acetonitrile. Methylamine hydrochloride (**18**) (48 mmol, 3.240 g, 1.2 eq.) was added, followed by the dropwise addition of triethylamine (48 mmol, 4.857 g, 1.2 eq.) under vigorous stirring at room temperature. Upon completion of the reaction, as monitored by TLC (EtOAc:Hex 1:3), the reaction mixture was poured into 40 mL of ice-cold water. The pH was adjusted to 7 using 1 M HCl. The resulting precipitate was collected by filtration, washed with cold water, and recrystallized from EtOAc/Hex. White solid, (%91)

^{1}H and ^{13}C NMR data of this compound compared with the literature (Wibowo et al., 2020).

^{1}H NMR (500 MHz, $CDCl_3$) δ 8.30 (s, 1H), 7.44 – 7.41 (m, 2H), 7.31 – 7.28 (m, 1H), 7.24 – 7.21 (m, 2H), 6.11 (s, 1H), 3.12 (s, 3H). ^{13}C NMR (126 MHz, $CDCl_3$) δ 181.4, 136.2, 130.1, 127.3, 125.4, 77.3, 77.1, 76.8, 32.0.

^{1}H NMR (500 MHz, $CDCl_3$) δ 7.89 (s, 1H), 7.43 (t, *J* = 7.8 Hz, 2H), 7.31 (t, *J* = 7.5 Hz, 1H), 7.21 (d, *J* = 7.7 Hz, 2H), 6.04 (s, 1H), 3.13 (d, *J* = 4.7 Hz, 3H). (lit.) ^{13}C NMR (126 MHz, $CDCl_3$) δ 181.7, 136.0, 130.2, 127.5, 125.5, 32.1. (lit.)

2.2.2 Synthesis Of Ethyl 3-Methyl-2-(Phenylimino)-2,3-Dihydrothiazole-4-Carboxylate (21)

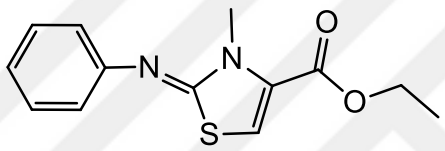

21

Compound **19** (34.494 mmol, 5.733 g, 1.0 eq.) was dissolved in 20 mL of dry EtOH in a round-bottomed flask. Ethyl bromopyruvate (**20**) (34.494 mmol, 6.622 g, 1.0 eq.) was added dropwise under vigorous stirring at room temperature. After the addition was complete, the reaction mixture was refluxed for 3 hours. The progress of the reaction was monitored by thin-layer chromatography (TLC) using ethyl acetate/hexane (1:3) as the mobile phase. Upon completion, the reaction mixture was poured into 40 mL of ice-cold water, and the pH was adjusted to 7 using 1 M Na_2CO_3 solution. The resulting precipitate was collected by vacuum filtration, washed with cold water, and recrystallized from an EtOAc/Hex mixture to afford the pure product.

Yellow powder, (88%); M.P. 110-111 ˚C, Rf: 0.78 (1:3 EtOAc:Hex), V̄max (ATR, cm^{-1}) 1716 (COOEt), 1606 (C=N). ^{1}H NMR (500 MHz, $CDCI_3$) δ 7.4-7.31 (m, 2H), 7.14-7.05 (m,1H), 7.09-7.03 (m,1H), 7.08-7.01 (m,1H), 6.95 (s, 1H, Thiazole),4.34 (q, *J*=7.1 Hz, 2H, CH_2), 3.76 (s,3H, N-CH_3), 1.38 (t, *J*=7.2 Hz, 3H, CH_3). ^{13}C NMR (125 MHz, $CDCl_3$) δ 159.1 (C=O), 158.5 (C=N), 151.3 (C-N), 130.4 (Thiazole C), 129.6 (C), 123.4 (C), 121.4 (C), 110.6 (Thiazole CH), 61.4

(CH_2), 33.3 (N-CH_3), 14.1 (CH_3). LC/MS $C_{13}H_{14}N_2O_2S$ m/z (ESI+) 263.3 (M+H 100%). HR/MS Calculated $C_{13}H_{14}N_2O_2S$ $[M+H]^+$ 262.0776, found 262.07877

2.2.33-Methyl-2-(Phenylimino)-2,3- Dihydrothiazole -4- Carbohydrazide (23)

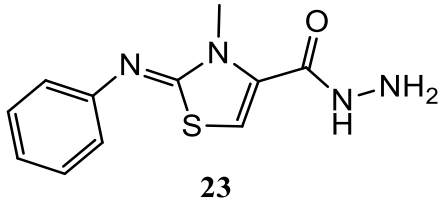

23

Compound **21** (26.726 mmol, 7.011 g, 1.0 eq.) was dissolved in 40 mL of dry ethanol in a round-bottomed flask. Hydrazine monohydrate (**22**) (50–60%, 200.445 mmol, 10.024 g, 7.5 eq.) was added dropwise under vigorous stirring at room temperature. After the addition was complete, the reaction mixture was stirred at room temperature for 6 hours. The progress of the reaction was monitored by TLC and EtOAc:Hex (1:1) as the mobile phase. After the reaction was completed the resulting precipitate was collected by vacuum filtration, washed with cold ethanol then recrystallized from ethanol to afford the pure product.

White powder, (88%); M.P. 194-195 ˚C, Rf: 0.10 (1:3 EtOAc:Hex), Vmax (ATR, cm-1) 1676 (CONH), 1606 (C=N). ^{1}H NMR (500 MHz, DMSO) δ 9.84 (s,1H, CONH), 7.32 (t, *J*=7.8 Hz,2H), 7.02 (t, *J*=7.4 Hz 1H), 6.98-6.94 (m,2H), 6.63 (s,1H, Thiazole), 4.53 (s,2H, NH_2), 3.46 (s,3H, N-CH_3). ^{13}C NMR (125 MHz, DMSO) δ 159.6 (C=O), 158.8 (C=N), 151.8 (C-N), 133.7 (Thiazole C), 130.0 (C), 123.2 (C), 121.5 (C), 102.1 (Thiazole CH), 32.9 (N-CH_3). LC/MS $C_{11}H_{12}N_4OS$ m/z (ESI+) 289.4 (M+Na+H_2O 100%) 290.4 (M+Na+H_2O+^{13}C 12%), HR/MS Calculated $C_{11}H_{12}N_4OS$ $[M+H]^+$ 248.07318, found 248.07444

2.2.4General Synthesis of 3-Methyl-N'-(Aryl)-2-(Phenylimino)-2,3-Dihydrothiazole -4- Carbohydrazone (24a-j)

Compound **23** (1.0 mmol, 1 eq.) and the corresponding aldehyde (1.0 mmol, 1 eq.) were dissolved in 10 mL of ethanol and refluxed overnight. The progress of the reaction was monitored by thin-layer chromatography (TLC). After completion,

the reaction mixture was allowed to cool to room temperature. The resulting precipitate was collected by vacuum filtration, recrystallized and washed with cold ethanol then dried to afford the pure product.

2.2.5 3-Methyl-N'-(4-Nitrobenzylidene)-2-(Phenylimino)-2,3-Dihydrothiazole-4-Carbohydrazone (24a)

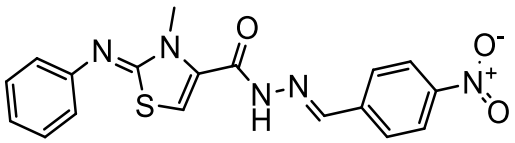

24a

Orange powder, (62%); M.P. 170-171 ˚C, Rf: 0.58 (1:2 EtOAc:Hex), Vmax (ATR, cm-1) 3120 (-NH), 1651 (CONH), 1606 (C=N), 1338 (NO_2). ^{1}H NMR (500 MHz, DMSO) δ 12.30 (s,1H, CONH), 8.44 (s, 1H, N=CH), 8.29 (d, *J*=8.4 Hz,2H), 7.98 (d, *J*=8.4, 2H), 7.33 (t, *J*=7.8, 2H), 7.04 (d, *J*=7.4, 1H), 7.01 (d, *J* = 6.5 Hz, 1H), 6.98 (d, *J* = 7.7 Hz, 2H), 3.37 (s, 3H, N-CH_3). ^{13}C NMR (125 MHz, DMSO) δ 158.7 (C=N), 156.3 (CONH), 151.7 (C-N),148.5 (C-NO_2), 146.5 (N=CH), 140.6 (CH-Ph), 133.2 (Thiazole C), 130.0 (C), 128.6 (C), 124.5 (C), 123.4 (C), 121.5 (C), 105.6 (Thiazole CH), 33.1 (N-CH_3). LC/MS $C_{18}H_{15}N_5O_3S$ m/z (ESI+) 382.5 (M+H 100%) 383.5 HR/MS Calculated $C_{18}H_{15}N_5O_3S$ $[M+H]^+$ 381.08956, found 381.09124

2.2.6 3-Methyl-N'-(4-Methoxybenzylidene)-2-(Phenylimino)-2,3-Dihydrothiazole-4-Carbohydrazone (24b)

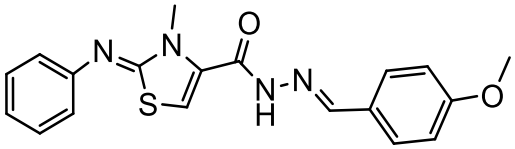

24b

Off-white powder, (61%); M.P. 180-181 ˚C, Rf: 0.63 (1:2 EtOAc:Hex), Vmax (ATR, cm-1) 3020 (-NH), 1622 (CONH), 1604 (C=N), 1249 (OCH_3). ^{1}H NMR (500 MHz, DMSO) δ 11.91 (s,1H, CONH), 8.31 (s, 1H, N=CH), 7.68 (d, *J*=8.3 Hz,2H), 7.34 (t, *J*=7.7, 2H), 7.05-6.98 (m, 5H), 6.92 (s,1H, Thiazole), 3.81 (s, 3H, O-CH_3), 3.51 (s, 3H, N-CH_3). ^{13}C NMR (125 MHz, DMSO) δ 161.6 (C=N), 158.8 (CONH), 156.1 (C-N),151.7 (C-OMe), 149.0 (N=CH), 133.7 (CH-Ph), 130.3 (Thiazole C), 129.3 (C), 126.9 (C), 123.3 (C), 121.5 (C), 114.8 (C), 104.2 (Thiazole CH), 55.7 (O- CH_3), 33.1 (N-CH_3). LC/MS $C_{19}H_{18}N_4O_2S$ m/z (ESI+) 367.5 (M+H 100%) 368.5 HR/MS Calculated $C_{19}H_{18}N_4O_2S$ $[M+H]^+$ 366.11677, found 366.11505

2.2.7 3-Methyl-N'-(4-Methylbenzylidene)-2-(Phenylimino)-2,3-Dihydrothiazole-4-Carbohydrazone (24c)

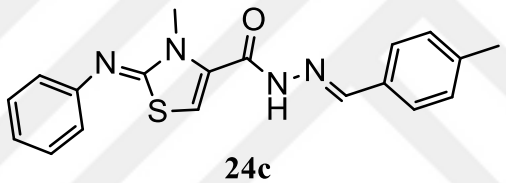

24c

White powder, (72%); M.P. 190-191 ˚C, Rf: 0.63 (1:2 EtOAc:Hex), Vmax (ATR, cm-1) 3024 (-NH), 1641 (CONH), 1618 (HC=N), 1608 (C=N). ^{1}H NMR (500 MHz, DMSO) δ 11.96 (s,1H, CONH), 8.33 (s, 1H, N=CH), 7.63 (d, *J*=7.7 Hz,2H), 7.39-7.23 (m, 4H), 7.04 (t, *J*=7.4 Hz,1H), 6.99 (d, *J*=7.7 Hz,2H), 6.94 (s,1H, Thiazole), 3.51 (s, 3H, N-CH_3), 2.35 (s, 3H, Ph-CH_3). ^{13}C NMR (125 MHz, DMSO) δ 158.7 (C=N), 156.1 (CONH), 151.7 (C-N),149.2 (N=CH), 140.7 (C), 133.6 (CH-Ph), 131.7 (Thiazole C), 130.0 (C), 129.9 (C), 127.7 (C), 123.3 (C), 121.5 (C), 104.5 (Thiazole CH), 33.1 (N-CH_3), 21.5 (Ph-CH_3). LC/MS $C_{19}H_{18}N_4OS$ m/z (ESI+) 351.5 (M+H 100%). HR/MS Calculated $C_{19}H_{18}N_4OS$ $[M+H]^+$ 350.12165, found 350.12013

2.2.8 3-Methyl-N'-(2,4-Dichlorobenzylidene)-2-(Phenylimino)-2,3-Dihydrothiazole-4-Carbohydrazone (24d)

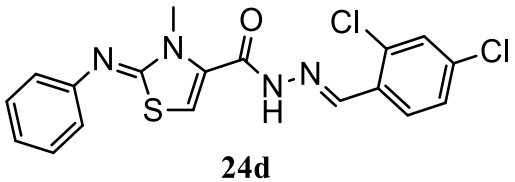

24d

Yellow crystals, (69%); M.P. 198-199 ˚C, Rf: 0.55 (1:2 EtOAc:Hex), Vmax (ATR, cm-1) 3039 (-NH), 1651 (CONH), 1620 (C=N). ^{1}H NMR (500 MHz, DMSO) δ 12.21 (s,1H, CONH), 8.72 (s, 1H, N=CH), 8.00 (d, *J*=8.9 Hz,1H), 7.71 (d, *J*=2.1 Hz 1H), 7.56-7.49 (m, 1H), 7.34 (t, *J*=7.7 Hz,2H), 7.02 (dt, *J*=22.0, 7.6 Hz,4H), 3.52 (s, 3H, N-CH_3). ^{13}C NMR (125 MHz, DMSO) δ 158.7 (C=N), 156.2 (CONH), 151.7 (C-N),143.9 (N=CH), 135.8 (C), 134.5 (CH-Ph), 133.3 (Thiazole C), 130.8 (C), 130.0 (C), 129.9 (C), 128.5 (C), 123.4 (C), 121.5 (C), 105.4 (Thiazole CH), 33.1 (N-CH_3). LC/MS $C_{18}H_{14}Cl_2N_4OS$ m/z (ESI+) 405.4 (M 100%). HR/MS Calculated $C_{18}H_{14}Cl_2N_4OS$ $[M+H]^-$ 404.02654, found 404.02803

2.2.9 3-Methyl-N'-(2,3-Dichlorobenzylidene)-2-(Phenylimino)-2,3-Dihydrothiazole-4-Carbohydrazone (24e)

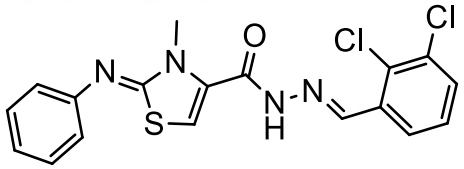

24e

Yellow needle crystals, (57%); M.P. 198-199 ˚C, Rf: 0.58 (1:2 EtOAc:Hex), Vmax (ATR, cm-1) 3051 (-NH), 1647 (CONH), 1600 (C=N). ^{1}H NMR (500 MHz, DMSO) δ 12.30 (s,1H, CONH), 8.79 (s,1H, N=CH), 7.97 (d, *J*=7.9 Hz,1H), 7.74-7.71 (m, 1H), 7.46 (t, *J*=8.0 Hz, 1H), 7.36-7.32 (m,2H), 7.06-7.02 (m, 2H), 7.00-6.97 (m, 2H), 3.52 (s, 3H, N-CH_3). ^{13}C NMR (125 MHz, DMSO) δ 158.7 (C=N), 156.2 (CONH), 151.7 (C-N),144.7 (N=CH), 134.1 (C), 133.2 (CH-Ph), 132.9 (Thiazole C), 132.3 (C), 131.6 (C), 130.0 (C), 129.0 (C), 126.0 (C), 123.4 (C), 121.5 (C) 105.5 (Thiazole CH), 33.2 (N-CH_3). LC/MS $C_{18}H_{14}Cl_2N_4OS$ m/z (ESI+) 405.4 (M 100%). HR/MS Calculated $C_{18}H_{14}Cl_2N_4OS$ $[M+H]^-$ 404.02654, found 404.02788

2.2.10 3-Methyl-N'-(2,6-Dichlorobenzylidene)-2-(Phenylimino)-2,3-Dihydrothiazole-4-Carbohydrazone (24f)

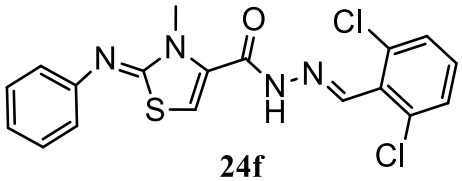

24f

Yellow powder (64%); M.P. 195-196˚C, Rf: 0.57 (1:2 EtOAc:Hex), Vmax (ATR, cm-1) 3120 (-NH), 1660 (CONH), 1610 (C=N). ^{1}H NMR (500 MHz, DMSO) δ 12.30 (s,1H, CONH), 8.59 (s,1H, N=CH), 7.58 (s,1H), 7.57 (s,1H), 7.46 (d, *J*=8.1 Hz, 1H), 7.33 (d, *J*=7.7 Hz,2H), 7.06-7.02 (m,2H), 6.99 (d, *J*=7.9 Hz,2H), 3.52 (s, 3H, N-CH_3). ^{13}C NMR (125 MHz, DMSO), 158.7 (C=N), 156.2 (CONH), 151.7 (C-N),144.5 (N=CH), 134.4 (C), 133.1 (CH-Ph), 131.8 (Thiazole C), 130.6 (C), 130.0 (C), 129.7 (C), 123.4 (C), 121.51 (C), 105.6 (Thiazole CH), 33.2 (N-CH_3). LC/MS $C_{18}H_{14}Cl_2N_4OS$ m/z (ESI+) 405.3 (M 100%) HR/MS Calculated $C_{18}H_{14}Cl_2N_4OS$ $[M+H]^-$ 404.02654, found 404.02786

2.2.11 3-Methyl-N'-(3-Hydroxybenzylidene)-2-(Phenylimino)-2,3-Dihydrothiazole-4-Carbohydrazone (24g)

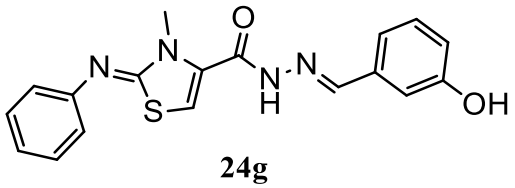

24g

Off-white powder (55%); M.P. 186-187˚C, Rf: 0.44 (1:2 EtOAc:Hex), Vmax (ATR, cm-1) 3392 (OH), 3051 (-NH), 1620 (CONH), 1604 (C=N). ^{1}H NMR (500 MHz, DMSO) δ 11.98 (s,1H, CONH), 9.69 (s,1H, OH), 8.27 (s,1H, N=CH), 7.34 (t, *J*=7.7 Hz,2H), 7.27 (t, *J*=7.8 Hz ,1H), 7.20 (s,1H), 7.11 (d, *J*=7.6 Hz,2H), 7.04 (t, *J*=7.4 Hz,1H), 7.00-6.91 (m,3H), 6.89-6.83 (m,1H), 3.51 (s, 3H, N-CH_3). ^{13}C NMR (125 MHz, DMSO) δ 158.8 (C=N), 158.1 (CONH), 156.1 (C-N),151.7 (N=CH), 149.2 (C), 135.6 (CH-Ph), 130.4 (Thiazole C), 130.0 (C), 123.4 (C), 121.5 (C), 119.4 (C), 118.2 (C), 113.1 (C), 104.6 (Thiazole CH), 33.1 (N-CH_3). LC/MS

$C_{18}H_{16}N_4O_2S$ m/z (ESI+) 353.4 (M+H 100%) HR/MS Calculated $C_{18}H_{16}N_4O_2S$ [M] 352.0994, found 352.10113

2.2.12 3-Methyl-N'-((3-MethylThiophen-2-yl) Methylene)-2-(Phenylimino)-2,3-Dihydrothiazole-4-Carbohydrazone (24h)

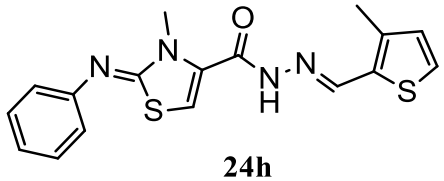

24h

Beige crystals (40%); M.P. 200-201˚C, Rf: 0.61 (1:2 EtOAc:Hex), Vmax (ATR, cm-1) 3041 (-NH), 1624 (CONH), 1606 (C=N). ^{1}H NMR (500 MHz, DMSO) δ 11.98 (s,1H, CONH), 8.62 (s,1H, N=CH), 7.60 (d, *J*=5.1 Hz,1H), 7.34 (t, *J*=7.8 Hz,2H), 7.06-6.91 (m,5H), 3.50 (s,3H, N-CH_3), 2.32 (s,3H, CH_3). ^{13}C NMR (125 MHz, DMSO) δ 158.8 (C=N), 155.80 (CONH), 151.7 (C-N),143.2 (N=CH), 141.1 (C), 138.3 (CH-Ph), 133.6 (Thiazole TZ C), 132.5 (C), 131.4 (C), 130.0 (C), 128.9 (C), 123.4 (C), 121.5 (C), 104.3 (Thiazole CH), 33.1 (N-CH_3), 14.0 (Thiophene-CH_3). LC/MS $C_{17}H_{16}N_4OS_2$ m/z (ESI+) 357.4 (M+H 100%) HR/MS Calculated $C_{17}H_{16}N_4OS_2$ [M] 356.07655, found 356.07844

2.2.13 3-Methyl-N'-(3-Benzylidene)-2-(Phenylimino)-2,3-Dihydrothiazole-4-Carbohydrazone (24i)

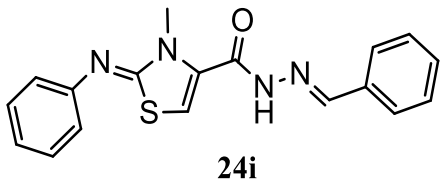

24i

Off-white powder, (78%); M.P. 211-212 ˚C, Rf: 0.52 (1:2 EtOAc:Hex), Vmax (ATR, cm-1) 3040 (-NH), 1622 (CONH), 1604 (C=N). ^{1}H NMR (500 MHz, DMSO) δ 11.95 (s,1H, CONH), 8.37 (s,1H, N=CH), 7.74 (s,2H), 7.47 (dd, *J*=5.4,1.9 Hz 3H), 7.36-7.32 (m,2H), 7.06-7.02 (m,1H), 7.01-6.98 (m,2H), 6.94 (s,1H), 3.51(s,3H,N-CH_3).^{13}C NMR (125 MHz, DMSO) δ 158.7 (C=N),156.2

(CONH),151.7 (C-N), 149.1 (N=CH), 134.4 (C), 133.5 (CH-Ph), 130.8 (Thiazole C), 130.0 (C), 129.3 (C), 127.7 (C), 123.4 (C), 121.5 (C), 104.7 (Thiazole CH), 33.1 (N-CH_3). LC/MS $C_{18}H_{16}N_4OS$ m/z (ESI+) 337.4 (M+H 100%) HR/MS Calculated $C_{18}H_{16}N_4OS$ [M] 336.10448, found 336.10486

2.2.14 3-Methyl-N'-(4-Hydroxybenzylidene)-2-(Phenylimino)-2,3-Dihydrothiazole-4-Carbohydrazone (24j)

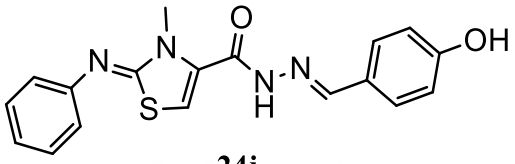

24j

White powder (59%); M.P. 190-191˚C, Rf: 0.43 (1:2 EtOAc:Hex), Vmax (ATR, cm-1) 3325 (OH), 3055 (-NH), 1618 (CONH), 1606 (C=N). ^{1}H NMR (500 MHz, DMSO) δ 11.76 (s,1H, CONH), 9.93 (s,1H, OH), 8.26 (s,1H, N=CH), 7.57 (d, *J*=8.3 Hz,2H), 7.34 (s,2H), 7.03 (s,1H), 6.99 (d, *J*=7.8 Hz,2H), 6.88 (s,1H), 6.85 (s,2H), 3.50 (s, 3H, N-CH_3). ^{13}C NMR (125 MHz, DMSO) δ 160.2 (C=N), 158.8 (CONH), 155.9 (C-N),151.7 (N=CH), 149.5 (C), 133.7 (CH-Ph), 130.0 (Thiazole C), 129.5 (C), 125.3 (C), 123.3 (C), 121.5 (C), 116.2 (C), 104.0 (Thiazole CH), 33.0 (N-CH_3). LC/MS $C_{18}H_{16}N_4O_2S$ m/z (ESI+) 353.4 (M+H 100%). HR/MS Calculated $C_{18}H_{16}N_4O_2S$ [M] 352.0994, found 352.1015

2.3 Molecular Docking Studies

Molecular docking studies were performed by using AutoDock Vina which evaluates the Gibbs free energy of ligands based on their binding affinity (Trott & Olson, 2010). For interaction analysis, Biova Discovery Studio Visualizer (v21.1.0.20298; Dassault Systèmes, San Diego 2021) and UCSF Chimera (Pettersen et al., 2004) were used. DeepSite was used to identify the binding site of the AChE (Jiménez et al., 2017). The co-crystallized complex file was obtained from the Protein Data Bank (PDB; www.rcsb.org) accession no: 4EY7 (Cheung et al., 2012). The docking protocols applied in this study followed those described in literature Stefano forli and his colleagues (Forli et al., 2016).

For the validation of the molecular docking method used, the well known method, re-docking was performed. The co-crystallized ligand (donepezil) was extracted from the crystal structure and subsequently re-docked into the active site using the same docking parameters applied throughout this study. Docking calculations were performed using UCSF Chimera 1.6 with integrated AutoDock Vina tools.

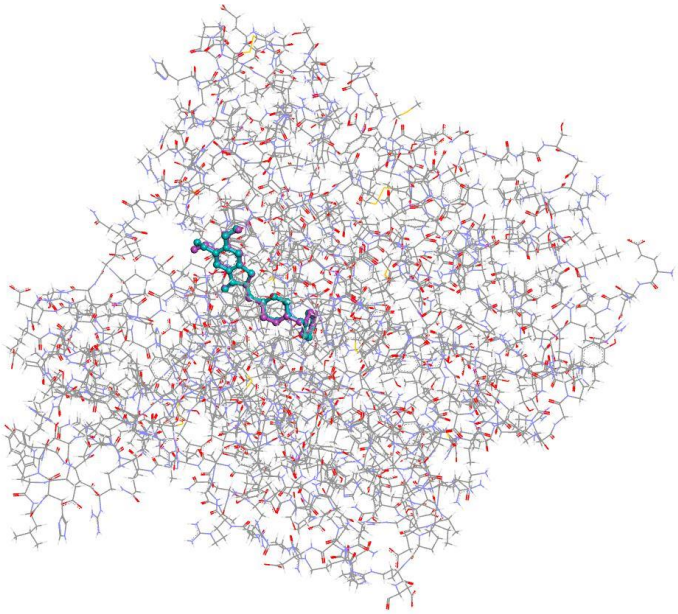

Figure 2.10 Co-crystallized and re-docked pose of Donepezil in AChE

The docking grid box was centered at coordinates (-14.075,-43.682, 27.588-X,Y,Z) with a box size of 20 × 20 × 20 Å. The number of binding modes was set to 10, with an exhaustiveness level of 8 to ensure adequate sampling of possible binding conformations. Prior to docking, protein structure integrity was evaluated using the Dunbrack 2010 rotamer library, and missing side chains or alternative conformations were corrected accordingly. Protonation states of the protein and the ligand were assigned using Gasteiger charges and prepared with ANTECHAMBER tools to ensure proper atom typing and charge distribution.

After docking, the best-scoring binding pose of donepezil was superimposed onto its original crystallographic conformation using UCSF Chimera 1.6. Heavy atoms (non-hydrogen atoms) were considered for alignment and the Root Mean Square Deviation was calculated. The RMSD between the docked and crystal

structure was determined as 0.253 Å, which indicates an excellent overlap and highly accurate reproduction of the experimentally observed binding conformation.

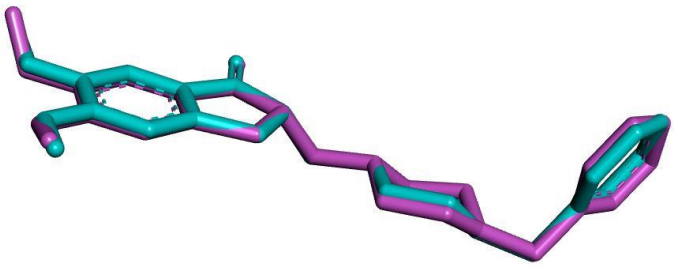

Figure 2.2 Superimpozed pose of donepezil (turquoise) and re-docked (purple)

An RMSD value below 2.0 Å is widely accepted as a successful re-docking validation, and the obtained value strongly supports the reliability, accuracy, and applicability of the docking protocol used in this study.

2.4 Biological Activity Studies

2.4.1 In Vitro ChE Enzymes Inhibition Assay

According to the modified Ellman approach outlined in our team's earlier work, the AChE and BChE inhibitory activities of the obtained compounds were evaluated (Ellman et al., 1961; Sağlık et al., 2016) The enzymes utilized in the experiment were human AChE (CAS No. 9000-81-1) and human BChE (CAS No. 9001-08-5).

2.4.1 In Vitro MAO Enzymes Inhibition Assay

The fluorometric approach, which was outlined in our team's earlier studies that were reported, was used to evaluate the synthesized compounds' inhibitory effects against MAO-A and MAO-B (Osmaniye et al., 2022). The enzymes employed in the experiment were recombinant human MAO-A and MAO-B enzymes

3. RESULTS

As supported by existing scientific evidence, the synthesis of 3-methyl-N'-(aryl)-2-(phenylimino)-2,3-dihydrothiazole-4-carbohydrazone derivatives **24a-j** was achieved.

The first step of the synthesis is the preparation of thiourea, namely 1-methyl-3-phenylthiourea (**19**) starting of phenylisothiocyanate (**17**) and methylamine hydrochloride (**18**), using the solvent acetonitrile and triethylamine as a base. Thin-layer chromatography was used to monitor the reaction's progress (TLC), and completion was achieved within 3 hours.

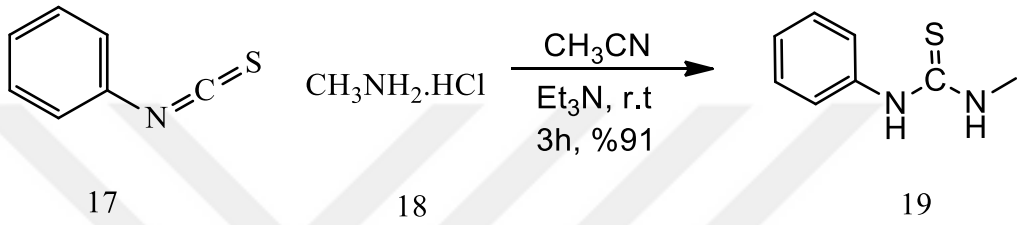

17 18 19

Photo 3.1 Synthesis of Compound **19**

FT-IR analysis of compound **19** showed two characteristic secondary amine peaks at 3259 cm^{-1} and 3157 cm^{-1}, along with a C=S stretching band at 1149 cm^{-1}.

The second step involved the cyclization of compound **19** to form a thiazole. The reaction proceeded smoothly in ethanol as the solvent, using ethyl bromopyruvate **20** under reflux conditions, and 3 hours were sufficient for the synthesis of compound **21**. The addition of ethyl bromopyruvate to a solution of compound **19** is exothermic; therefore, it is important to perform the addition at room temperature until the heat of the reaction is dissipated. Otherwise, the formation of side products was observed.

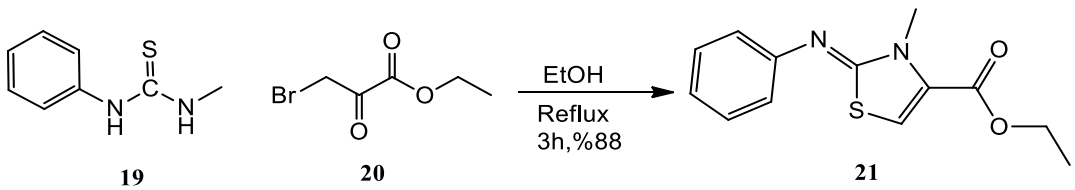

19 20 21

Photo 3.2 Synthesis of compound **21**

In FT-IR analysis, compound **21** showed a characteristic ester carbonyl peak at 1716 cm^{-1}.

The synthesis of the final intermediate compound was completed by reacting compound **21** with hydrazine monohydrate (**22**) at room temperature, furnishing compound **23**. The reaction was performed in ethanol under ambient conditions using a large excess of **22**. Experimental trials showed that the absence of excess **22** is not sufficient to fully convert the starting material into the target compound. On the other hand, the initial temperature of the reaction during the addition of **22** to the solution of compound **21** is critical. Rapid addition causes an uncontrolled exothermic reaction, turning the mixture into a tar-like mass.

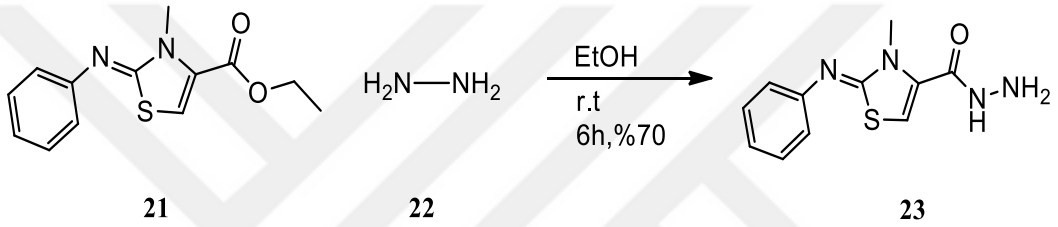

21 **22** **23**

Photo 3.3 Synthesis of compound **23**

FT-IR analysis of compound **23** revealed that the absence of the ester carbonyl peak is strong evidence of complete conversion. Additionally, the presence of an amide peak at 1676 cm^{-1} and an asymmetric N–H stretching band between 3300–3500 cm^{-1} confirms the formation of compound **23**. The synthesis of the target molecules **24a–j** under reflux conditions allowed for easy isolation and work-up. The physical and spectroscopic properties of all compounds were determined using FT-IR, ^{1}H NMR, ^{13}C NMR, LC-MS, HR-MS, and melting point (Mp) analysis. Since the formation of carbohydrazones proceeds via a condensation reaction, the presence of water has a negative effect on the reaction progress. Therefore, the dryness of ethanol is essential to achieve good yields. Otherwise, the reaction requires significantly more time to reach completion compared to when dry ethanol is used. Additionally, the substituents on the aromatic aldehydes influence the reaction time. Aldehydes bearing electron-withdrawing groups (EWGs), especially at the ortho position, completed the reaction within a few hours. In contrast, aldehydes containing electron-donating groups (EDGs) required substantially more time for full conversion.

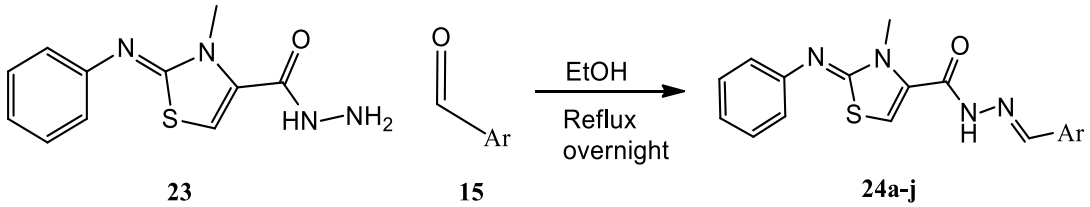

23 **15** **24a-j**

Photo 3.4 Synthesis of carbohydrazone derivatives **(24a-j)**

Compound	Ar	% Yield	Melting Point °C
24a	4-$O_2NC_6H_4$	62	170-171
24b	4-$MeOC_6H_4$	61	180-181
24c	4-$H_3CC_6H_4$	72	190-191
24d	2,4-$DiClC_6H_3$	69	198-199
24e	2,3-$DiClC_6H_3$	57	198-199
24f	2,6-$DiClC_6H_3$	64	195-196
24g	3-HOC_6H_4	55	186-187
24h	3-MeThienyl	40	200-201
24i	C_6H_5	78	211-212
24j	4-HO-C_6H_4	59	190-191

Table 3.1 Yields and substituents of compounds **24a-j**

Compounds	**Affinity for AChE binding (Kcal/Mol)**
21	**-7.9**
23	**-7.6**
24a	**-**
24b	**-9.9**
24c	**-**
24d	**-9.4**
24e	**-9.0**
24f	**-9.6**
24g	**-**
24h	**-9.5**
24i	**-9.0**

24j	**-**
Donepezil	**-12**

Table 3.2 Docking results between AChE and synthesized compounds.

Compounds	**IC_{50} values (µM)**			
	AChE enzyme	**BChE enzyme**	**MAO-A enzyme**	**MAO-B enzyme**
21	0.105±0.004	>1000	0.142±0.006	0.117±0.005
23	0.233±0.011	>1000	>100	0.162±0.006
24a	>100	>100	>100	>100
24b	0.052±0.002	>100	0.072±0.003	0.064±0.002
24c	>100	>100	0.185±0.007	0.249±0.011
24d	0.066±0.002	>1000	>100	0.083±0.004
24e	0.310±0.014	>100	>100	>100
24f	0.076±0.003	>1000	0.091±0.004	0.081±0.003
24g	>100	>100	>100	>100
24h	0.114±0.004	>1000	>1000	>100
24i	0.192±0.008	>100	0.202±0.009	0.139±0.005
24j	>100	>100	>100	0.208±0.009
Donepezil	0.0201±0.0001	-	-	-
Tacrine	-	0.0064±0.0002	-	-
Moclobemide	-	-	6.0613±0.262	-
Selegiline	-	-	-	0.0374±0.0016

Table 3.3 IC_{50} value of the selected compounds against the AChE, BChE, MAO-A and MAO-B enzymes.

4. DISCUSSION

4.1 Spectroscopic Analysis

Comprehensive spectroscopic analyses, including FT-IR, ^{13}C NMR, ^{1}H NMR, LC-MS, and LC-QTOF-MS, provided strong and conclusive evidence for the accurate structural determination and characterization of the synthesized compounds. Among them, compound **24c** 3-methyl-N'-(4-methylbenzylidene)-2-(phenylimino)-2,3-dihydrothiazole-4-carbohydrazide was selected as a representative example for detailed discussion. Careful evaluation of all spectroscopic data confirmed that the observed signals were fully consistent with the proposed structure, thereby verifying the successful synthesis of the target molecule.

The FT-IR spectrum of compound **24c** (**Figure 4.1**) showed peaks at 1641 cm^{-1} corresponding to the amide carbonyl group (CONH), at 1618 cm^{-1} for the azomethine group (HC=N) and at 1608 cm^{-1} for imine (C=N) stretch.

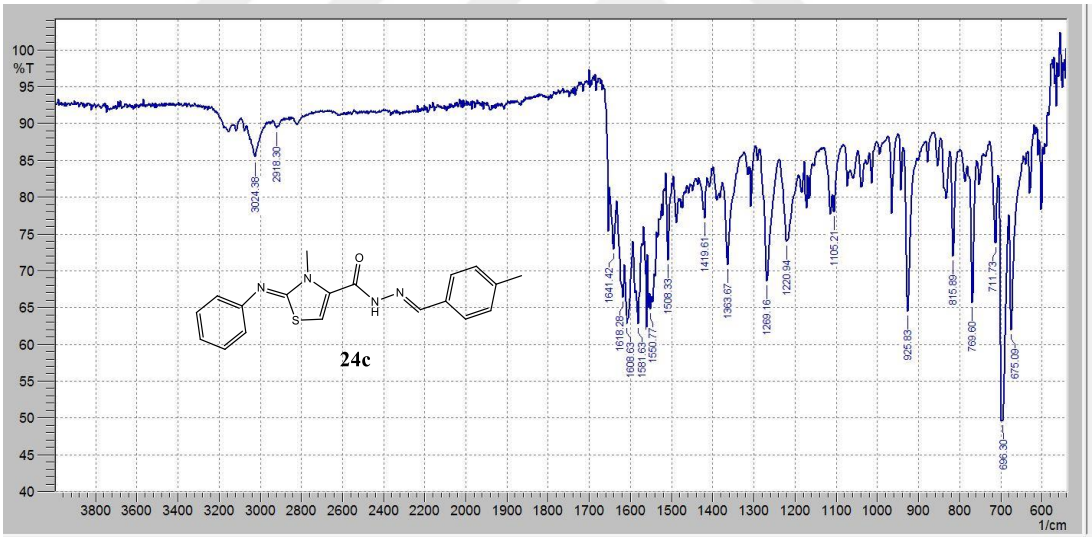

Figure 4.1 FT-IR of compound **24c**

The structural elucidation based on ^{1}H NMR spectroscopy was carried out by analyzing the chemical shifts, splitting patterns, and integration values corresponding to the hydrogen atoms present in the molecule. The chemical shift of the amidic NH proton in compound **24c** was observed at 11.96 ppm, while in other derivatives it appeared within the 11.91–12.30 ppm range. The characteristic

imine proton (N=CH) was detected at 8.33 ppm, with corresponding signals for other compounds falling within the 8.30–8.80 ppm range, depending on the substituents. The N-methyl protons were identified as a singlet at 3.51 ppm in compound **24c**, and generally appeared in the 3.30–3.55 ppm range across the series. In addition to the expected aromatic proton signals, compound **24c** showed a singlet at 2.35 ppm corresponding to para-methyl protons on the aromatic ring (**Figure 4.2**). Compound **24c** contains a total of 18 hydrogen atoms, and the integration of the ^{1}H NMR signals confirmed this, demonstrating consistency with the proposed molecular structure.

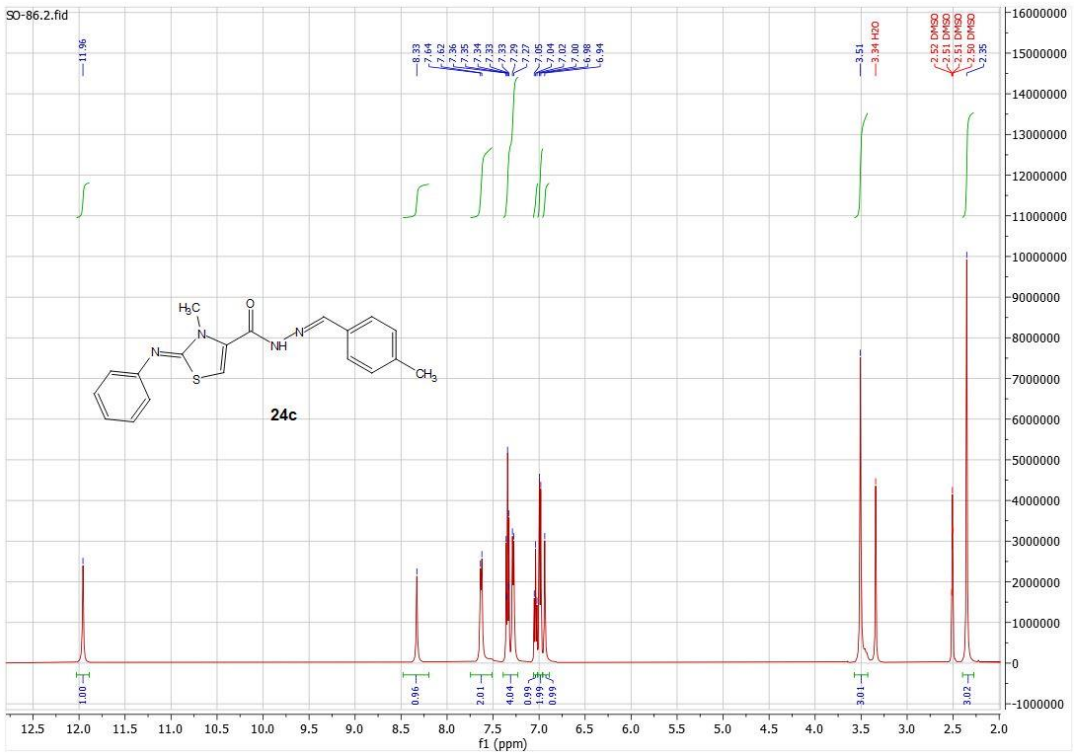

Figure 4.2 ^{1}H NMR of compound **24c**

The ^{13}C NMR spectra of compound **24c** and related derivatives revealed characteristic chemical shifts consistent with the proposed structures. The iminic carbon of the thiazole ring was observed in the range of 158–159 ppm, while the carbonyl carbon appeared between 156–157 ppm. The aliphatic N-methyl group showed signals in the 32–34 ppm range. Additionally, the thiazole ring carbon was detected between 104–105 ppm. In compound **24c**, a signal at 21.53 ppm was attributed to the para-methyl group on the aromatic ring (**Figure 4.3**). These

chemical shifts collectively support the structural integrity of the synthesized compounds.

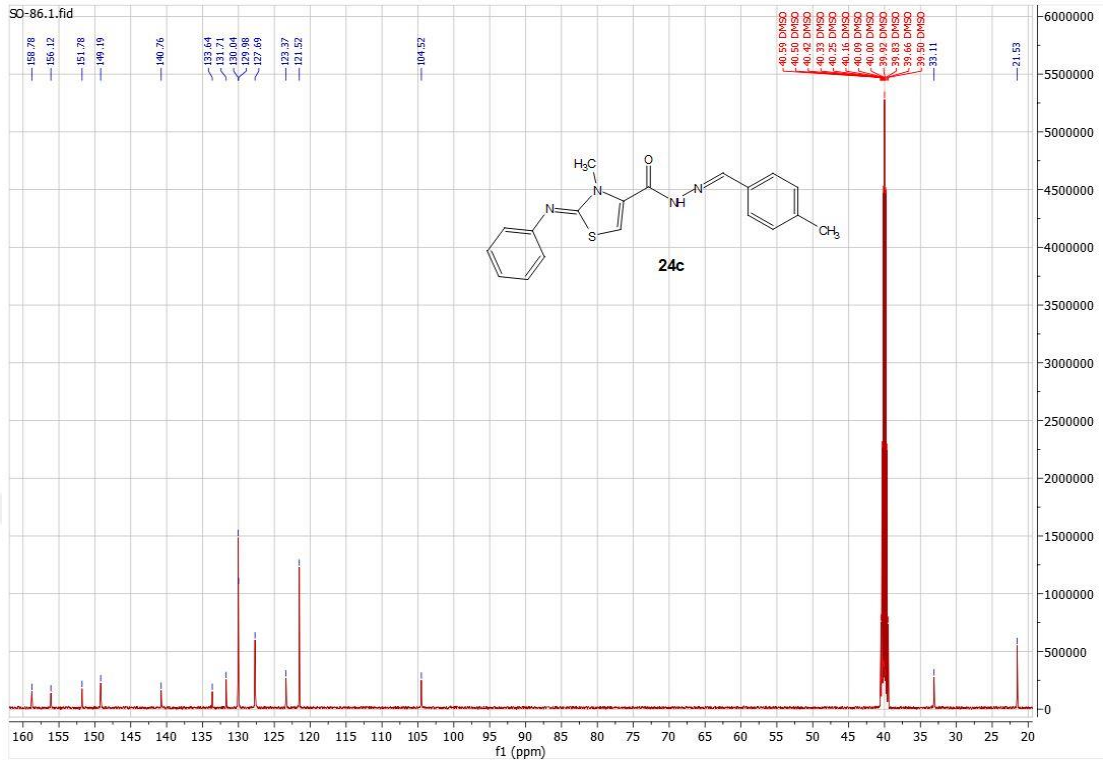

Figure 4.3 ^{13}C NMR of compound **24c**

The LC-QTOF-MS spectrum of compound **24c** was acquired in ESI^+ and spectrum showed a prominent peak at m/z 351.13 corresponding to $[M+H]^+$. Additional minor peak at 352.13 which can be attributed to isotopic patterns or adducts (**Figure 4.4**). The experimental monoisotopic mass (351.13) matched the theoretical value which is 350.12, confirming the molecular formula $C_{19}H_{18}N_4OS$.

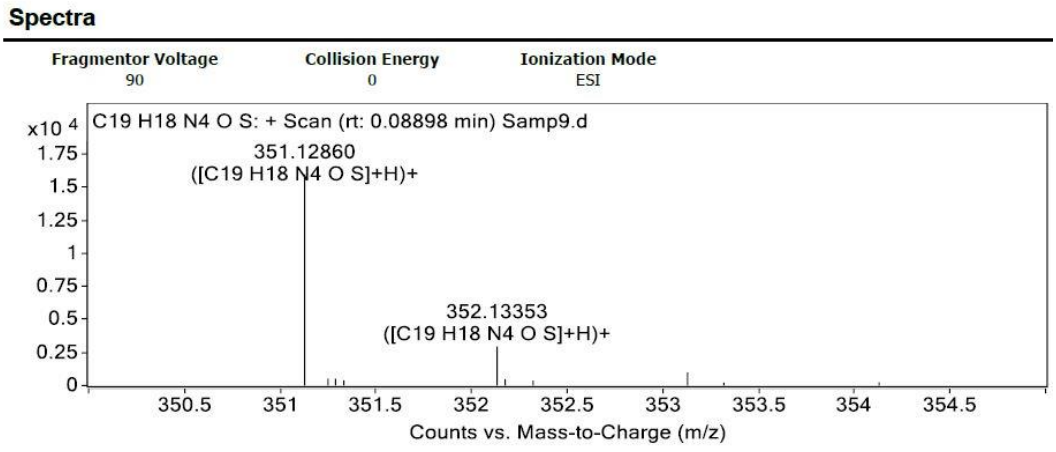

Figure 4.4 LC-QTOF-MS of compound **24c**

The LC/MS spectra of compound **24c** ($C_{19}H_{18}N_4OS$; MW = 350.40 g mol^{-1}) was analyzed on a ZQ Micromass mass spectrometer. The base peak at m/z 351.50 $[M+H]^+$ (100%) corresponds to the protonated molecular ion (350.40+1.01=351.41). No significant sodium or potassium adducts were observed. The expected molecular ion, clean isotopic pattern, and characteristic fragment peaks collectively confirm the correct molecular composition of **24c**.

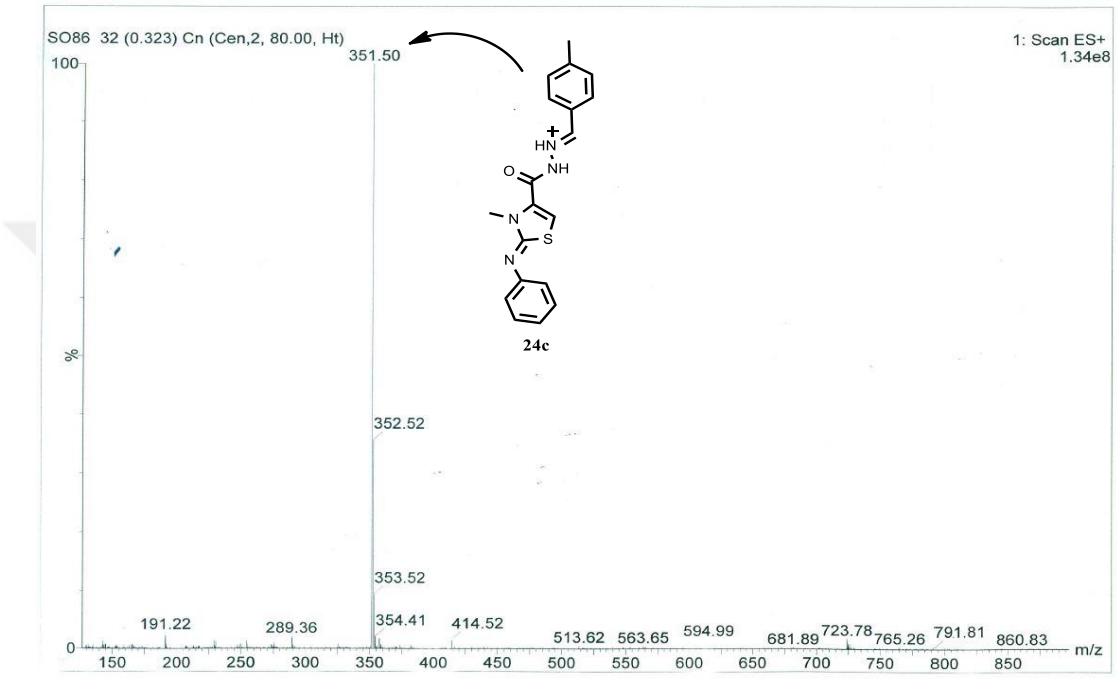

Figure 4.5 LC/MS of compound **24c**

The synthesis of compound **(21)** proceeds through a multistep mechanism beginning with the S-alkylation of 1-phenyl-3-methylthiourea (**19**) by ethyl bromopyruvate (**20**). In the first step, the nucleophilic sulfur atom attacks the electrophilic α-carbon of ethyl bromopyruvate, displacing bromide and forming a thioether intermediate. This is followed by an intramolecular nucleophilic attack in which the lone pair of the methyl-substituted nitrogen attacks the adjacent ester carbonyl carbon. This step initiates 5-exo-trig cyclization, leading to a cyclic intermediate. Subsequent proton transfers and elimination of HBr further stabilize the structure. Final rearrangement and reformation of the carbon-nitrogen bond yield the 2,3-dihydrothiazole-4-carboxylate structure of **(21)** which is depicted in **Photo 4.1**.

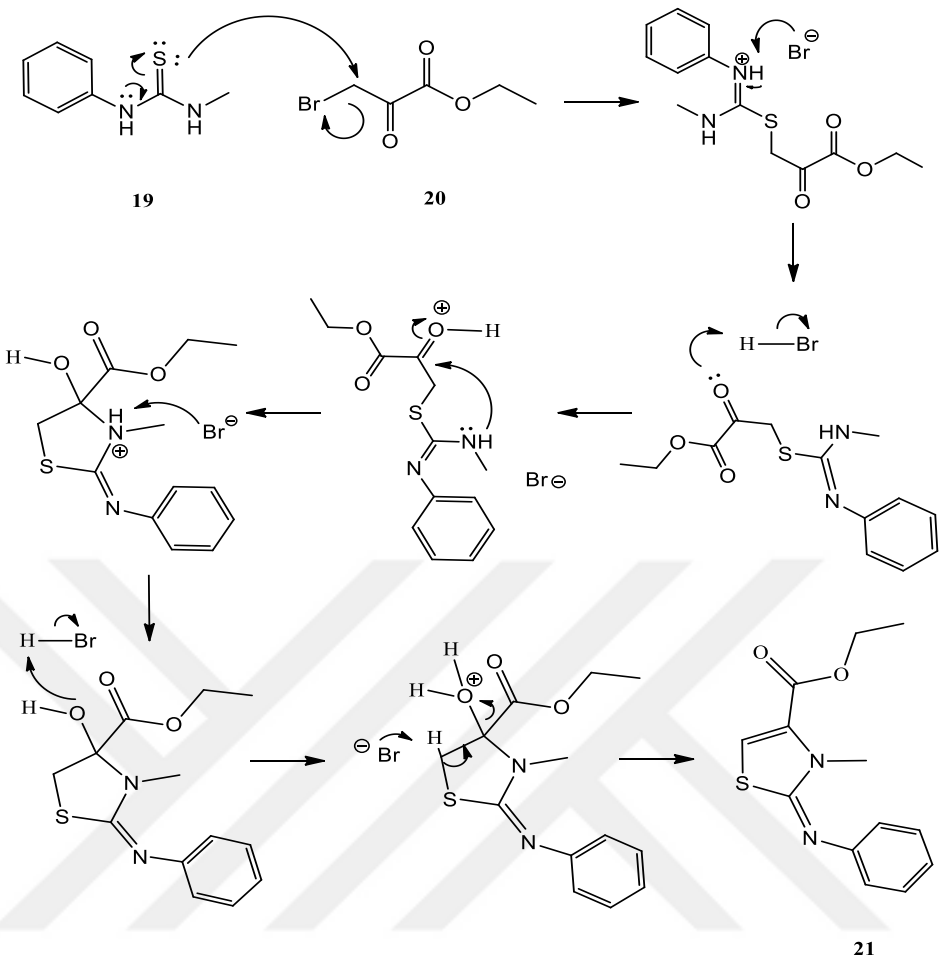

Photo 4.1 Proposed Reaction Mechanism for Thiazole Ring Formation

The synthesis of carbohydrazone derivatives **24a–j** proceeds via a classical condensation reaction between carbohydrazide compound **23** and various aromatic aldehydes **15**. The reaction initiates with the nucleophilic attack of the –NH_2 group on the carbonyl carbon of the aldehyde, forming a intermediate. Then this intermediate undergoes proton transfers that facilitate the departure of a water molecule, ultimately leading to the formation of a carbon-nitrogen double bond. The resulting products, **24a–j**, possess a hydrazone functional group conjugated to the thiazole ring system. The reaction is performed under reflux in dry ethanol, as the presence of water hinders condensation by shifting the equilibrium toward the reactants. The electronic properties of the substituents on the aromatic aldehydes significantly influences the reaction rate; aldehydes bearing electron-withdrawing groups, particularly in the ortho position, promote faster reaction completion

compared to those with electron-donating groups. The formation of **24a–j** is thus governed by both electronic factors and reaction conditions, enabling the efficient generation of structurally diverse hydrazone derivatives.

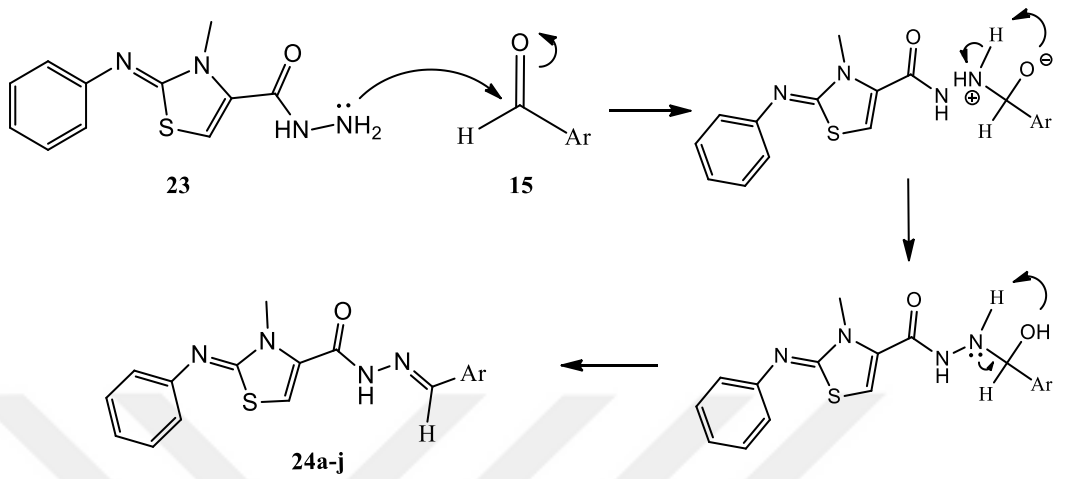

Photo 4.2 Proposed Hydrazide Condensation Reaction Mechanism

4.2 Molecular Docking Analysis

The molecular docking studies of the synthesized compounds **21,23,24b,24d,24e,24f,24h and 24i** with AChE revealed consistent binding patterns. For example, thiazole ring of compound **24b** forms interaction with Trp-86 in the catalytic anionic site of AChE. Its substituted phenyl ring also forms interactions with Tyr-341 and Trp-286 in the peripheral anionic site (**Figure 4.6**). These results demonstrate that **24b** is capable of simultaneously occupying both the catalytic site and the peripheral anionic region of AChE. The molecular docking scores of all newly synthesized compounds against AChE are summarized in **Table 3.2**. As evident from the data, compounds featuring the carbohydrazone moiety exhibit enhanced binding affinities, likely due to stronger interactions with the enzyme's peripheral anionic site. Furthermore, variations in the substituents on the phenyl ring linked to the carbohydrazone scaffold also appear to significantly modulate these docking scores. Although these binding modes resemble those of donepezil, differences in rotatable bonds, torsion angles, substituent identity and overall electronic environment produce variability across the synthesized series. Nevertheless, the conserved interactions indicate that the carbohydrazone moiety is

critical for enhancing peripheral anionic site whereas the phenylimino-2,3-dihydrothiazole core forms interaction with the catalytic anionic site.

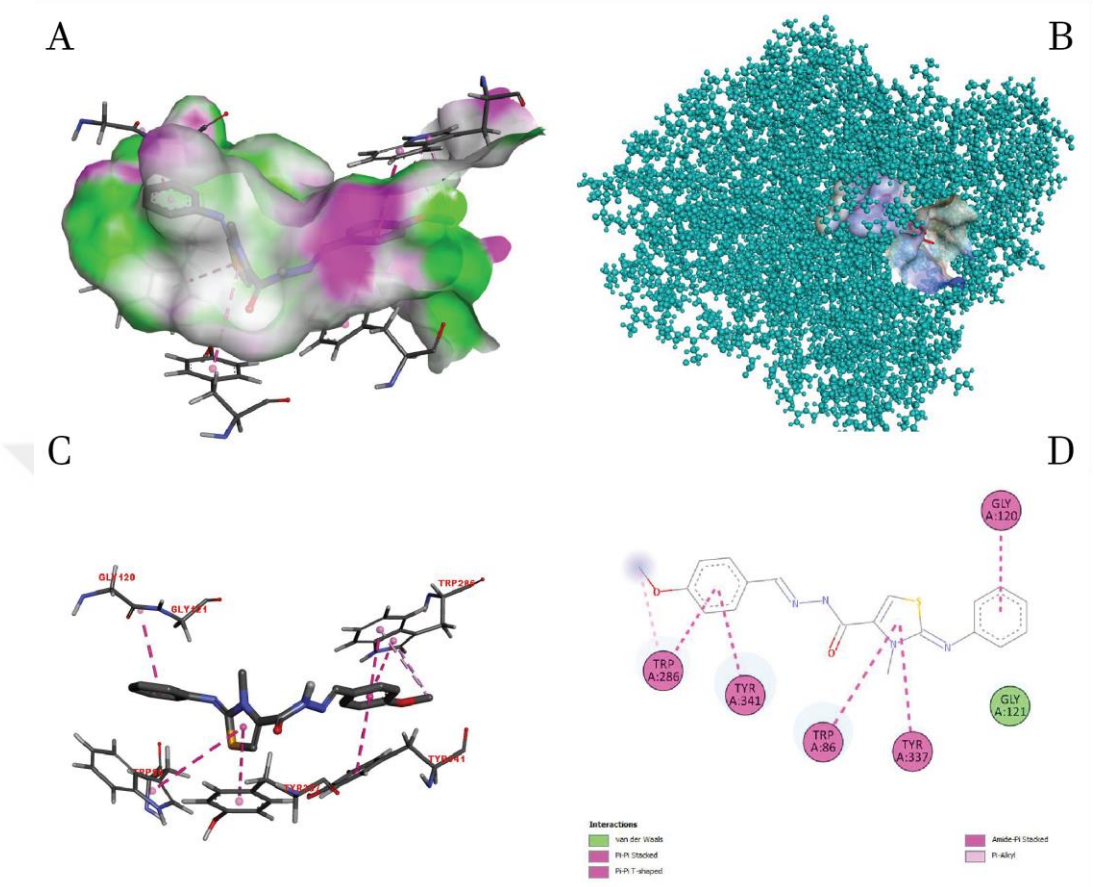

Figure 4.6 A) Interactions between hydrogen donors and acceptors at the AChE binding site with **24b. B)** Binding orientation of ligand 24c within the AChE active site **C)** Diagram of ligand **24b** interactions with AChE residues. **D)** Diagram of **24b** interactions.

4.3 Structure-Activity Relationship

The synthesized derivatives **21**, **23**, and **24a–j** were evaluated for their inhibitory potency against human AChE, BChE, MAO-A, and MAO-B. Donepezil, tacrine, moclobemide, and selegiline served as reference inhibitors.

AChE inhibition: Intermediates **21** ($IC_{50} = 0.105$ µM) and **23** (0.233 µM) show modest activity. Among the hydrazones, compounds **24b** (0.052 µM), **24d** (0.066 µM), **24f** (0.076 µM), and **24h** (0.114 µM) inhibit AChE in the sub-0.2 µM

range approaching donepezil's potency (0.0201 μM). Compounds **24a**,**24c**,**24g** and **24j** are inactive (IC_{50} > 100 μM).

BChE inhibition: None of the new analogs show significant BChE inhibition.

MAO-A inhibition: Compound **24b** exhibits the strongest MAO-A inhibition (0.072 μM), followed by **24f** (0.091 μM) and **24i** (0.202 μM). Intermediates and most analogs (**23**,**24-a**,**d,e,g,h,j**) are inactive (IC_{50} > 100 μM).

MAO-B inhibition: The best MAO-B inhibitors are **24b** (0.064 μM) and **24f** (0.081 μM); compound **23** shows moderate activity (0.162 μM). Selegiline (0.0374 μM) remains the most potent reference.

4-Methoxy (**24b**): delivers the highest dual AChE/MAO-A,B potency (IC_{50} = 0.052/0.072/0.064 μM), suggesting that the methoxy group enhances both hydrophobic and H-bond interactions in both active sites. **24i** retains good AChE (0.192 μM) and moderate MAO activity (MAO-B 0.139 μM), indicating that a benzylidene group still supports binding but less effectively than methoxy.

Dichloro (**24d**,**24f**) show strong AChE inhibition (0.066 and 0.076 μM) and dual MAO inhibition (**24f**: MAO-A 0.091 μM, MAO-B 0.081 μM). Halogens likely engage in van der Waals interactions within the gorges. 2-,3-Dichloro analog (**24e**) inactive or weak, highlighting the critical importance of chlorine positioning for optimal binding.

Hydroxy-Substitution (**24g**, **24j**) Free OH groups abolish AChE activity (IC_{50} > 100 μM) and generally MAO-A activity, likely due to unfavorable desolvation and steric hindrance in the active-site cavities.

5. CONCLUSION

The primary aim of this study was to synthesize and characterize a novel intermediate, ethyl 3-methyl-2-(phenylimino)-2,3-dihydrothiazole-4-carboxylate, and its corresponding carbohydrazone derivatives through a multi-step synthetic approach. Initially, 1-methyl-3-phenylthiourea and ethyl bromo pyruvate were reacted to yield compound **21** (ethyl 3-methyl-2-(phenylimino)-2,3-dihydrothiazole-4-carboxylate.

Compound **21** was then converted into its corresponding hydrazide derivative. Subsequently, the hydrazide was further modified to produce the desired carbohydrazone derivatives. According to the literature, the thiazole scaffold is present in several known cholinesterase inhibitors. Therefore, the newly synthesized compounds were evaluated for their potential to inhibit acetylcholinesterase (AChE) activity a key therapeutic target in the treatment of neurodegenerative disorders such as Alzheimer's disease. Additionally, *in silico* molecular docking studies were conducted to predict the interactions of the synthesized derivatives with the active site of the AChE enzyme, providing valuable insights into their binding affinities, potential interactions, and possible mechanisms of action.

Series of novel compounds fully characterized. In vitro profiling identified **24b** and **24f** as the most potent dual AChE and MAO-A,B inhibitors. The carbohydrazone linkage and specific aryl substituents are critical for strong and multi target engagement. The absence of BChE inhibition across all analogs underscores their selectivity. These findings validate the thiazole-hydrazone scaffold as a promising candidate for further lead optimization in neurodegenerative research.

REFERENCES

Alajarín, M., Cabrera, J., Pastor, A., Sánchez-Andrada, P., & Bautista, D. (2006). On the [2+2] Cycloaddition of 2-Aminothiazoles and Dimethyl Acetylenedicarboxylate. Experimental and Computational Evidence of a Thermal Disrotatory Ring Opening of Fused Cyclobutenes. *The Journal of Organic Chemistry*, *71*(14), 5328–5339. https://doi.org/10.1021/jo060664c

Arduengo, A. J., Goerlich, J. R., & Marshall, W. J. (1997). A Stable Thiazol-2-ylidene and Its Dimer. *Liebigs Annalen*, *1997*(2), 365–374. https://doi.org/10.1002/jlac.199719970213

Ariantari, N. P., & Putri, N. W. P. S. (2023). PRODUCTION OF HUPERZINE A BY FUNGAL ENDOPHYTES ASSOCIATED WITH HUPERZIACEAE PLANTS. *Journal of Pharmaceutical Science and Application*, *5*(1), 45. https://doi.org/10.24843/JPSA.2023.v05.i01.p06

B. Billones, J., & T. Bangalan, M. A. (2019). Structure-Based Discovery of Inhibitors Against MurE in Methicillin-Resistant Staphylococcus Aureus. *Oriental Journal of Chemistry*, *35*(2), 618–625. https://doi.org/10.13005/ojc/350216

Bag, S. S., Sinha, S., Dutta, S., Baishya, H. J., & Paul, S. (2023). *Targeting the SARS-CoV-2 RNA Dependent RNA Polymerase (RdRp) With Synthetic/Designer Unnatural Nucleoside Analogues: An In Silico Study*. https://doi.org/10.21203/rs.3.rs-2576209/v1

Bharti, S. K., Patel, S. K., Nath, G., Tilak, R., & Singh, S. K. (2010). Synthesis, characterization, DNA cleavage and in vitro antimicrobial activities of copper(II) complexes of Schiff bases containing a 2,4-disubstituted thiazole. *Transition Metal Chemistry*, *35*(8), 917–925. https://doi.org/10.1007/s11243-010-9412-8

Borcea, A.-M., Ionuț, I., Crișan, O., & Oniga, O. (2021). An Overview of the Synthesis and Antimicrobial, Antiprotozoal, and Antitumor Activity of Thiazole and Bisthiazole Derivatives. *Molecules*, *26*(3), 624. https://doi.org/10.3390/molecules26030624

Breitung, E. M., Shu, C.-F., & McMahon, R. J. (2000). Thiazole and Thiophene Analogues of Donor−Acceptor Stilbenes: Molecular Hyperpolarizabilities and Structure−Property Relationships. *Journal of the American Chemical Society*, *122*(6), 1154–1160. https://doi.org/10.1021/ja9930364

Burle, S. S., Gupta, K. R., Jibhkate, Y. J., Hemke, A. T., & Umekar, M. J. (2023). Insights into molecular docking: A comprehensive view. *International Journal of Pharmaceutical Chemistry and Analysis*, *10*(3), 175–184. https://doi.org/10.18231/j.ijpca.2023.030

Čačić, M., & Molnar, M. (2011). Design, Synthesis and Characterization of Some Novel 3-Coumarinyl- 5-aryliden-1,3-thiazolidine-2,4-diones and Their Antioxidant Activity.

Zeitschrift Für Naturforschung B, *66*(2), 177–183. https://doi.org/10.1515/znb-2011-0210

Chen, S., Lin, C., Xu, Y., Liu, X., & Shen, L. (2022). Pd(II)-Catalyzed Selective Amination of Inert γ-C(sp 3)−O Bonds of Aliphatic Amides with Hydrazines. *Asian Journal of Organic Chemistry*, *11*(2). https://doi.org/10.1002/ajoc.202100765

Cheung, J., Rudolph, M. J., Burshteyn, F., Cassidy, M. S., Gary, E. N., Love, J., Franklin, M. C., & Height, J. J. (2012). Structures of Human Acetylcholinesterase in Complex with Pharmacologically Important Ligands. *Journal of Medicinal Chemistry*, *55*(22), 10282–10286. https://doi.org/10.1021/jm300871x

Chimenti, F., Bizzarri, B., Bolasco, A., Secci, D., Chimenti, P., Granese, A., Carradori, S., D'Ascenzio, M., Lilli, D., & Rivanera, D. (2011). Synthesis and biological evaluation of novel 2,4-disubstituted-1,3-thiazoles as anti-Candida spp. agents. *European Journal of Medicinal Chemistry*, *46*(1), 378–382. https://doi.org/10.1016/j.ejmech.2010.10.027

D'Auria, M., Racioppi, R., Viggiani, L., & Zanirato, P. (2009). Photochemical Reactivity of 2-Azido-1,3-thiazole and 2-Azido-1,3-benzothiazole: A Procedure for the Aziridination of Enol Ethers. *European Journal of Organic Chemistry*, *2009*(6), 932–937. https://doi.org/10.1002/ejoc.200800959

Davis, M. R., Singh, E. K., Wahyudi, H., Alexander, L. D., Kunicki, J. B., Nazarova, L. A., Fairweather, K. A., Giltrap, A. M., Jolliffe, K. A., & McAlpine, S. R. (2012). Synthesis of sansalvamide A peptidomimetics: triazole, oxazole, thiazole, and pseudoproline containing compounds. *Tetrahedron*, *68*(4), 1029–1051. https://doi.org/10.1016/j.tet.2011.11.089

Doroszkiewicz, J., & Mroczko, B. (2022). New Possibilities in the Therapeutic Approach to Alzheimer's Disease. *International Journal of Molecular Sciences*, *23*(16), 8902. https://doi.org/10.3390/ijms23168902

Dotevall, G., & Herner, B. (1957). Treatment of Acute Primidone Poisoning with Bemegride and Amiphenazole. *BMJ*, *2*(5042), 451–452. https://doi.org/10.1136/bmj.2.5042.451

Easwaran potti, M., Kurup, M. R. P. P., & Fun, H.-K. (2007). Macrocyclic molecular square complex of zinc(II) self-assembled with a carbohydrazone ligand. *Inorganic Chemistry Communications*, *10*(3), 324–328. https://doi.org/10.1016/j.inoche.2006.11.009

Ellman, G. L., Courtney, K. D., Andres, V., & Featherstone, R. M. (1961). A new and rapid colorimetric determination of acetylcholinesterase activity. *Biochemical Pharmacology*, *7*(2), 88–95. https://doi.org/10.1016/0006-2952(61)90145-9

Ferreira, L., Dos Santos, R., Oliva, G., & Andricopulo, A. (2015). Molecular Docking and Structure-Based Drug Design Strategies. *Molecules*, *20*(7), 13384–13421. https://doi.org/10.3390/molecules200713384

Fikes, A. G., & Srougi, M. C. (2023). Design and Implementation of an Accessible and Open-Sourced *In Silico* Drug Screening Activity for Cancer Drug Discovery. *Journal of Chemical Education*, *100*(10), 4125–4130. https://doi.org/10.1021/acs.jchemed.3c00307

Forli, S., Huey, R., Pique, M. E., Sanner, M. F., Goodsell, D. S., & Olson, A. J. (2016). Computational protein–ligand docking and virtual drug screening with the AutoDock suite. *Nature Protocols*, *11*(5), 905–919. https://doi.org/10.1038/nprot.2016.051

Gann, H., Hartig, K., Feige, B., Brueck, R., Hohagen, F., Weske, G., van Calker, D., & Riemann, D. (2005). The effects of clomethiazole on polysomnographically recorded sleep in healthy subjects. *European Archives of Psychiatry and Clinical Neuroscience*, *255*(4), 284–290. https://doi.org/10.1007/s00406-005-0589-3

Gentile, F., Agrawal, V., Hsing, M., Ton, A.-T., Ban, F., Norinder, U., Gleave, M. E., & Cherkasov, A. (2020). Deep Docking: A Deep Learning Platform for Augmentation of Structure Based Drug Discovery. *ACS Central Science*, *6*(6), 939–949. https://doi.org/10.1021/acscentsci.0c00229

Gomha, S. M., & Khalil, K. D. (2012). A Convenient Ultrasound-Promoted Synthesis of Some New Thiazole Derivatives Bearing a Coumarin Nucleus and Their Cytotoxic Activity. *Molecules*, *17*(8), 9335–9347. https://doi.org/10.3390/molecules17089335

Grodner, B., Pisklak, D. M., & Szeleszczuk, Ł. (2024). Succinimide Derivatives as Acetylcholinesterase Inhibitors—In Silico and In Vitro Studies. *Current Issues in Molecular Biology*, *46*(6), 5117–5130. https://doi.org/10.3390/cimb46060307

Hantzsch Thiazole Synthesis. (2010). In *Comprehensive Organic Name Reactions and Reagents* (pp. 1330–1334). Wiley. https://doi.org/10.1002/9780470638859.conrr296

Huang, N., Luo, J., Liao, L., & Zhao, X. (2024). Catalytic Enantioselective Aminative Difunctionalization of Alkenes. *Journal of the American Chemical Society*, *146*(10), 7029–7038. https://doi.org/10.1021/jacs.4c00307

Huang, Y., Gan, H., Li, S., Xu, J., Wu, X., & Yao, H. (2010). Oxidation of 4-carboxylate thiazolines to 4-carboxylate thiazoles by molecular oxygen. *Tetrahedron Letters*, *51*(13), 1751–1753. https://doi.org/10.1016/j.tetlet.2010.01.091

Jacquet, P., Rémy, B., Bross, R. P. T., van Grol, M., Gaucher, F., Chabrière, E., de Koning, M. C., & Daudé, D. (2021). Enzymatic Decontamination of G-Type, V-Type and Novichok Nerve Agents. *International Journal of Molecular Sciences*, *22*(15), 8152. https://doi.org/10.3390/ijms22158152

Jiménez, J., Doerr, S., Martínez-Rosell, G., Rose, A. S., & De Fabritiis, G. (2017). DeepSite: protein-binding site predictor using 3D-convolutional neural networks. *Bioinformatics*, *33*(19), 3036–3042. https://doi.org/10.1093/bioinformatics/btx350

John Oluwafemi Teibo, Samuel Abidemi Bello, Oluwaseun Abraham Adebisi, Jeremiah Olorunjuwon Olugbami, & Titilade Kehinde Ayandeyi. (2021). Anti-diabetic drug discovery using bioactive compounds: Molecular docking insights. *GSC Biological and Pharmaceutical Sciences*, *14*(3), 075–0178. https://doi.org/10.30574/gscbps.2021.14.3.0048

Kamila, S., Mendoza, K., & Biehl, E. R. (2012). Microwave-assisted Hantzsch thiazole synthesis of N-phenyl-4-(6-phenylimidazo[2,1-b]thiazol-5-yl)thiazol-2-amines from the reaction of 2-chloro-1-(6-phenylimidazo[2,1-b]thiazol-5-yl)ethanones and thioureas. *Tetrahedron Letters*, *53*(37), 4921–4924. https://doi.org/10.1016/j.tetlet.2012.06.116

Karunakaran, K. B., Thiyagaraj, A., & Santhakumar, K. (2022). Novel insights on acetylcholinesterase inhibition by Convolvulus pluricaulis, scopolamine and their combination in zebrafish. *Natural Products and Bioprospecting*, *12*(1), 6. https://doi.org/10.1007/s13659-022-00332-5

Kumawat, A., Raheem, S., Ali, F., Dar, T. A., Chakrabarty, S., & Rizvi, M. A. (2021). Organoselenium Compounds as Acetylcholinesterase Inhibitors: Evidence and Mechanism of Mixed Inhibition. *The Journal of Physical Chemistry B*, *125*(6), 1531–1541. https://doi.org/10.1021/acs.jpcb.0c08111

Li, J. J. (2003). Cook-Heilbron thiazole synthesis. In *Name Reactions* (pp. 82–82). Springer Berlin Heidelberg. https://doi.org/10.1007/978-3-662-05336-2_66

Li, Y., Liu, X., Liu, J., Gao, L., Jin, K., Sheng, L., Yang, H., Lin, L., & Li, J. (2020). Synthesis and Protein Tyrosine Phosphatase 1B (PTP1B) Inhibitory Activity Evaluation of Novel Carbazole-Based Carbohydrazone Derivatives. *Chinese Journal of Organic Chemistry*, *40*(2), 478. https://doi.org/10.6023/cjoc201907043

Maheswari, B. U., & Kalaiselvi, G. (2024). Exploring Neophytadiene from Ampelocissus araneosa: A Molecular Docking Approach to Inhibit Biofilm Formation in Staphylococcus aureus. *UTTAR PRADESH JOURNAL OF ZOOLOGY*, *45*(3), 59–70. https://doi.org/10.56557/upjoz/2024/v45i33875

Meng, X.-Y., Zhang, H.-X., Mezei, M., & Cui, M. (2011). Molecular Docking: A Powerful Approach for Structure-Based Drug Discovery. *Current Computer Aided-Drug Design*, *7*(2), 146–157. https://doi.org/10.2174/157340911795677602

Meşeli, T., Doğan, Ş. D., Gündüz, M. G., Kökbudak, Z., Skaro Bogojevic, S., Noonan, T., Vojnovic, S., Wolber, G., & Nikodinovic-Runic, J. (2021). Design, synthesis, antibacterial activity evaluation and molecular modeling studies of new sulfonamides containing a sulfathiazole moiety. *New Journal of Chemistry*, *45*(18), 8166–8177. https://doi.org/10.1039/D1NJ00150G

Mishra, C. B., Kumari, S., & Tiwari, M. (2015). Thiazole: A promising heterocycle for the development of potent CNS active agents. *European Journal of Medicinal Chemistry*, *92*, 1–34. https://doi.org/10.1016/j.ejmech.2014.12.031

Mishra, I., & Sachan, N. (2022). Thiazole Scaffold: An Overview on Its Synthetic and Pharmaceutical Aspects. *ECS Transactions*, *107*(1), 17745–17768. https://doi.org/10.1149/10701.17745ecst

Modrić, M., Božičević, M., Odak, I., Talić, S., Barić, D., Mlakić, M., Raspudić, A., & Škorić, I. (2022). The structure-activity relationship and computational studies of 1,3-thiazole derivatives as cholinesterase inhibitors with anti-inflammatory activity. *Comptes Rendus Chimie*, *25*, 267–279. https://doi.org/10.5802/crchim.201

Murugesan, & kaleeswaran. (2024). *In Silico Drug Discovery: Unveiling Potential Targets in Plasmodium falciparum through Molecular Docking Analysis*. https://doi.org/10.21203/rs.3.rs-3981337/v1

Natarajan, P., Subramaniam, S. V., & Peruncheralathan, S. (2024). Organocatalytic Dearomatization of 5-Aminopyrazoles: Synthesis of 4-Hydroxypyrazolines. *The Journal of Organic Chemistry*, *89*(14), 10258–10271. https://doi.org/10.1021/acs.joc.4c01160

Nkpaa, K. W., Owoeye, O., Amadi, B. A., Adedara, I. A., Abolaji, A. O., Wegwu, M. O., & Farombi, E. O. (2021). Ethanol exacerbates manganese-induced oxidative/nitrosative stress, pro-inflammatory cytokines, nuclear factor-κB activation, and apoptosis induction in rat cerebellar cortex. *Journal of Biochemical and Molecular Toxicology*, *35*(3). https://doi.org/10.1002/jbt.22681

Obushak, N. D., Matiichuk, V. S., Vasylyshin, R. Ya., & Ostapyuk, Yu. V. (2004). Heterocyclic Syntheses on the Basis of Arylation Products of Unsaturated Compounds: X. 3-Aryl-2-chloropropanals as Reagents for the Synthesis of 2-Amino-1,3-thiazole Derivatives. *Russian Journal of Organic Chemistry*, *40*(3), 383–389. https://doi.org/10.1023/B:RUJO.0000034976.75646.85

Osmaniye, D., Evren, A. E., Sağlık, B. N., Levent, S., Özkay, Y., & Kaplancıklı, Z. A. (2022). Design, synthesis, biological activity, molecular docking, and molecular dynamics of novel benzimidazole derivatives as potential AChE/MAO-B dual inhibitors. *Archiv Der Pharmazie*, *355*(3). https://doi.org/10.1002/ardp.202100450

Parthasarathy, A., Borrego, E. J., Savka, M. A., Dobson, R. C. J., & Hudson, A. O. (2021). Amino acid–derived defense metabolites from plants: A potential source to facilitate novel antimicrobial development. *Journal of Biological Chemistry*, *296*, 100438. https://doi.org/10.1016/j.jbc.2021.100438

Pendiukh, V., Yakovleva, H., Stadniy, I., Pashenko, O., Volovenko, O., Rozhenko, A., Ryabukhin, S., & Volochnyuk, D. (2024). *Harnessing Diazoketones for the Efficient Synthesis of 2,4-Disubstituted-(1,3)Thiazoles: Scalable and Versatile Approach to Important Heterocyclic Scaffolds*. https://doi.org/10.26434/chemrxiv-2024-r2knw

Pérez-Sánchez, H., den Haan, H., Pérez-Garrido, A., Peña-García, J., Chakraborty, S., Erdogan Orhan, I., Senol Deniz, F. S., & Villalgordo, J. M. (2021). Combined Structure and Ligand-Based Design of Selective Acetylcholinesterase Inhibitors. *Journal of Chemical Information and Modeling*, *61*(1), 467–480. https://doi.org/10.1021/acs.jcim.0c00463

Pettersen, E. F., Goddard, T. D., Huang, C. C., Couch, G. S., Greenblatt, D. M., Meng, E. C., & Ferrin, T. E. (2004). UCSF Chimera—A visualization system for exploratory research and analysis. *Journal of Computational Chemistry*, *25*(13), 1605–1612. https://doi.org/10.1002/jcc.20084

Pinzi, L., & Rastelli, G. (2019). Molecular Docking: Shifting Paradigms in Drug Discovery. *International Journal of Molecular Sciences*, *20*(18), 4331. https://doi.org/10.3390/ijms20184331

Reyadh, L., KhAhmed, A., Abachi, F., Abdu-Rahem, L. R., Kh Ahmad, A., & Abachi, F. T. (2021). Synthesis And Medicinal Attributes Of Thiazole Derivatives: A Review. In *Systematic Reviews in Pharmacy* (Vol. 12, Issue 1). https://www.researchgate.net/publication/348310059

Sadigova, S. E., Magerramov, A. M., Allakhverdiev, M. A., & Vekilova, T. M. (2004). Some Transformations of 2-Amino-4-phenyl-1,3-thiazole. *Russian Journal of Applied Chemistry*, *77*(5), 787–789. https://doi.org/10.1023/B:RJAC.0000038813.35580.37

Sağlık, B. N., Ilgın, S., & Özkay, Y. (2016). Synthesis of new donepezil analogues and investigation of their effects on cholinesterase enzymes. *European Journal of Medicinal Chemistry*, *124*, 1026–1040. https://doi.org/10.1016/j.ejmech.2016.10.042

Schaffel, R., Nucci, M., Portugal, R., Castro, M. B., Ferreira, S. B., Almeida, L., Spector, N., & Pulcheri, W. (2000). Thiabendazole for the Treatment of Strongyloidiasis in Patients with Hematologic Malignancies. *Clinical Infectious Diseases*, *31*(3), 821–822. https://doi.org/10.1086/314023

Şener, N., Erişkin, S., Yavuz, S., & Şener, İ. (2017). Synthesis, Characterization, Solvatochromic Properties, and Antimicrobial-radical Scavenging Activities of New Diazo Dyes Derived from Pyrazolo[1,5-a]pyrimidine. *Journal of Heterocyclic Chemistry*, *54*(6), 3538–3548. https://doi.org/10.1002/jhet.2977

Sharma, S., Devgun, M., Narang, R., Lal, S., & Rana, A. C. (2022). Thiazoles: A Retrospective Study on Synthesis, Structure-activity Relationship and Therapeutic Significance. *Indian Journal of Pharmaceutical Education and Research*, *56*(3), 646–666. https://doi.org/10.5530/ijper.56.3.113

Shen, S.-S., Lei, M.-Y., Wong, Y.-X., Tong, M.-L., Teo, P. L.-Y., Chiba, S., & Narasaka, K. (2009). Intramolecular nucleophilic substitution at an sp2 carbon: synthesis of substituted thiazoles and imidazole-2-thiones. *Tetrahedron Letters*, *50*(26), 3161–3163. https://doi.org/10.1016/j.tetlet.2008.12.118

Shih, J. C., Chen, K., & Ridd, M. J. (1999). MONOAMINE OXIDASE: From Genes to Behavior. *Annual Review of Neuroscience*, *22*(1), 197–217. https://doi.org/10.1146/annurev.neuro.22.1.197

Siddiqui, N., Arshad, M. F., Ahsan, W., & Alam, M. S. (2009). THIAZOLES: A VALUABLE INSIGHT INTO THE RECENT ADVANCES AND BIOLOGICAL ACTIVITIES.

International Journal of Pharmaceutical Sciences and Drug Research, 136–143. https://doi.org/10.25004/IJPSDR.2009.010302

Singh, K. R., Santhosh, C., Sheela, K., & Sadashiva, M. P. (2024). Regioselective Synthesis of 2,4- and 2,5-Disubstituted 1,3-Thiazoles from 2-Oxo-2-(amino)ethanedithioates via Base-Catalyzed Cyclization. *Synthesis*, *56*(05), 878–886. https://doi.org/10.1055/a-2210-6357

Taghizadeh, M. S., Niazi, A., Moghadam, A., & Afsharifar, A. (2022). Experimental, molecular docking and molecular dynamic studies of natural products targeting overexpressed receptors in breast cancer. *PLOS ONE*, *17*(5), e0267961. https://doi.org/10.1371/journal.pone.0267961

Tang, X., Yang, J., Zhu, Z., Zheng, M., Wu, W., & Jiang, H. (2016). Access to Thiazole via Copper-Catalyzed [3+1+1]-Type Condensation Reaction under Redox-Neutral Conditions. *The Journal of Organic Chemistry*, *81*(22), 11461–11466. https://doi.org/10.1021/acs.joc.6b02124

Tomassetti, M., Lupidi, G., Gabrielli, S., Rossi, F. V., Lillini, S., Bianchini, G., Aramini, A., Canestrari, D., & Marcantoni, E. (2021). The Appropriate Acyclic Precursors to Build Biologically Active 5-acylamino-1,3-thiazoles. In *Current Advances in Chemistry and Biochemistry Vol. 8* (pp. 40–56). Book Publisher International (a part of SCIENCEDOMAIN International). https://doi.org/10.9734/bpi/cacb/v8/9618D

Trott, O., & Olson, A. J. (2010). AutoDock Vina: Improving the speed and accuracy of docking with a new scoring function, efficient optimization, and multithreading. *Journal of Computational Chemistry*, *31*(2), 455–461. https://doi.org/10.1002/jcc.21334

Umar, B. A., Uzairu, A., Shallangwa, G. A., & Uba, S. (2019). RATIONAL DRUG DESIGN OF POTENT V600E-BRAF KINASE INHIBITORS THROUGH MOLECULAR DOCKING SIMULATION. *The Journal of Engineering and Exact Sciences*, *5*(5), 0469–0481. https://doi.org/10.18540/jcecvl5iss5pp0469-0481

Walter, A., Chaikuad, A., Loaëc, N., Preu, L., Knapp, S., Meijer, L., Kunick, C., & Koch, O. (2017). Identification of CLK1 Inhibitors by a Fragment–linking Based Virtual Screening. *Molecular Informatics*, *36*(4). https://doi.org/10.1002/minf.201600123

Wang, X., Qiu, X., Wei, J., Liu, J., Song, S., Wang, W., & Jiao, N. (2018). Cu-Catalyzed Aerobic Oxidative Sulfuration/Annulation Approach to Thiazoles via Multiple Csp 3 –H Bond Cleavage. *Organic Letters*, *20*(9), 2632–2636. https://doi.org/10.1021/acs.orglett.8b00840

Watkins, J. C., & Jane, D. E. (2006). The glutamate story. *British Journal of Pharmacology*, *147*(S1). https://doi.org/10.1038/sj.bjp.0706444

Wibowo, J. P., Xiao, Z., Voet, J. M., Dekker, F. J., & Quax, W. J. (2020). Development of phenylthiourea derivatives as allosteric inhibitors of pyoverdine maturation enzyme PvdP tyrosinase. *Bioorganic & Medicinal Chemistry Letters*, *30*(17), 127409. https://doi.org/10.1016/j.bmcl.2020.127409

Ye, M., Han, B. H., Kim, J. S., Kim, K., & Shim, I. (2020). Neuroprotective Effect of Bean Phosphatidylserine on TMT-Induced Memory Deficits in a Rat Model. *International Journal of Molecular Sciences*, *21*(14), 4901. https://doi.org/10.3390/ijms21144901

Zhao, D., Liu, Y., Li, Y., & Chen, Y. (2022). A green synthesis and antibacterial activity of ferrocene-based thiazole derivatives in choline chloride/glycerol eutectic solvent. *RSC Advances*, *12*(34), 22054–22059. https://doi.org/10.1039/D2RA04587G

APPENDICES

APPENDIX 1 Molecular Docking Data

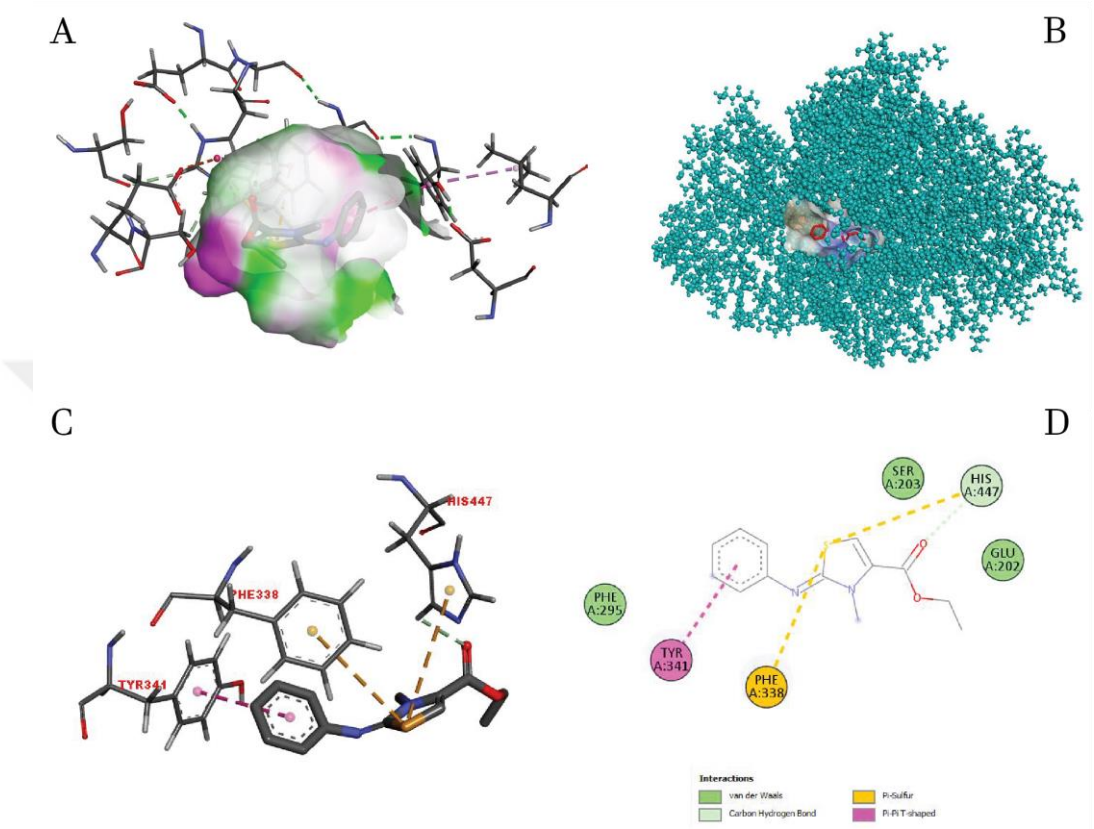

Figure 4.7 Molecular Docking of **21**

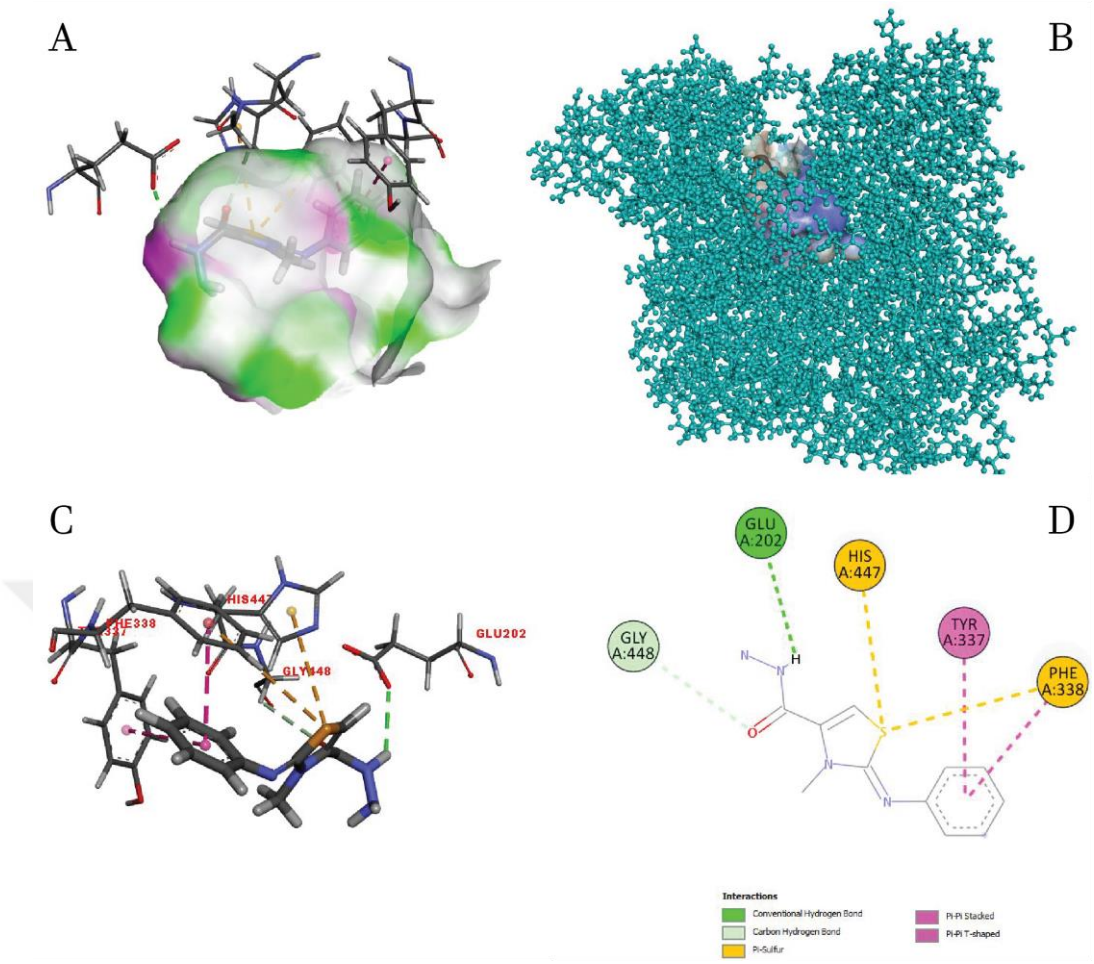

Figure 4.8 Molecular Docking of **23**

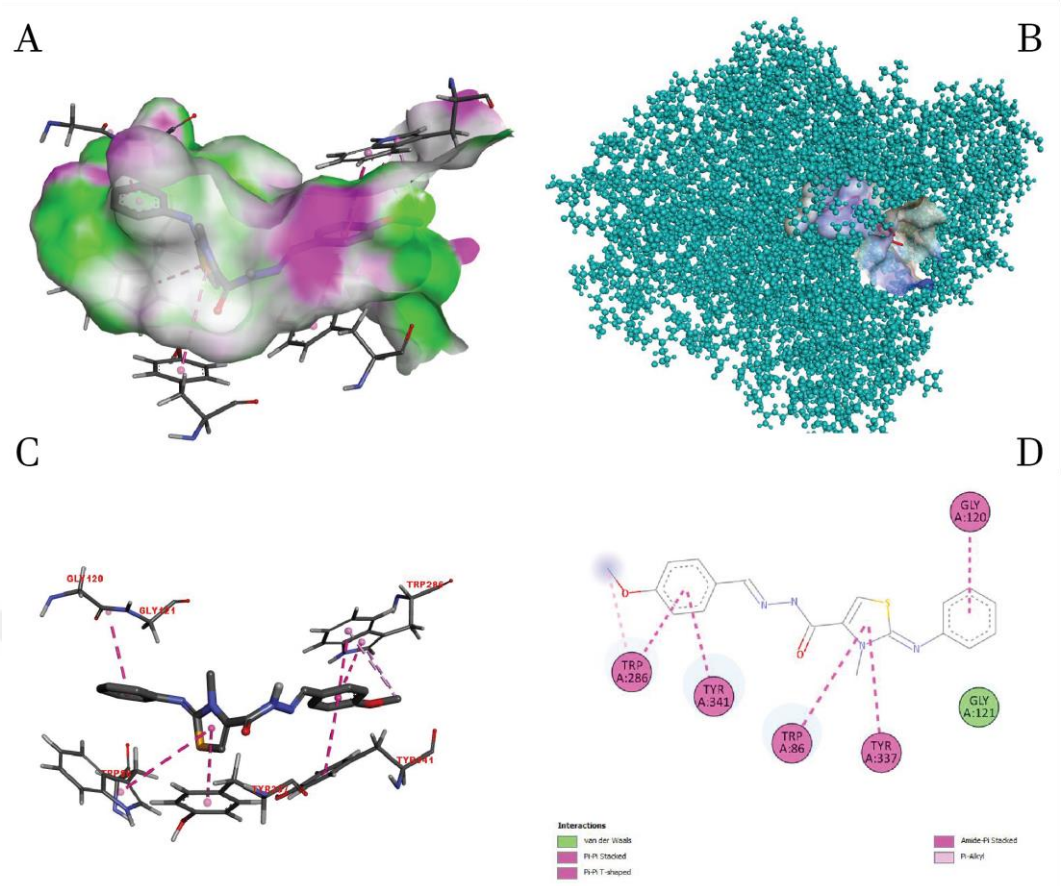

Figure 4.9 Molecular Docking of **24b**

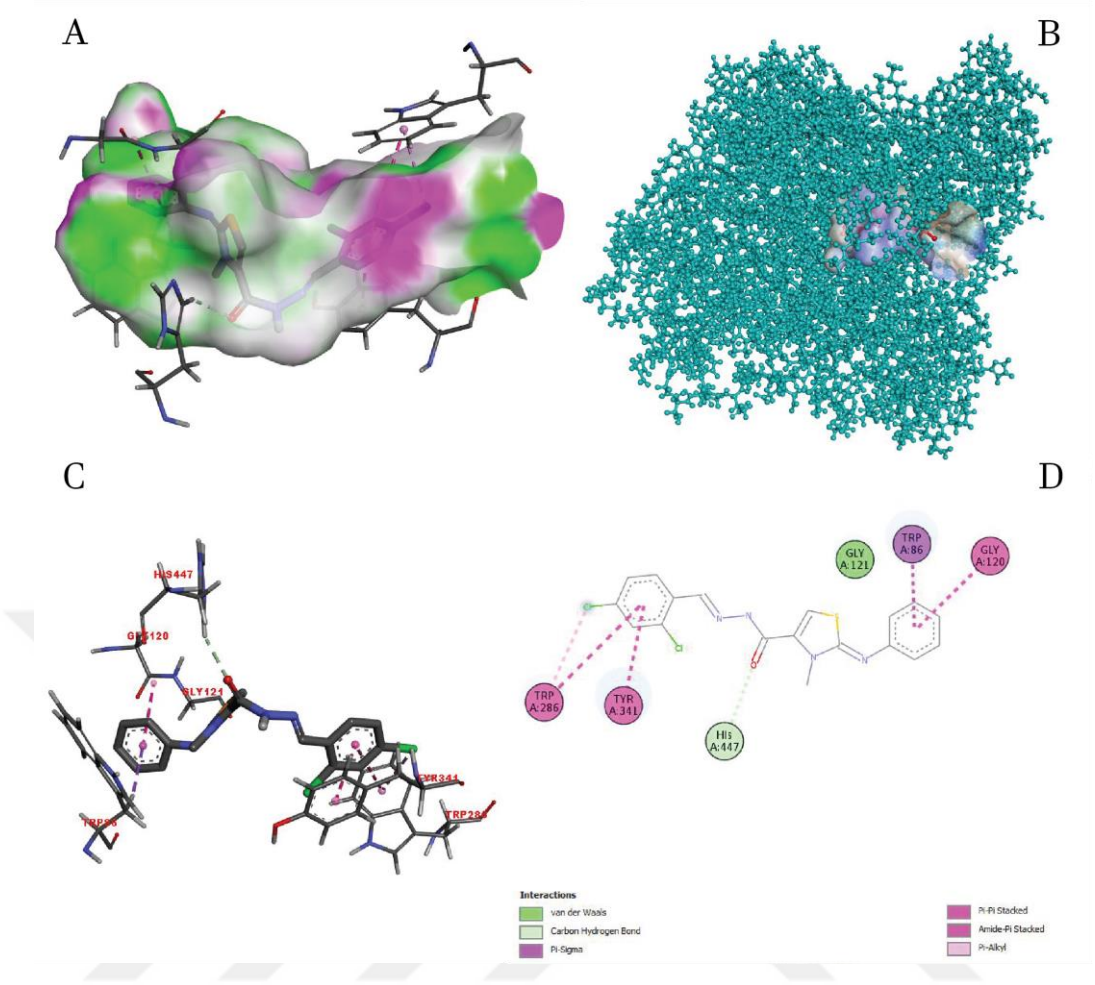

Figure 4.10 Molecular Docking of **24d**

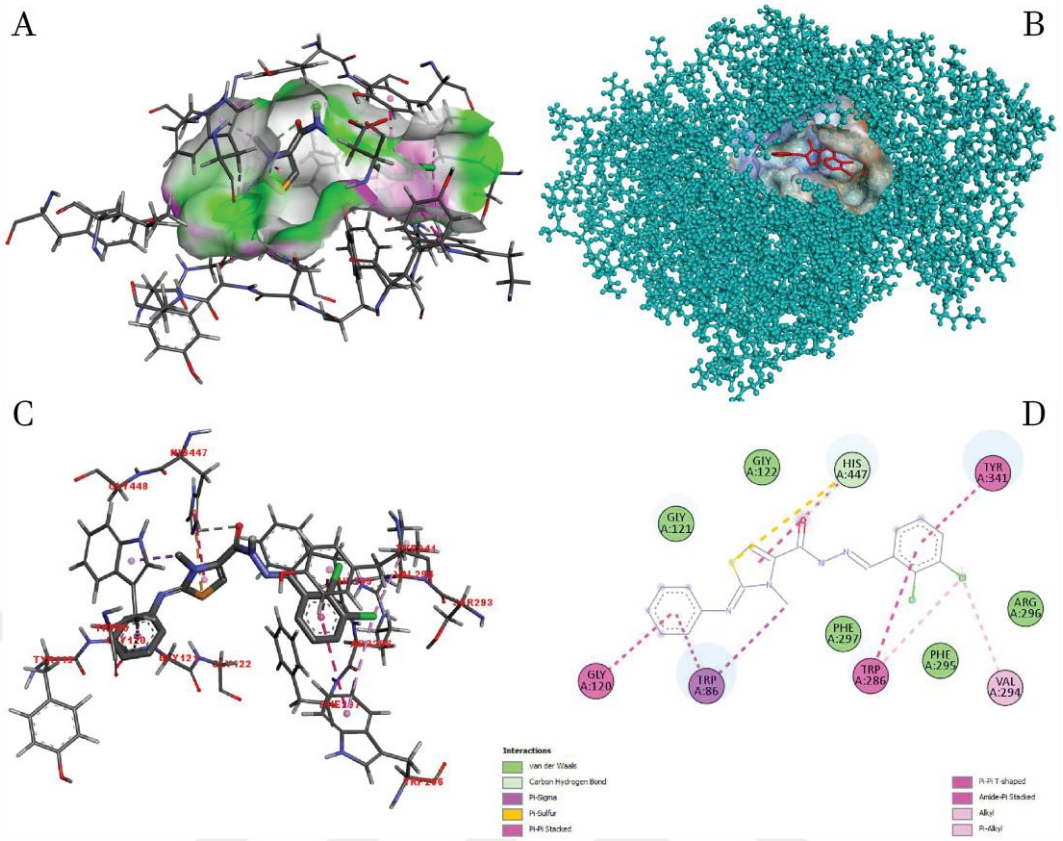

Figure 4.11 Molecular Docking of **24e**

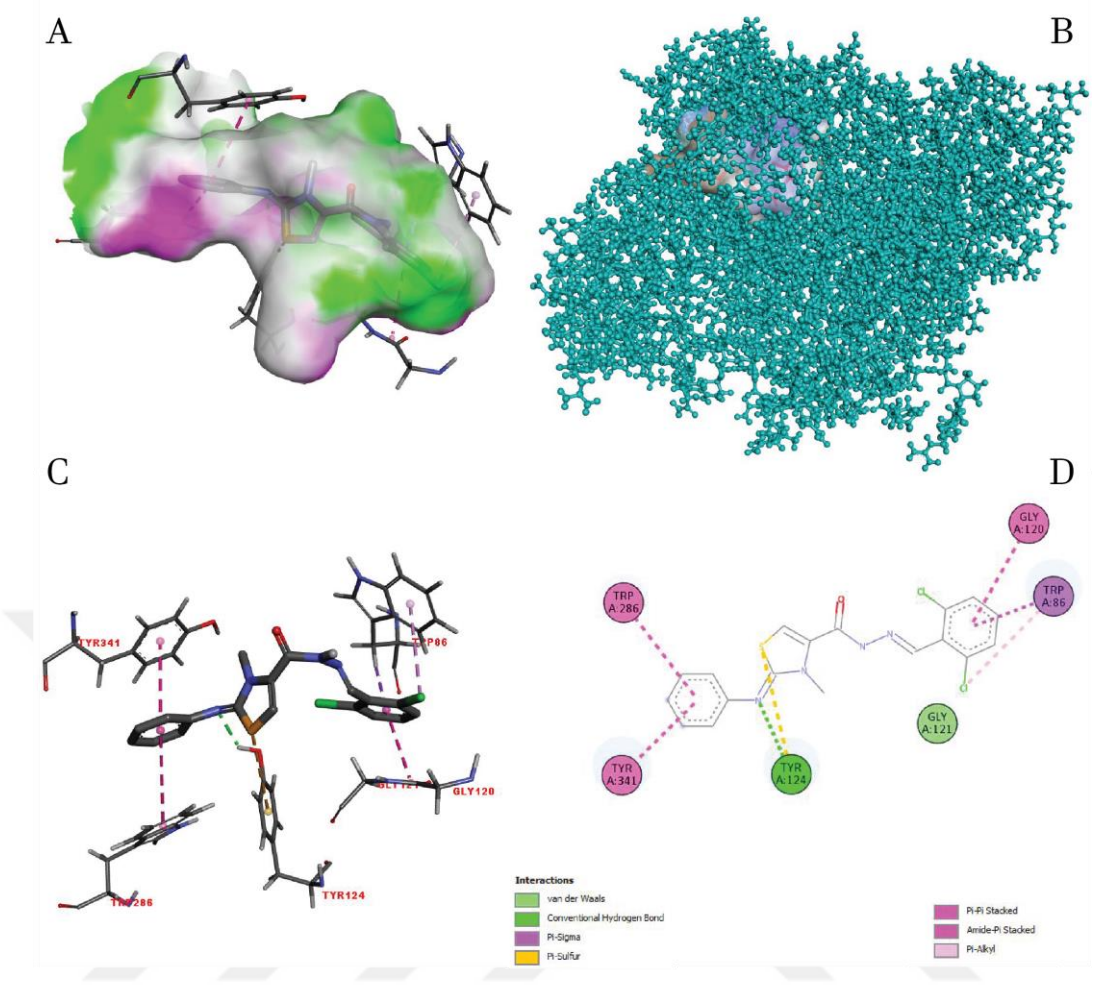

Figure 4.12 Molecular Docking of **24f**

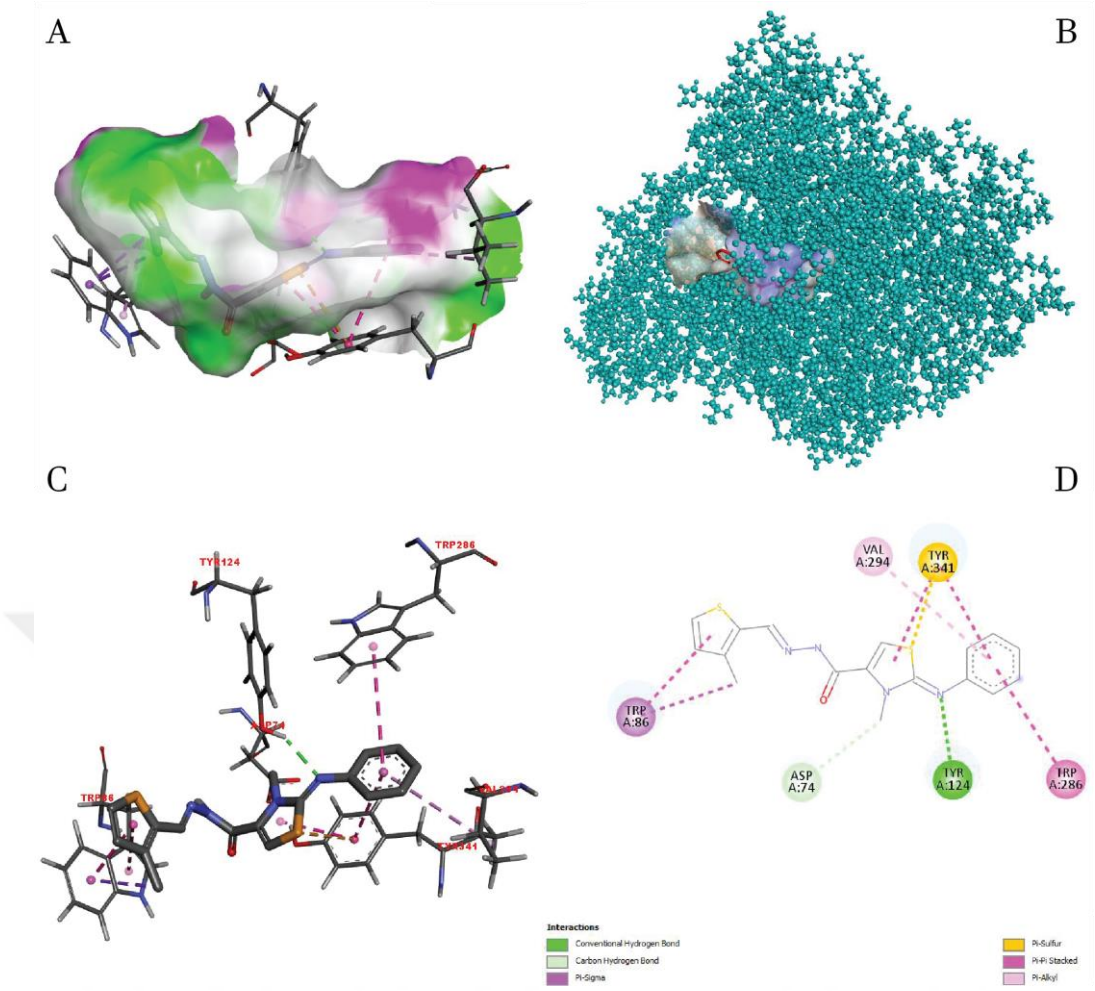

Figure 4.13 Molecular Docking of **24h**

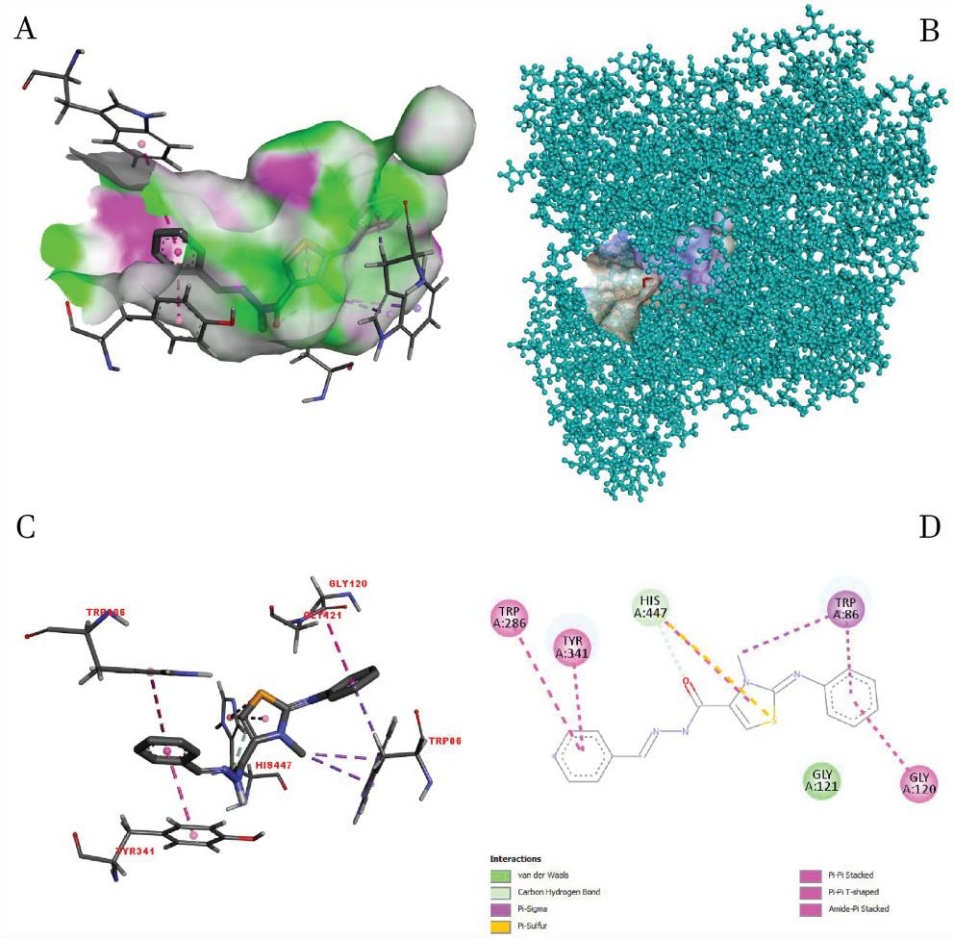

Figure 4.14 Molecular Docking of **24i**

APPENDIX 2 Spectrum Data

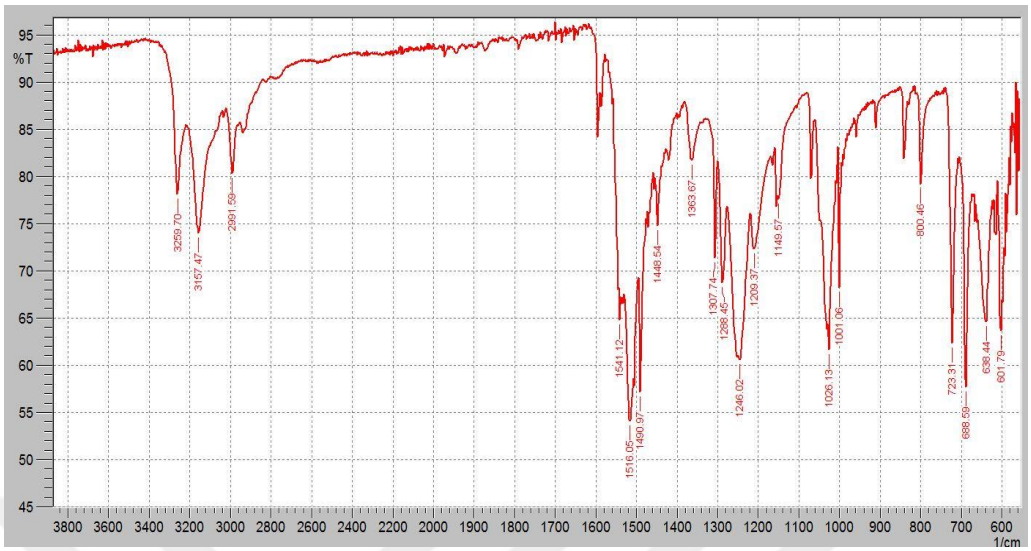

Figure 4.15 FT-IR of **19**

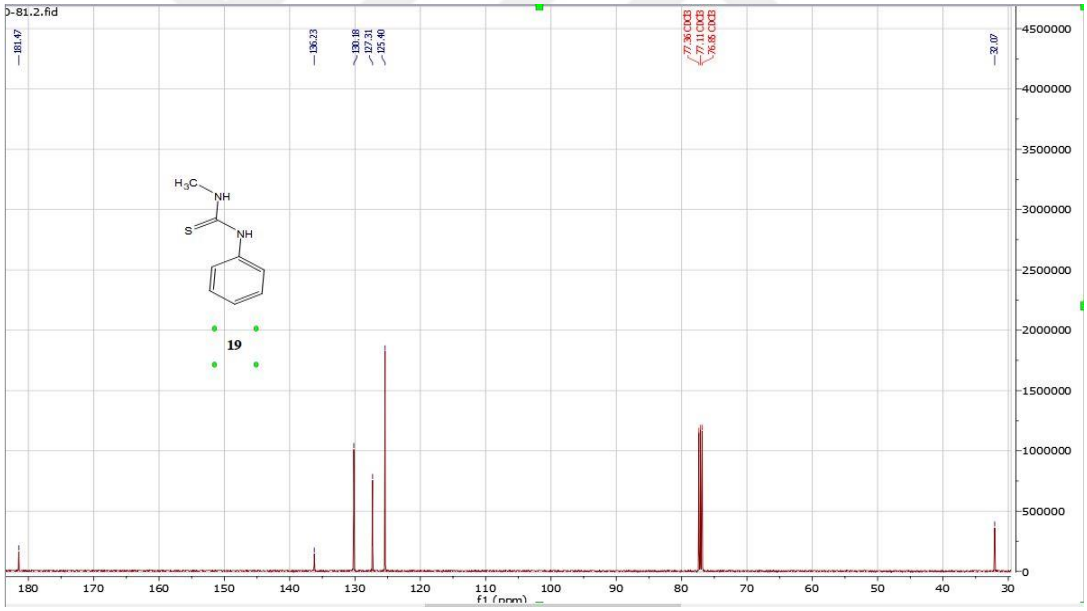

Figure 4.16 ^{13}C NMR of **19**

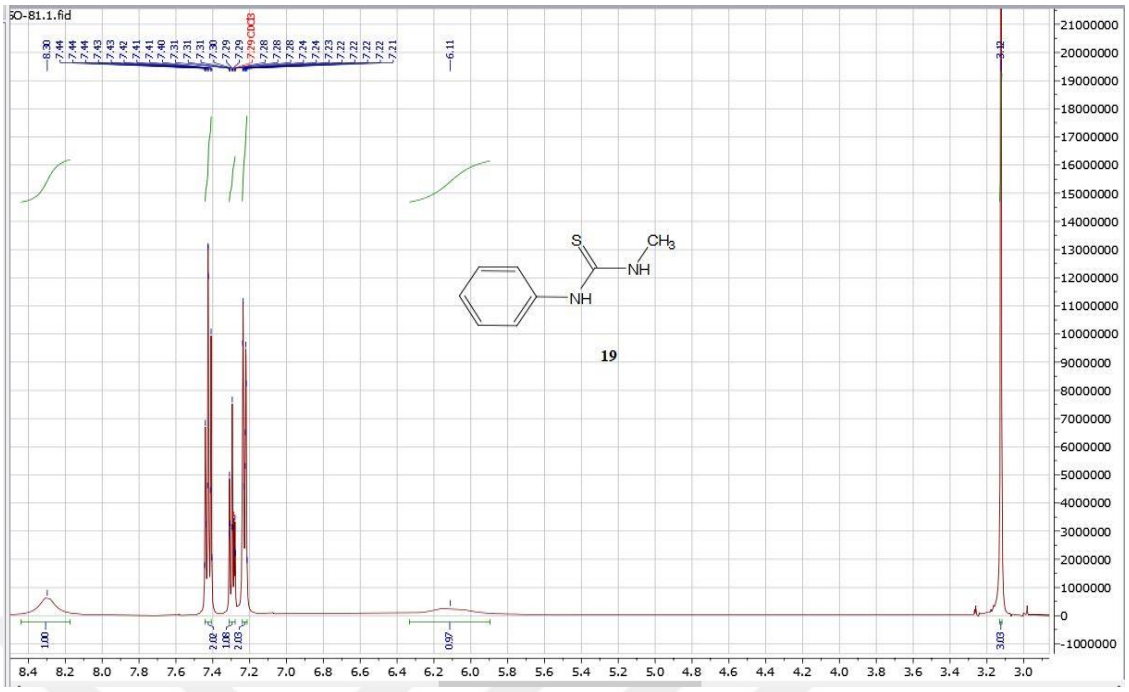

Figure 4.17 ^{1}H NMR of **19**

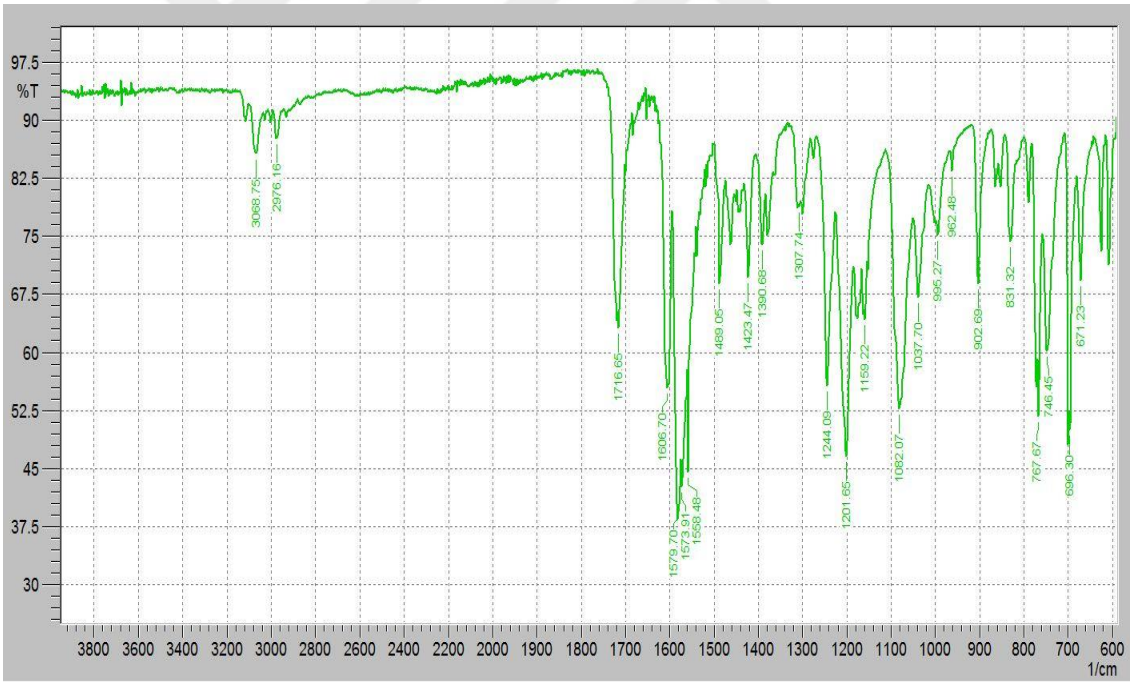

Figure 4.18 FT-IR of **21**

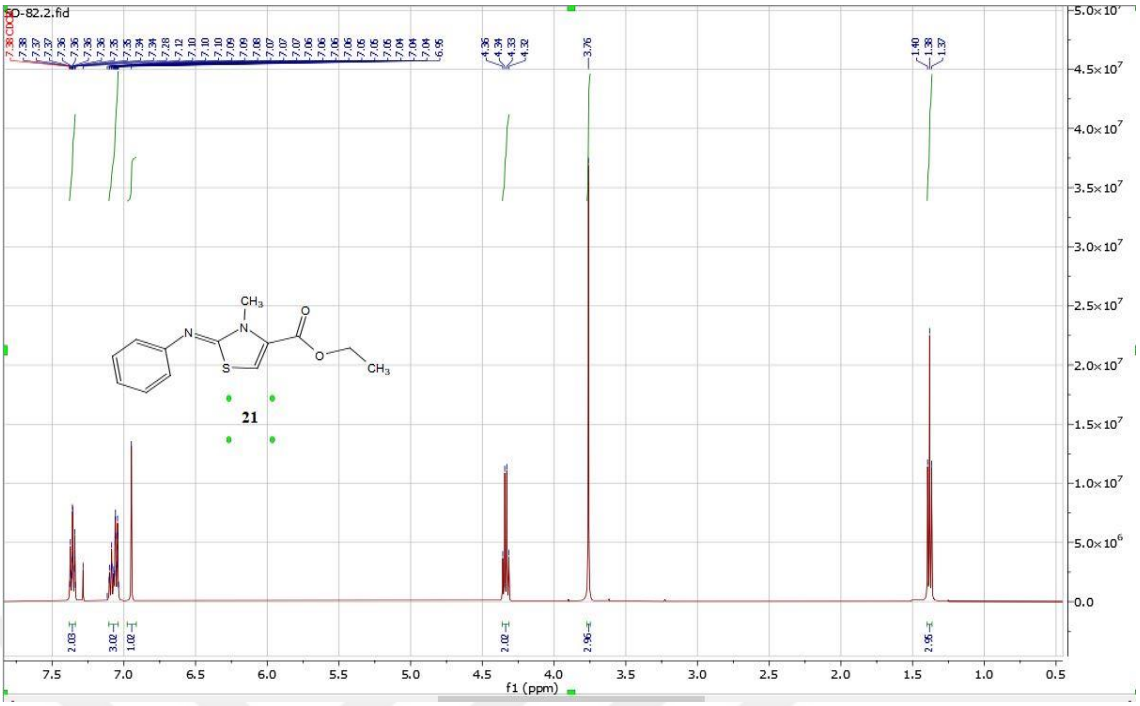

Figure 4.19 ^{1}H NMR of **21**

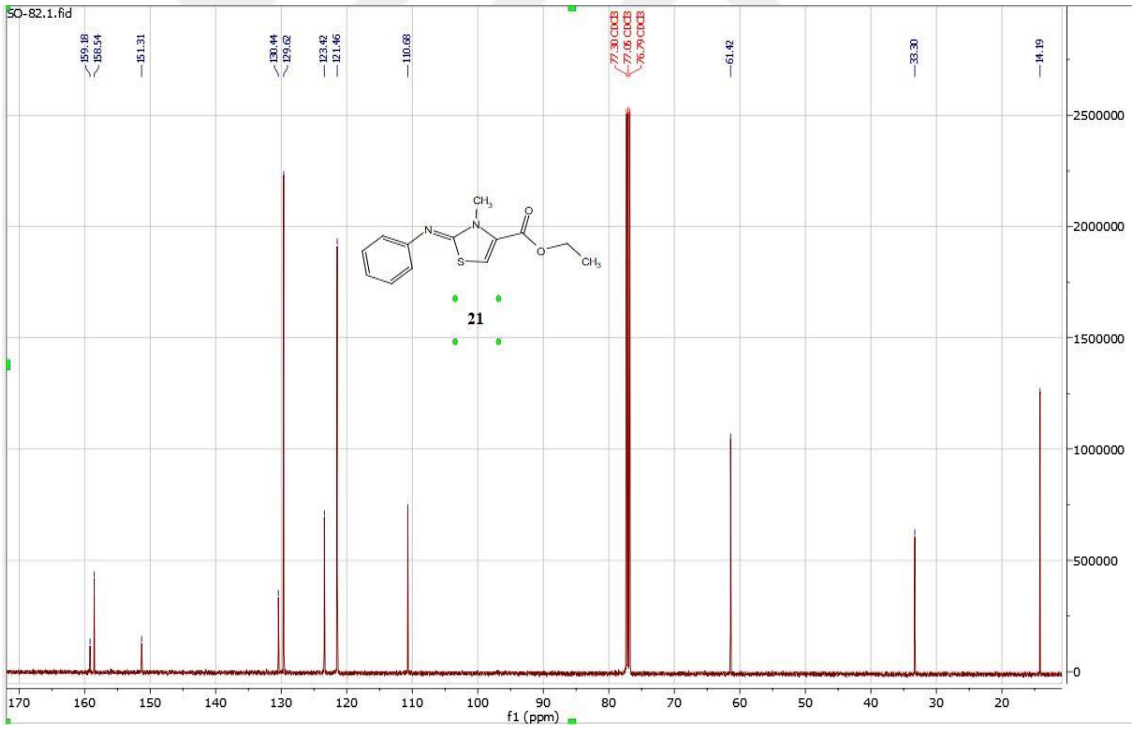

Figure 4.20 ^{13}C NMR of **21**

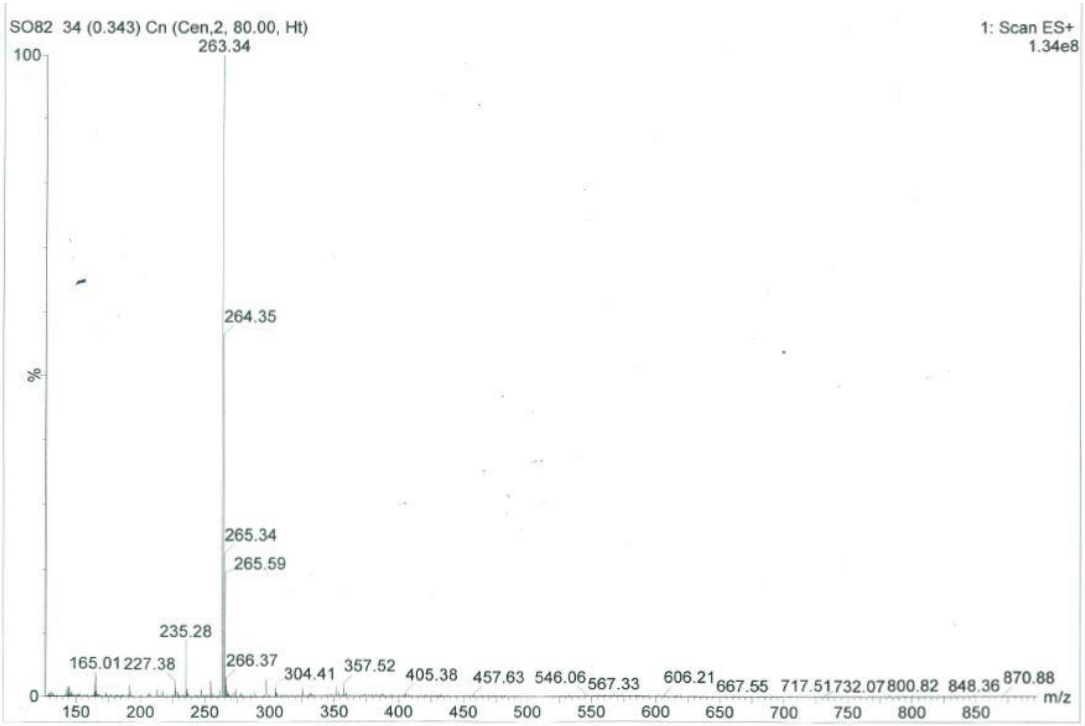

Figure 4.21 LC/MS of **21**

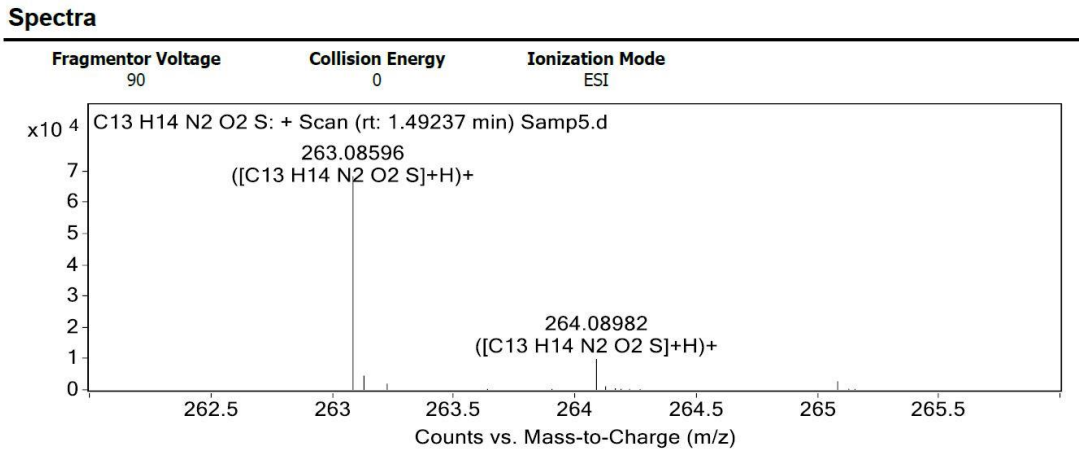

Figure 4.22 LC-QTOF-MS spectrum of compound **21**

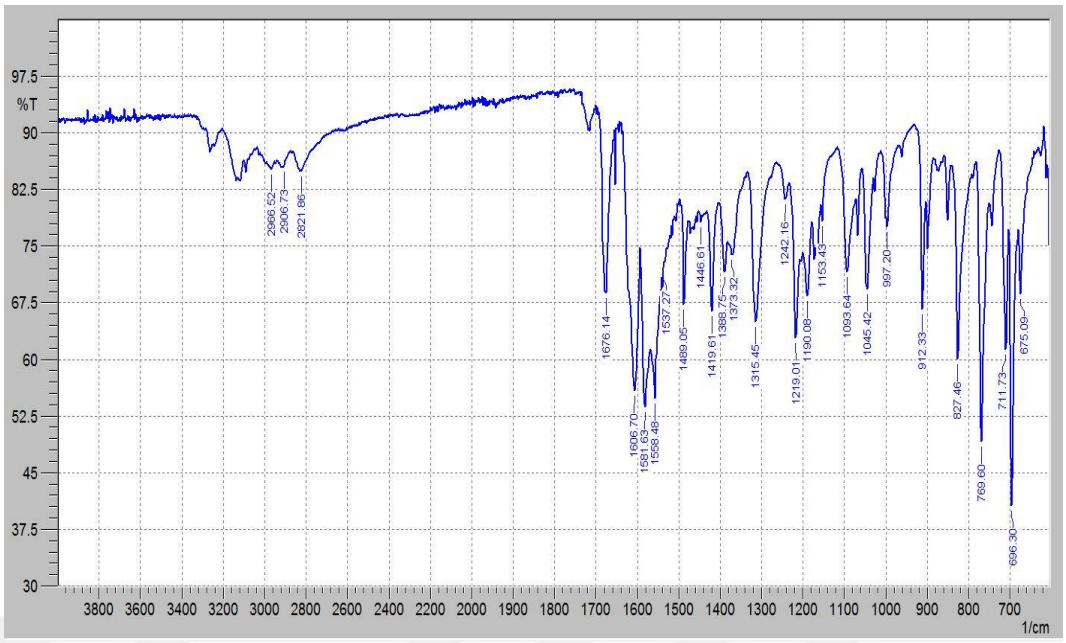

Figure 4.23 FT-IR of **23**

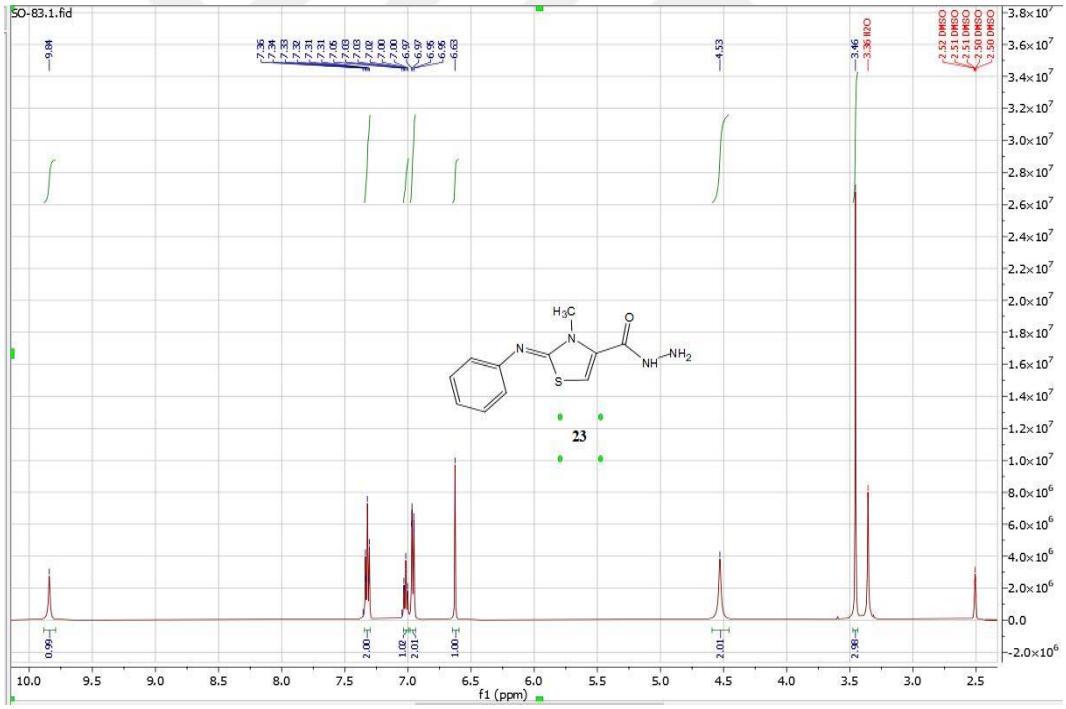

Figure 4.24 ^{1}H NMR of **23**

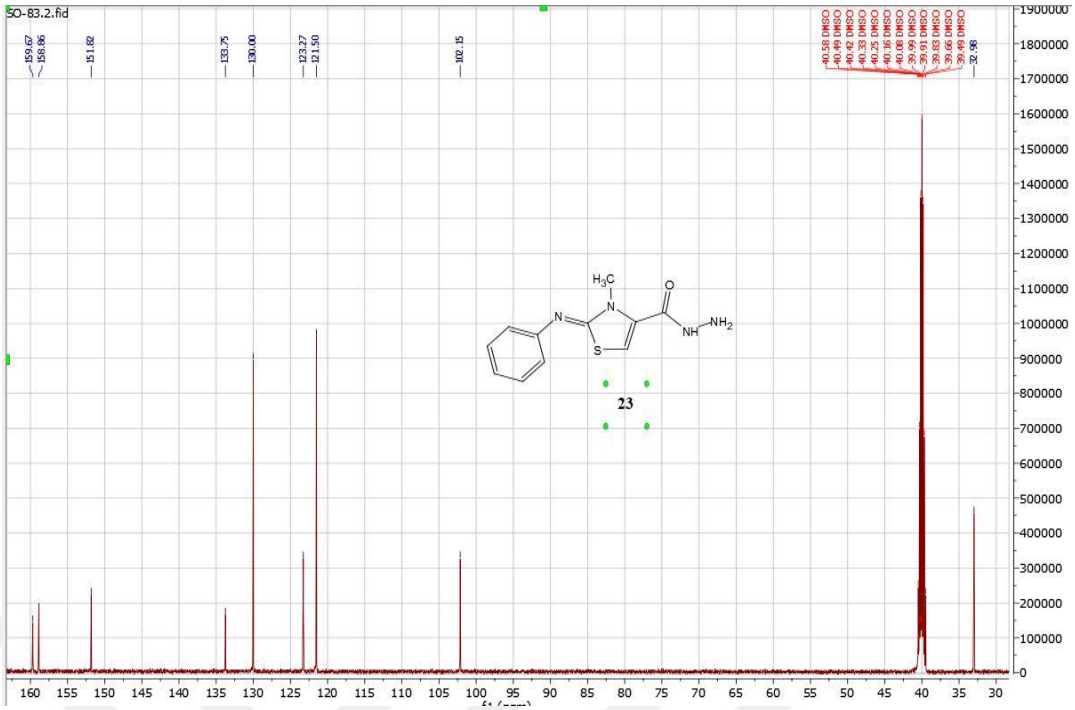

Figure 4.25 ^{13}C NMR of **23**

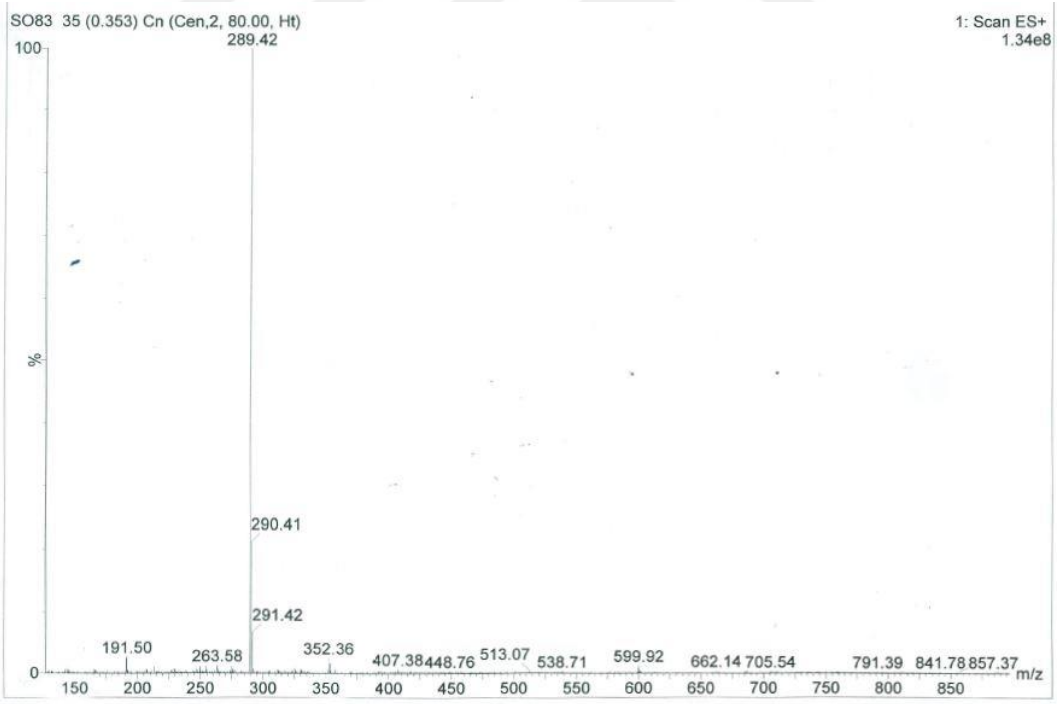

Figure 4.26 LC/MS of **23**

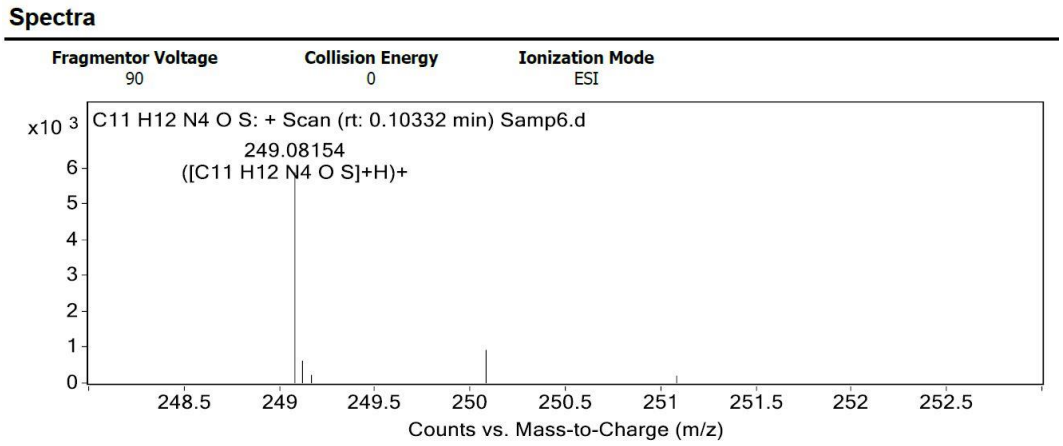

Figure 4.27 LC-QTOF-MS spectrum of compound **23**

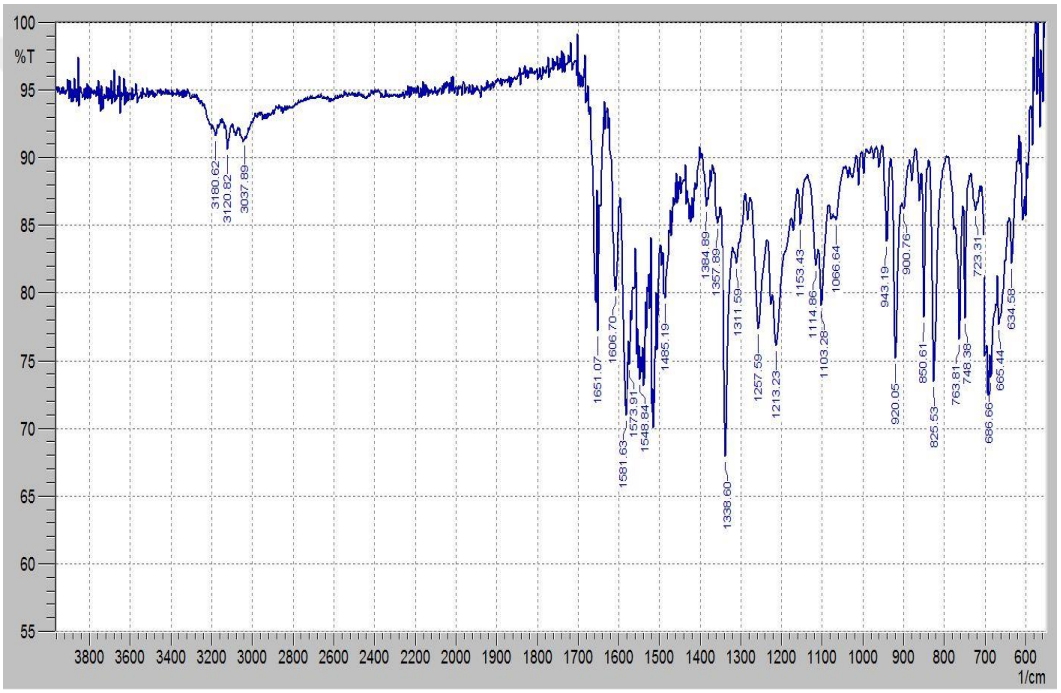

Figure 4.28 FT-IR of **24a**

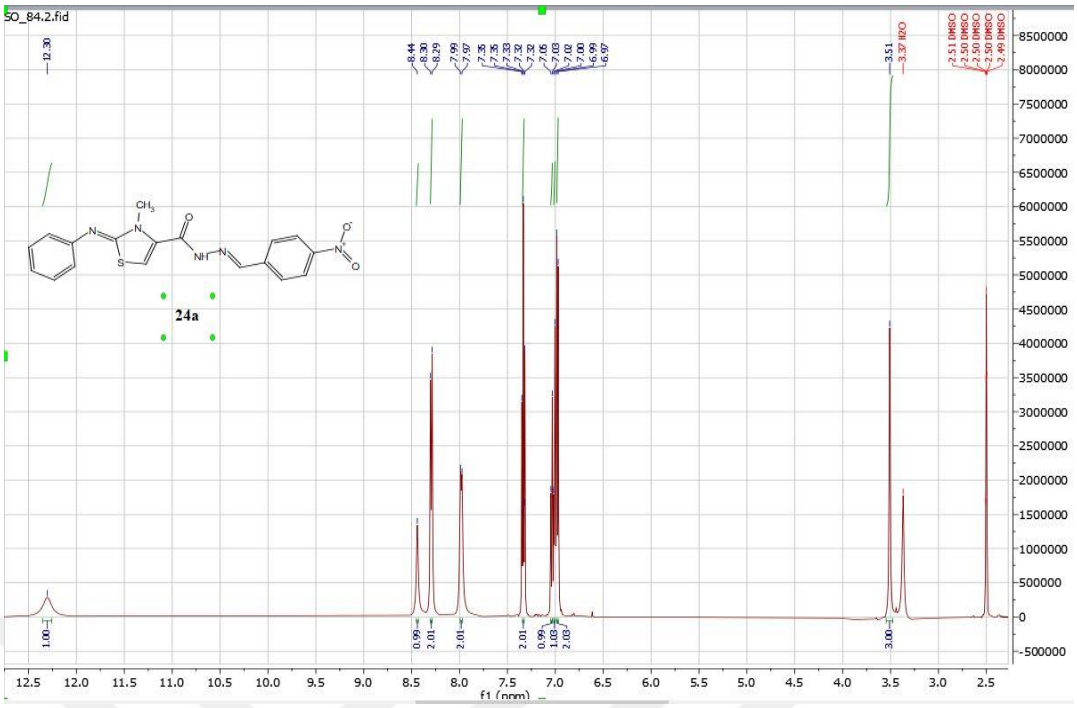

Figure 4.29 ^{1}H NMR of **24a**

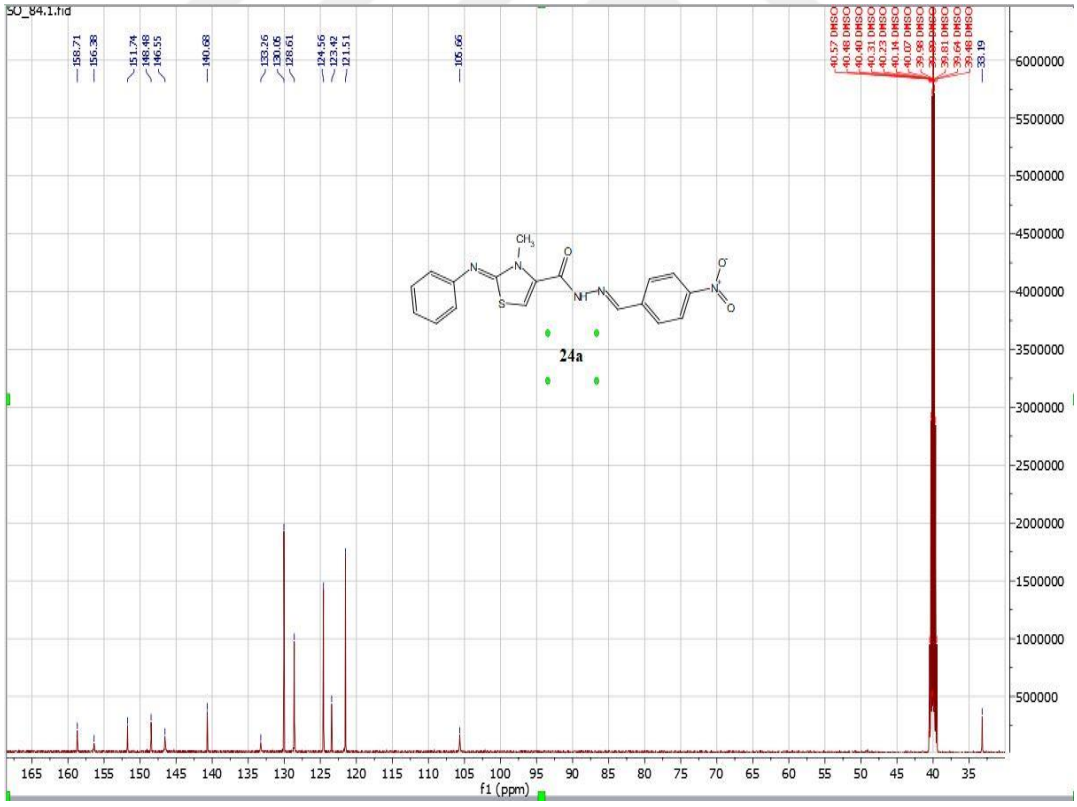

Figure 4.30 ^{13}C NMR of **24a**

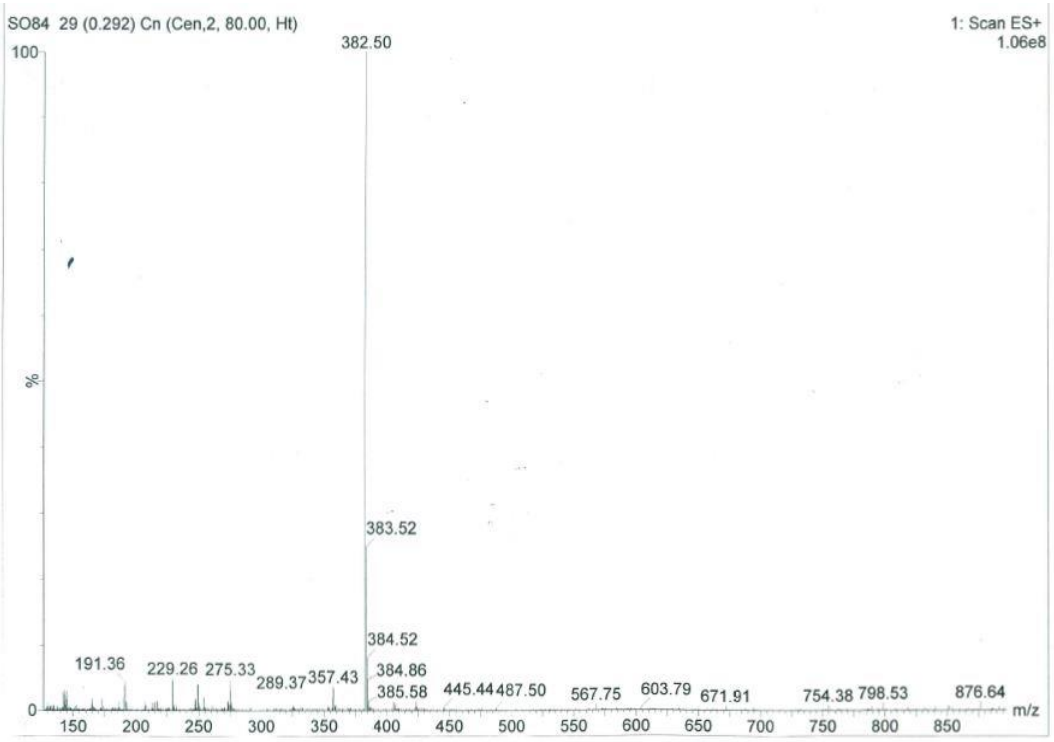

Figure 4.31 LC/MS of **24a**

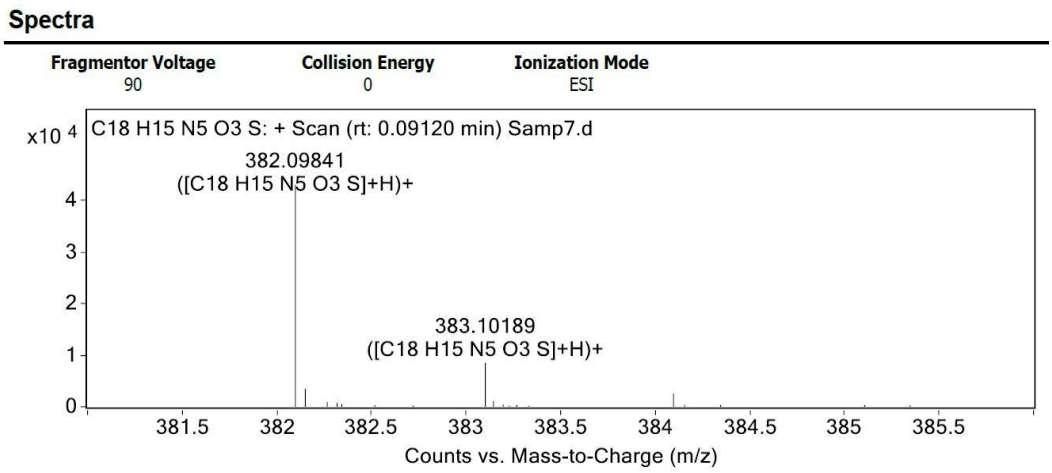

Figure 4.32 LC-QTOF-MS spectrum of compound **24a**

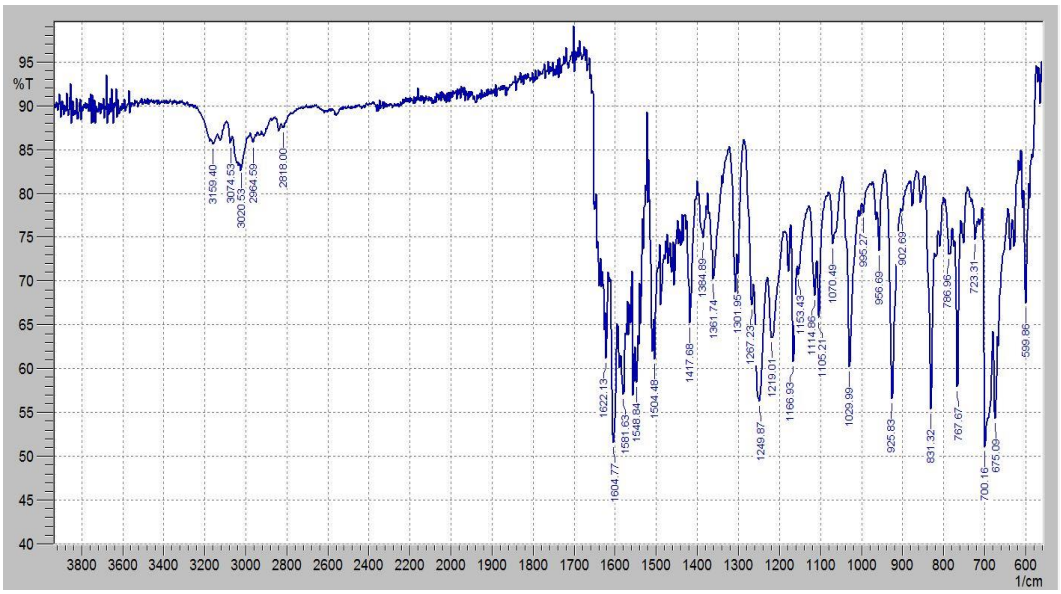

Figure 4.33 FT-IR of **24b**

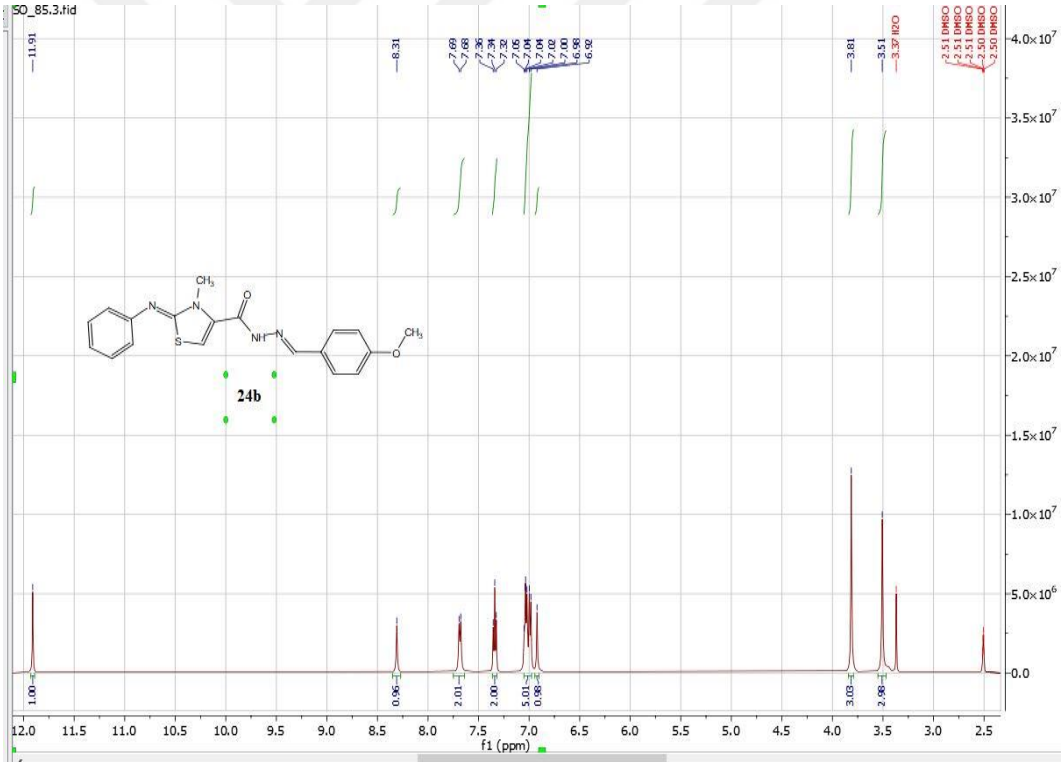

Figure 4.34 ^{1}H NMR of **24b**

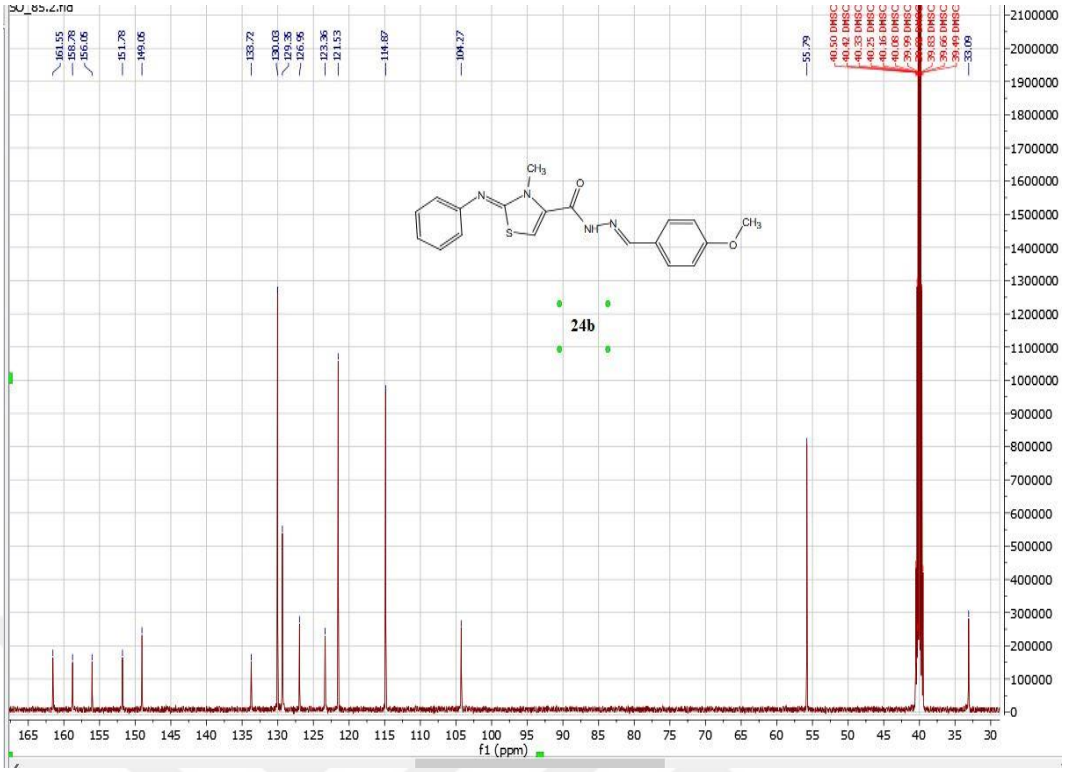

Figure 4.35 ^{13}C NMR of **24b**

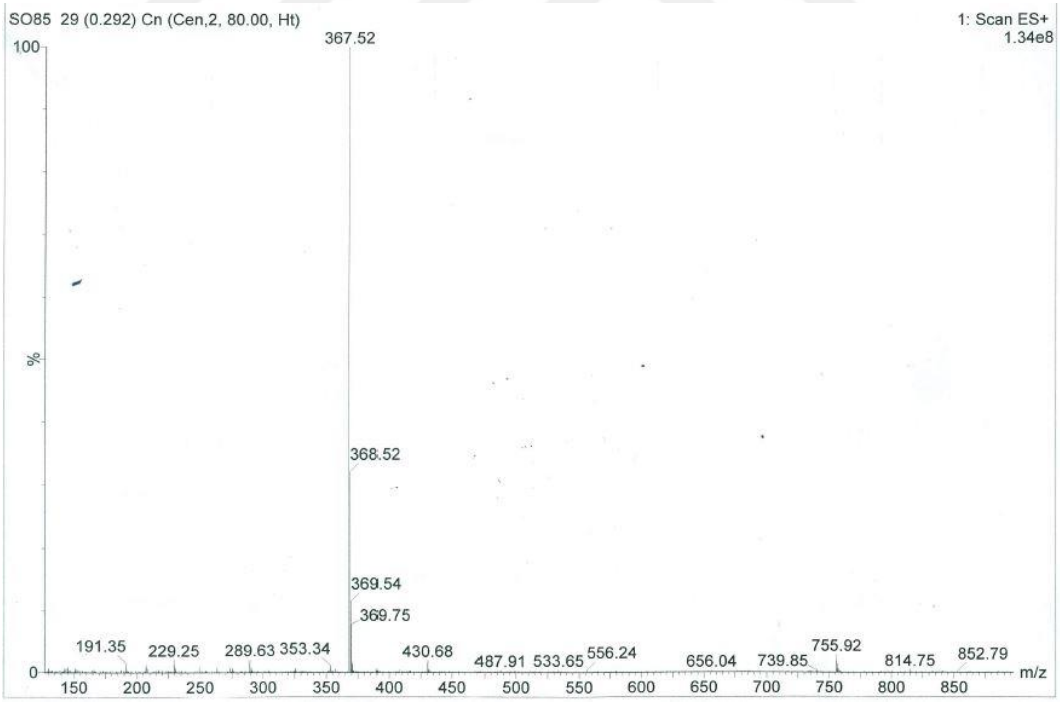

Figure 4.36 LC/MS of **24b**

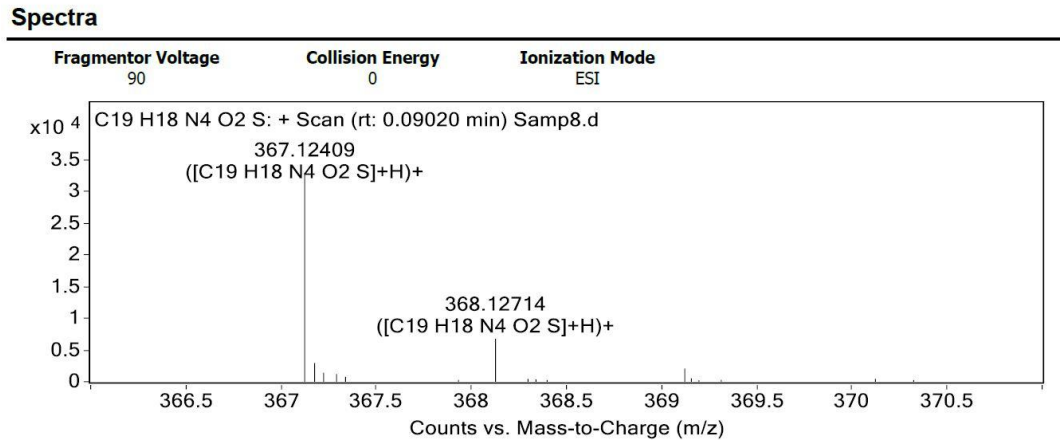

Figure 4.37 LC-QTOF-MS spectrum of compound **24b**

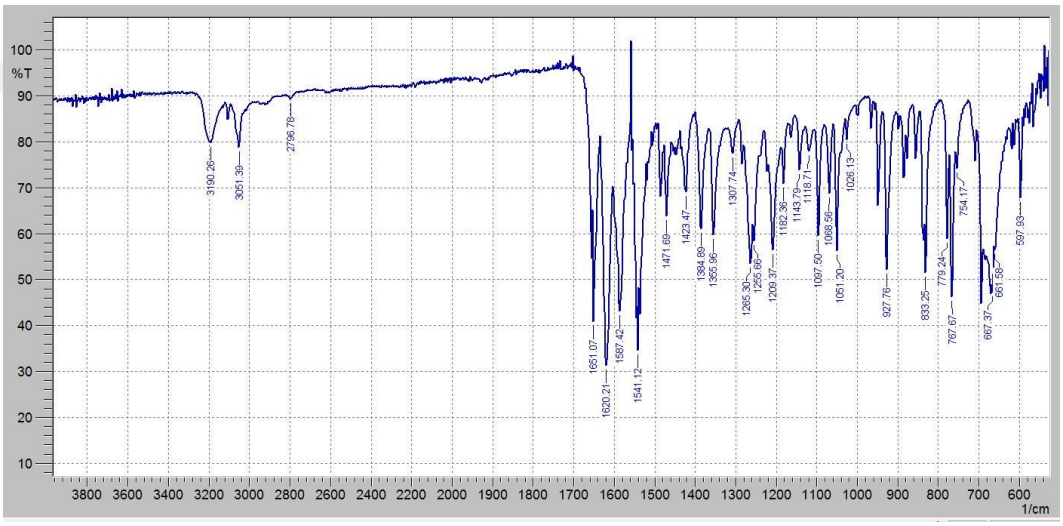

Figure 4.38 FT-IR of **24d**

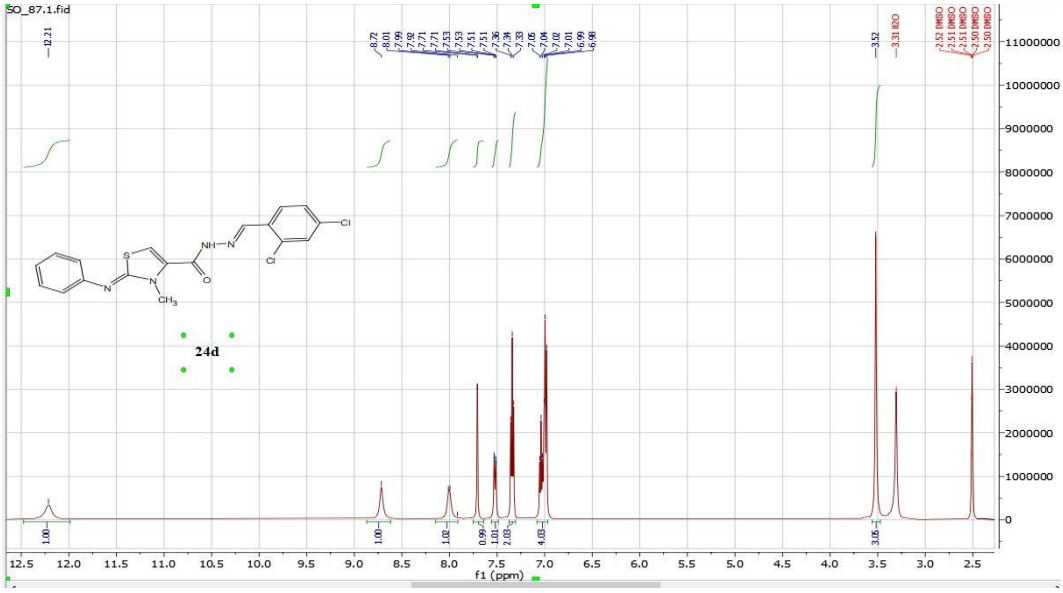

Figure 4.39 ^{1}H NMR of **24d**

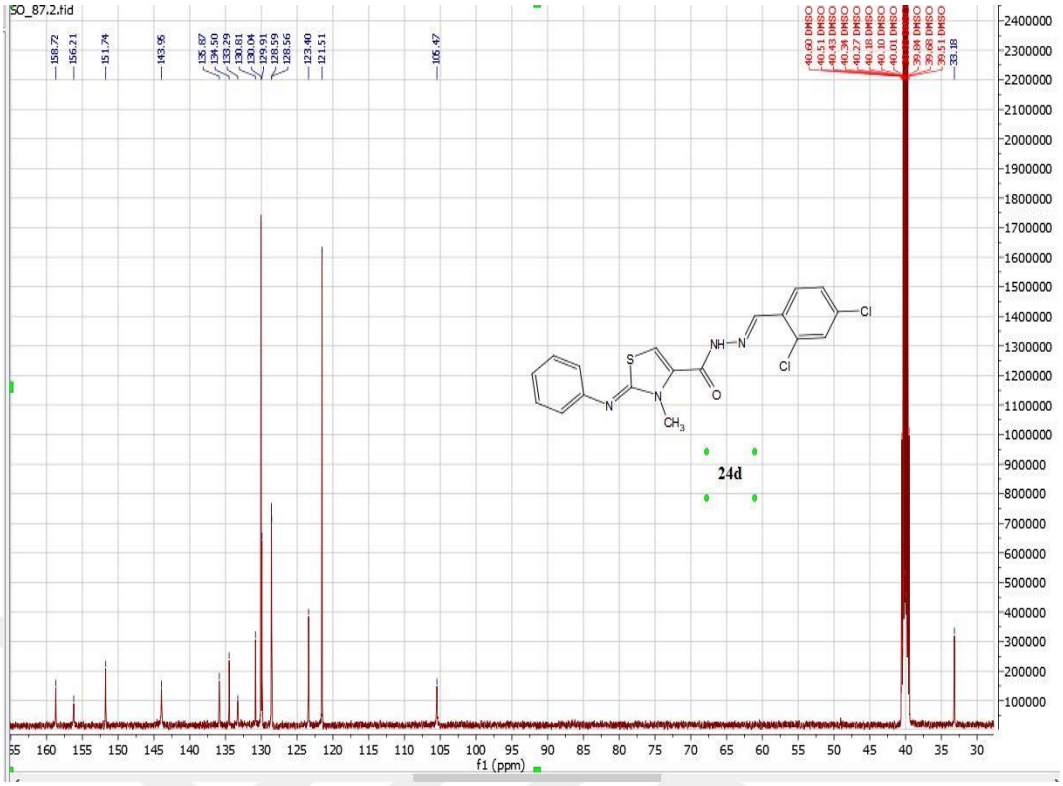

Figure 4.40 ^{13}C NMR of **24d**

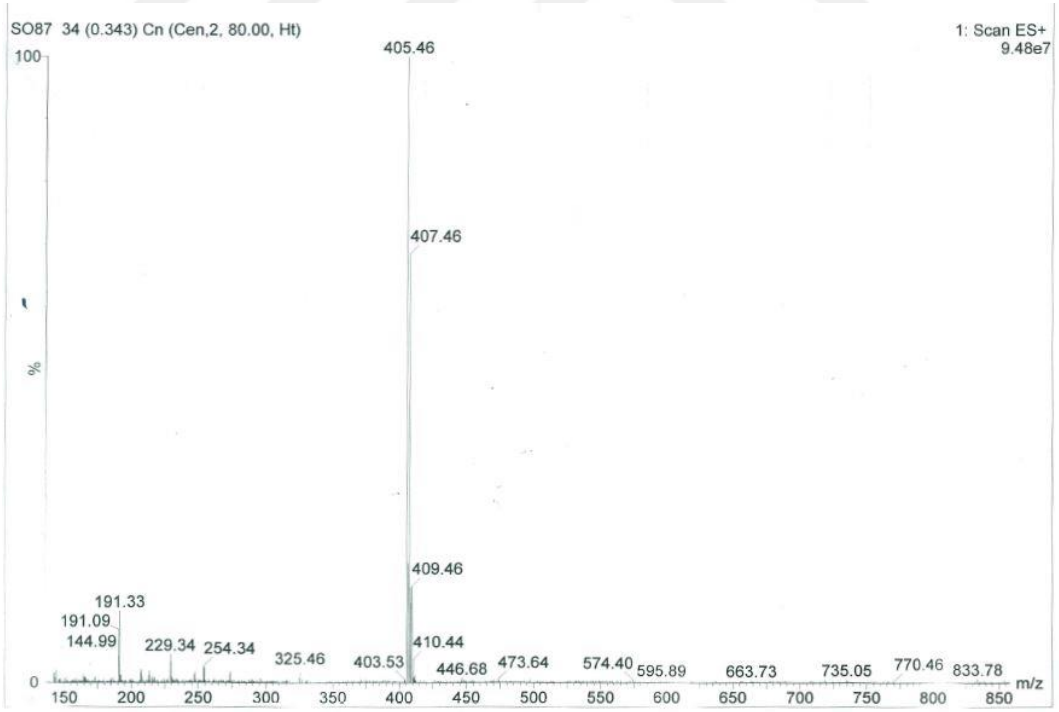

Figure 4.41 LC/MS of **24d**

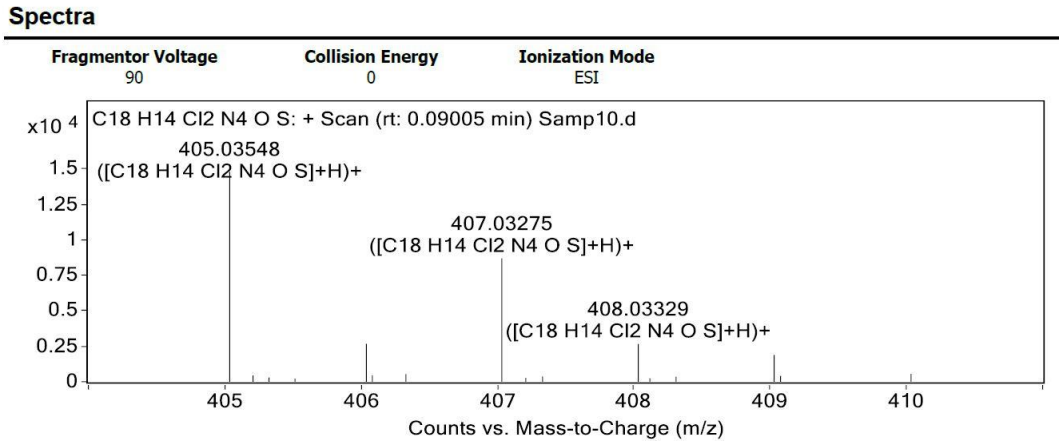

Figure 4.42 LC-QTOF-MS spectrum of compound **24d**

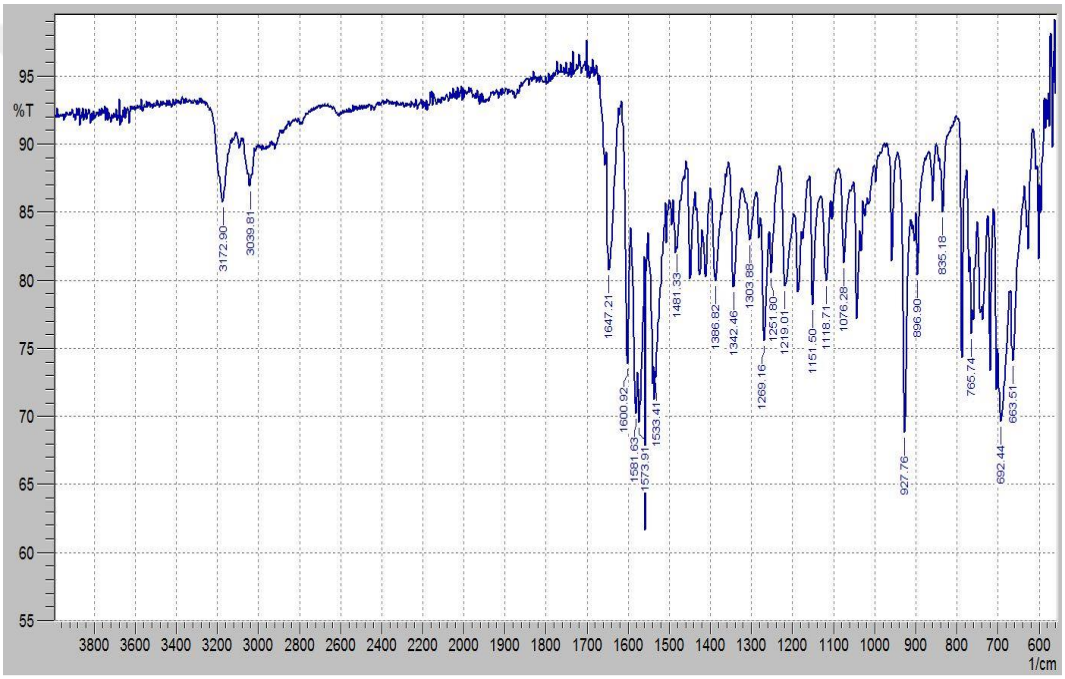

Figure 4.43 FT-IR of **24e**

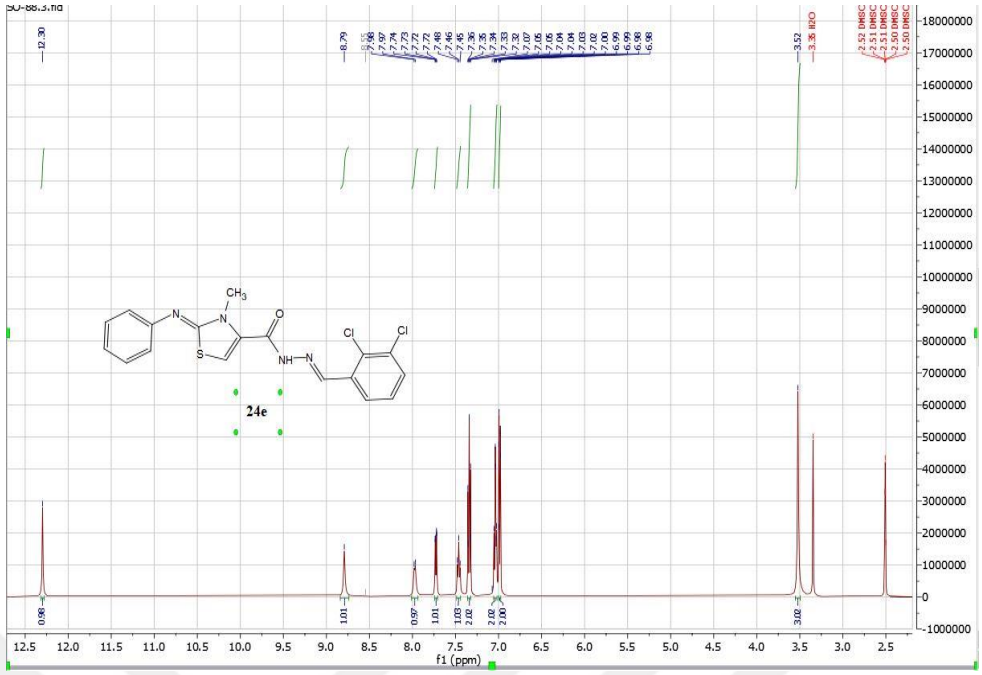

Figure 4.44 ^{1}H NMR of **24e**

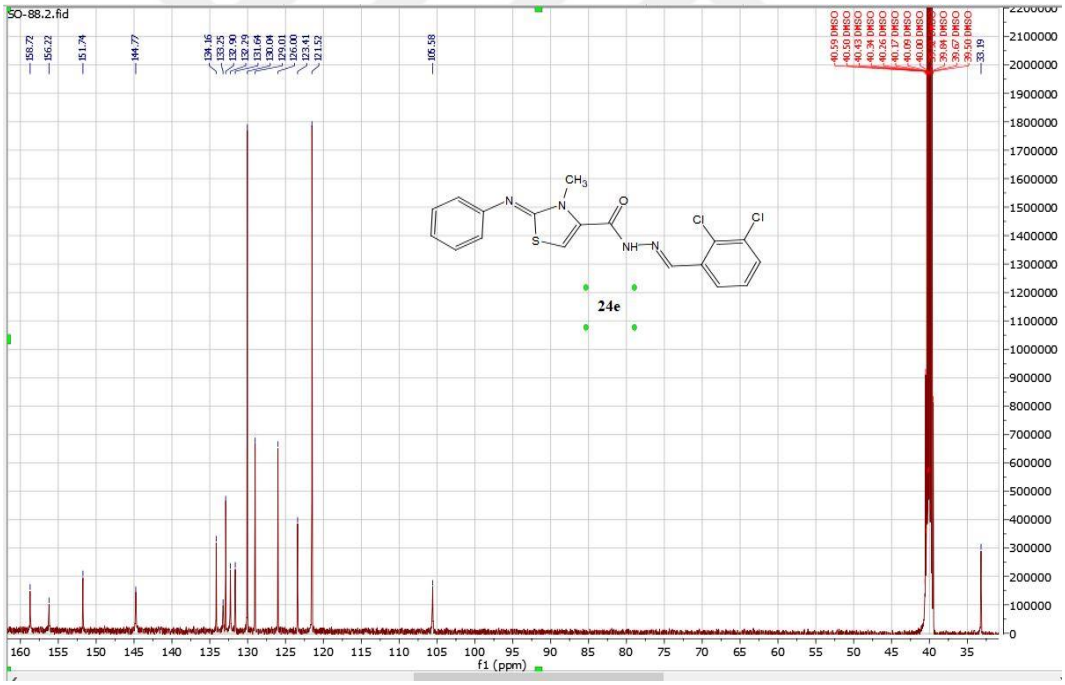

Figure 4.45 ^{13}C NMR of **24e**

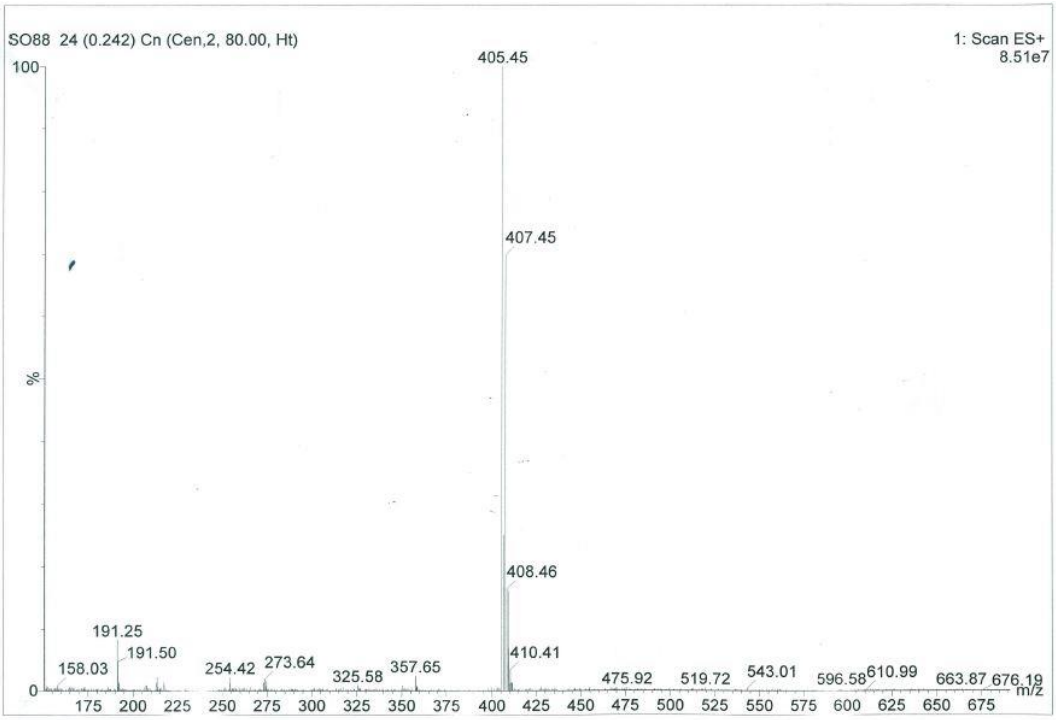

Figure 4.46 LC/MS of **24e**

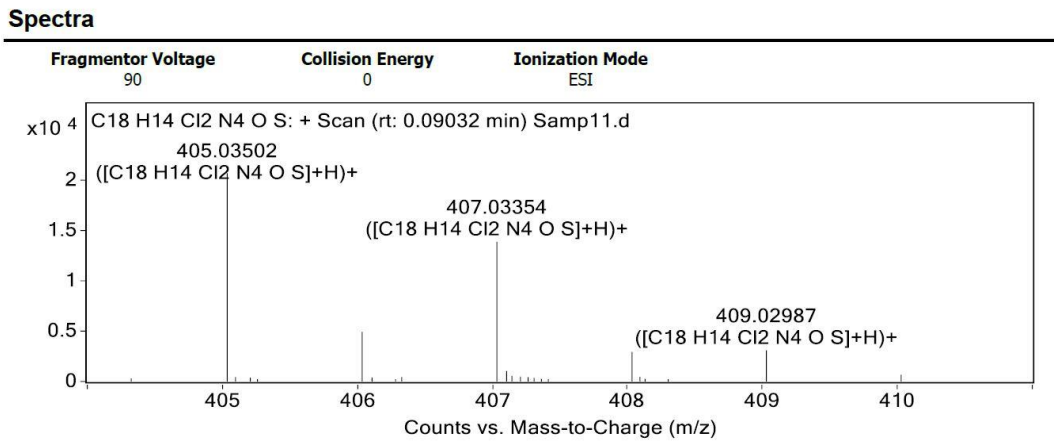

Figure 4.47 LC-QTOF-MS spectrum of compound **24e**

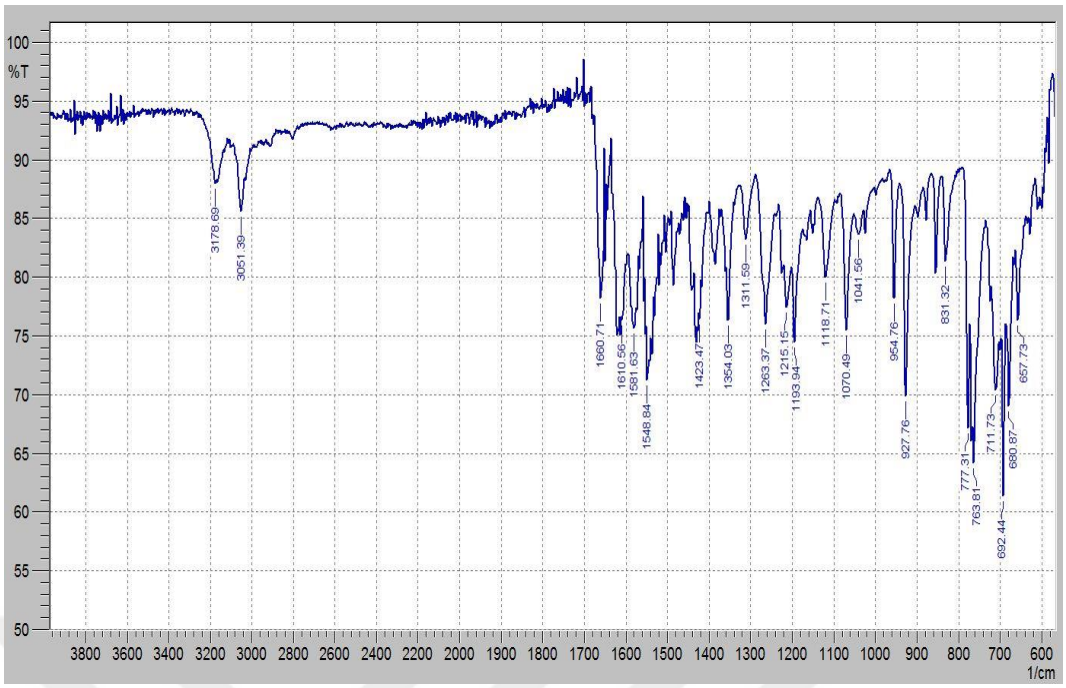

Figure 4.48 FT-IR of **24f**

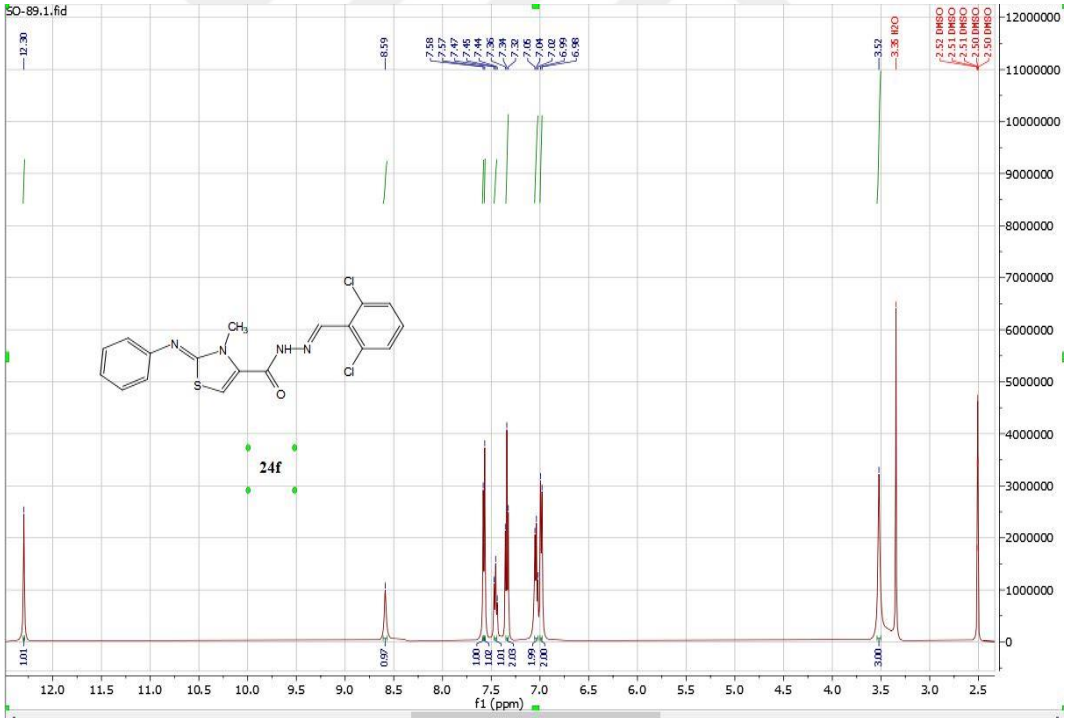

Figure 4.49 ^{1}H NMR of **24f**

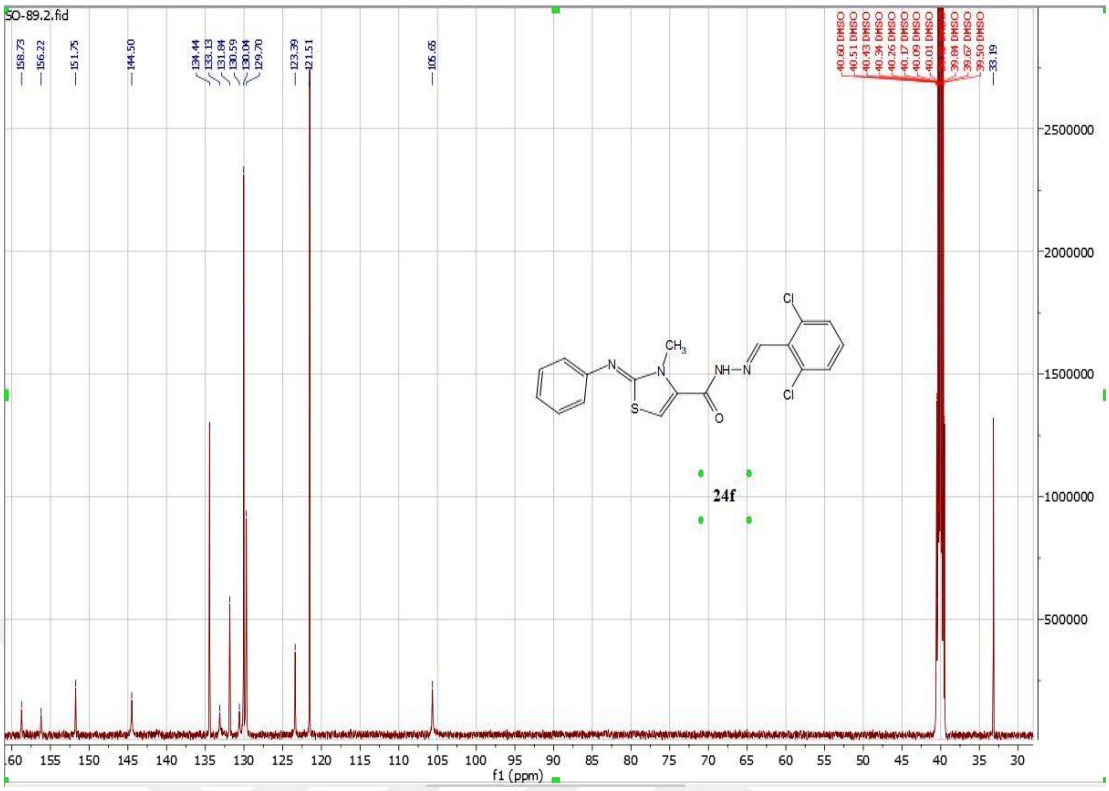

Figure 4.50 ^{13}C NMR of **24f**

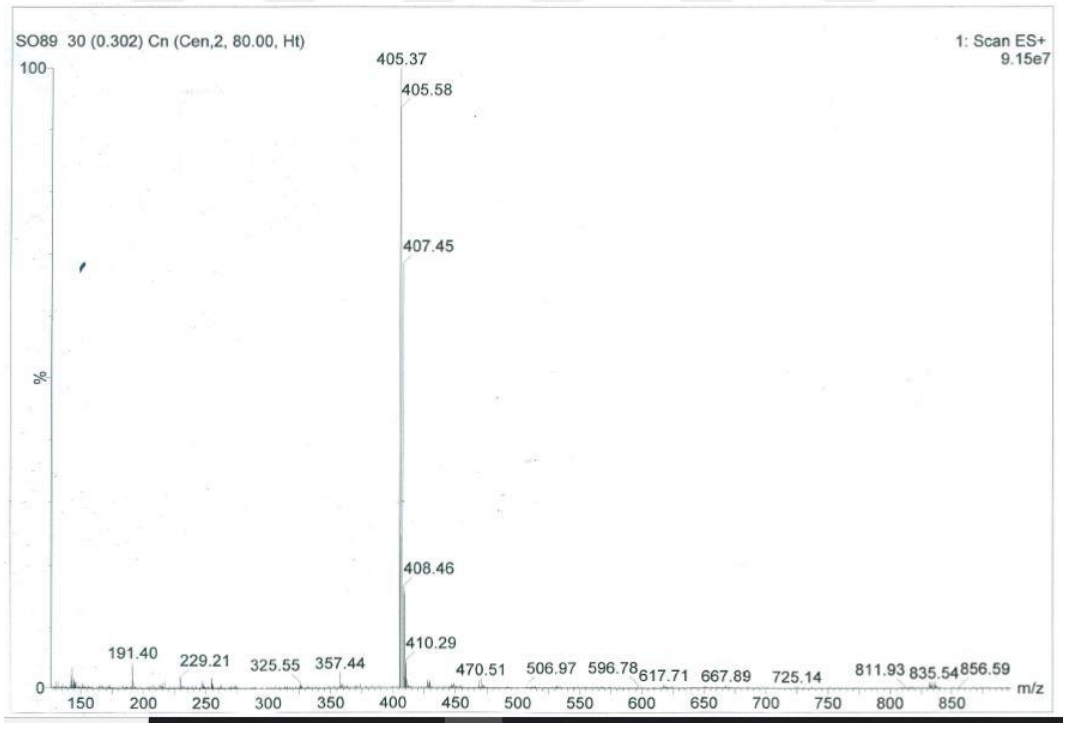

Figure 4.51 LC/MS of **24f**

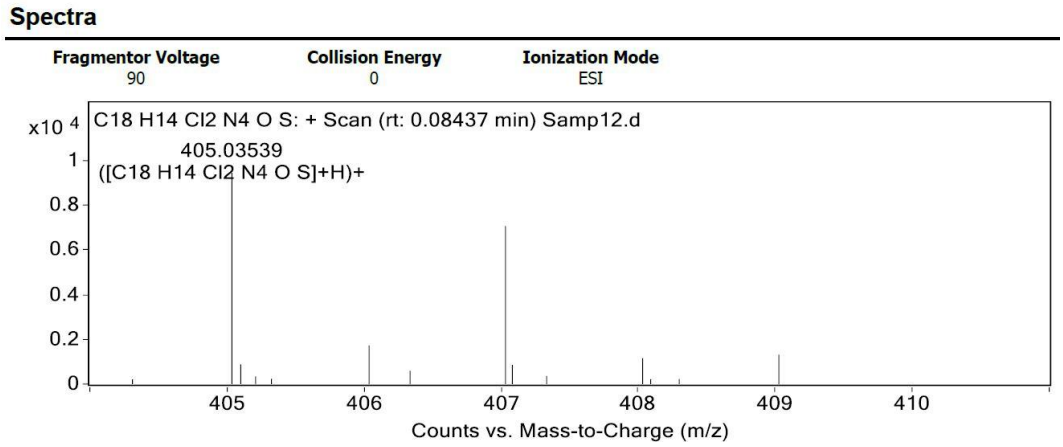

Figure 4.52 LC-QTOF-MS spectrum of compound **24f**

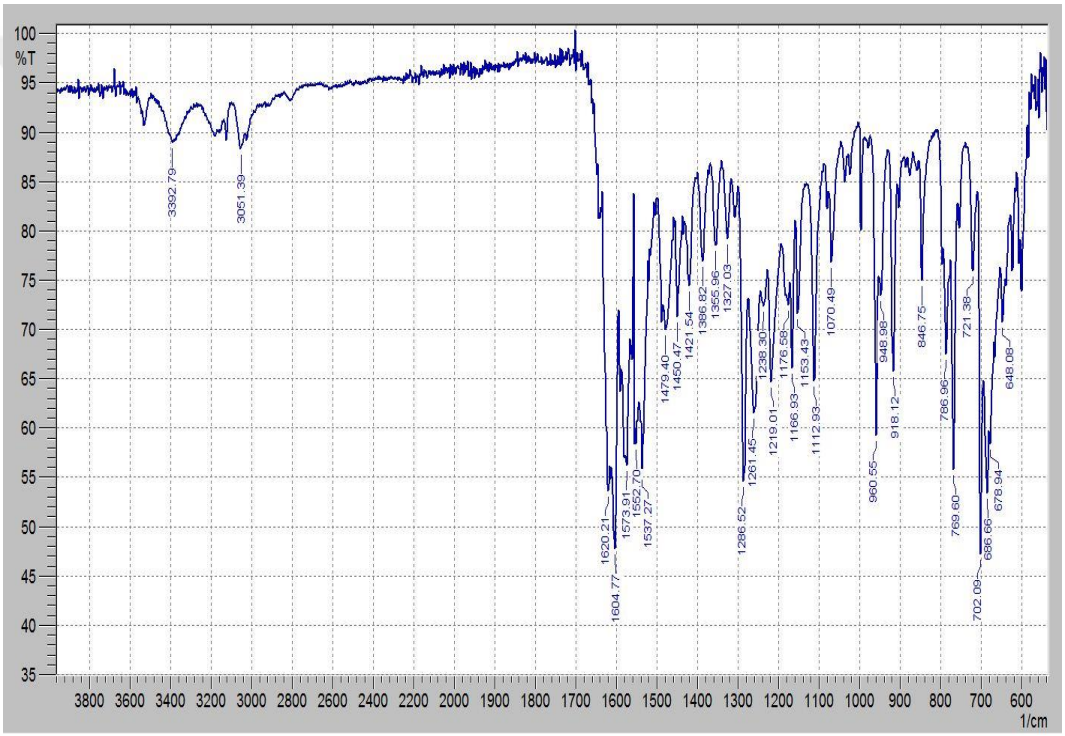

Figure 4.53 FT-IR of **24g**

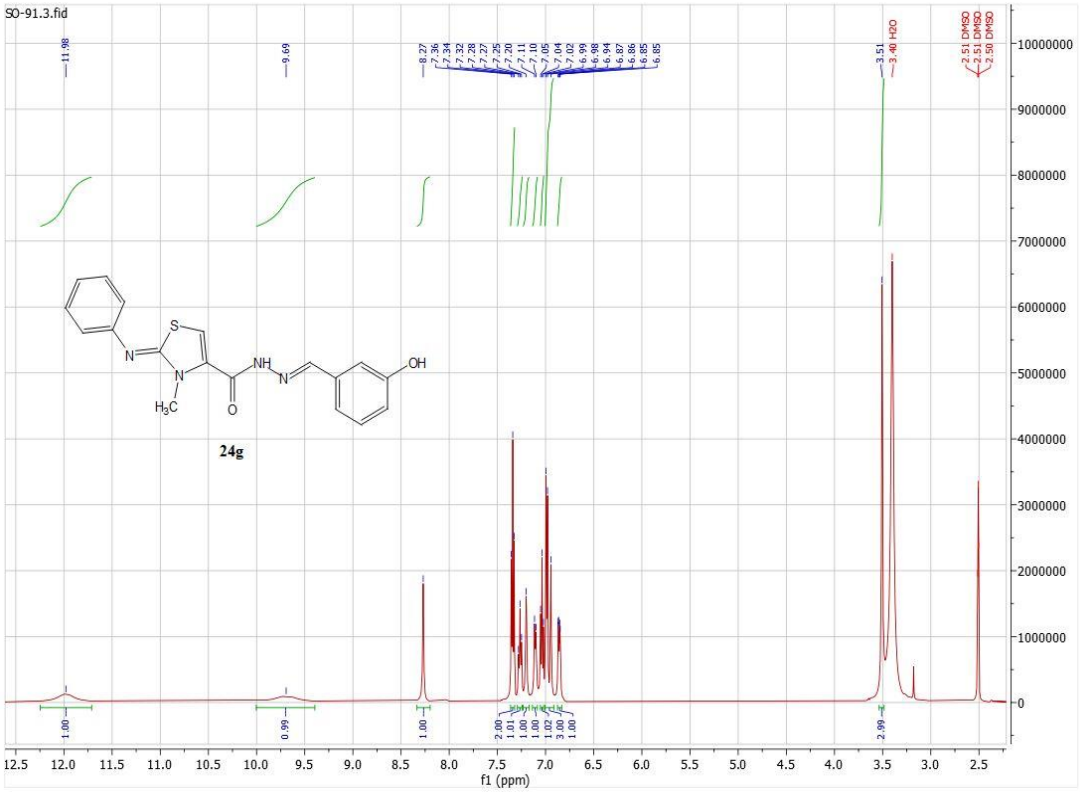

Figure 4.54 ^{1}H NMR of **24g**

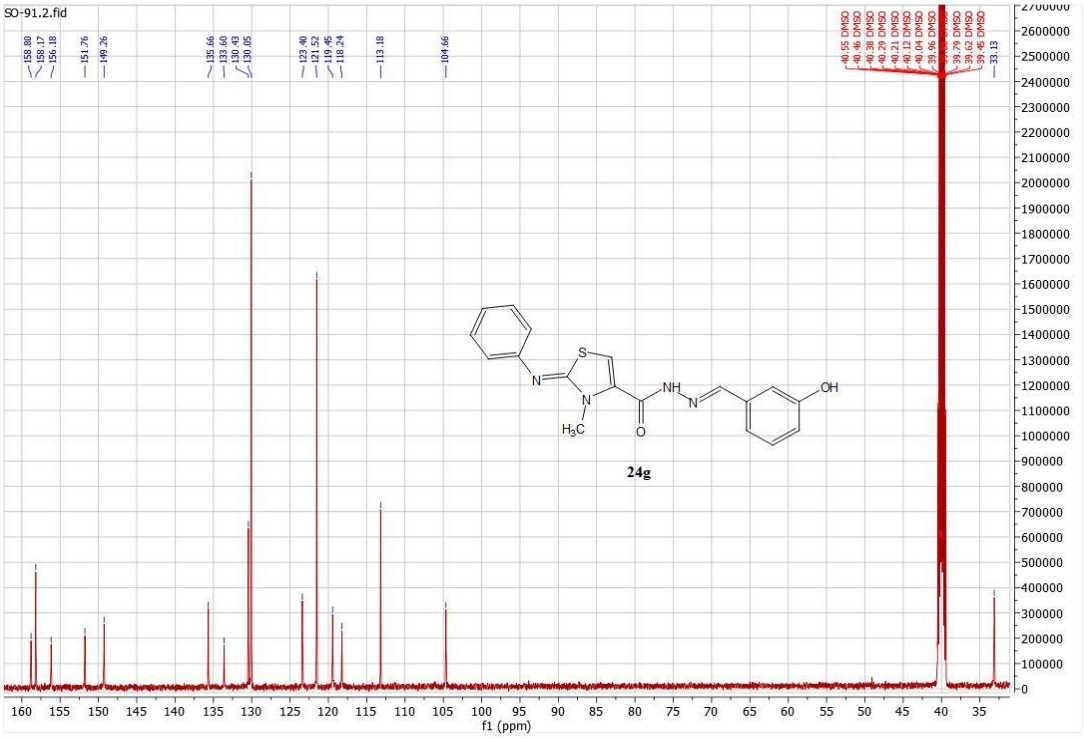

Figure 4.55 ^{13}C NMR of **24g**

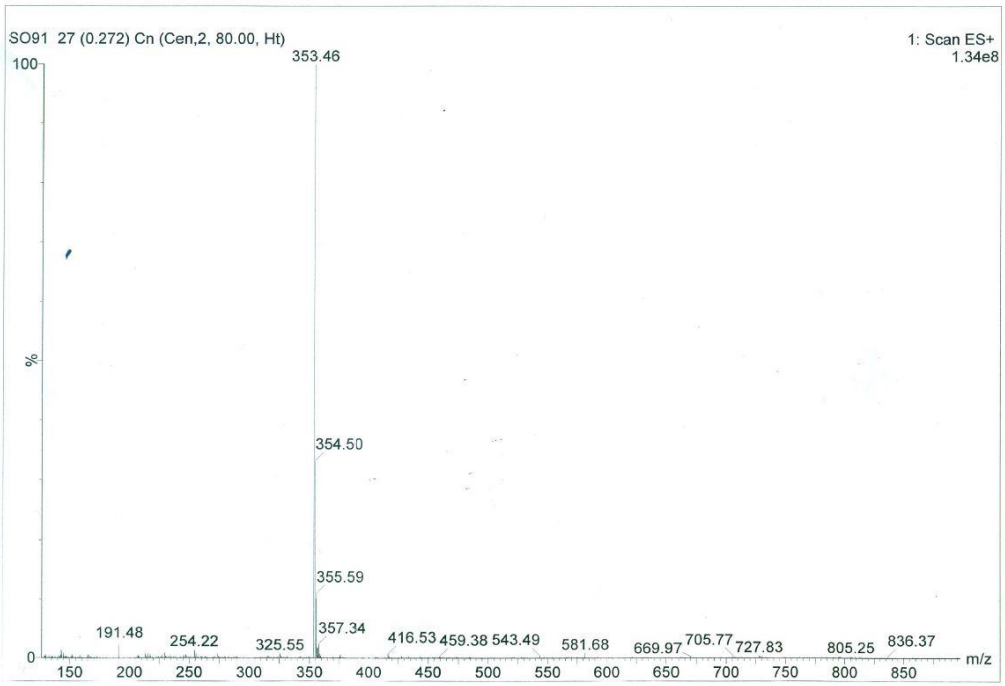

Figure 4.56 LC/MS of **24g**

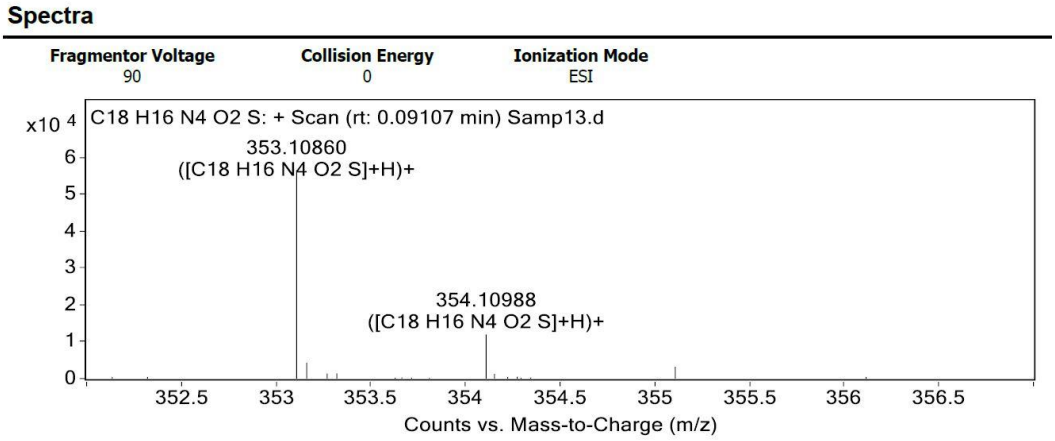

Figure 4.57 LC-QTOF-MS spectrum of compound **24g**

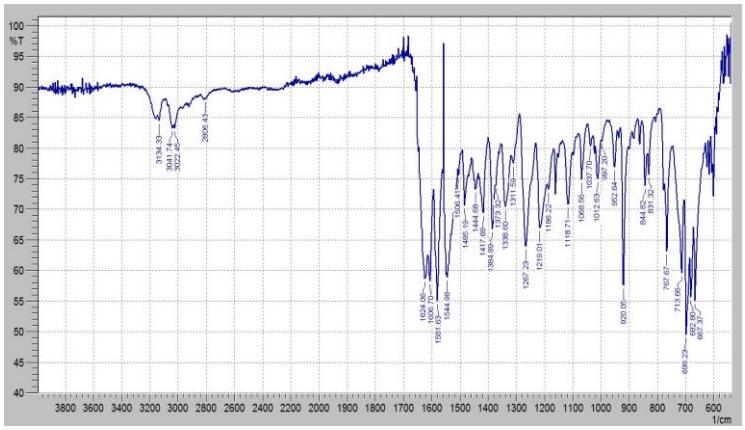

Figure 4.58 FT-IR of **24h**

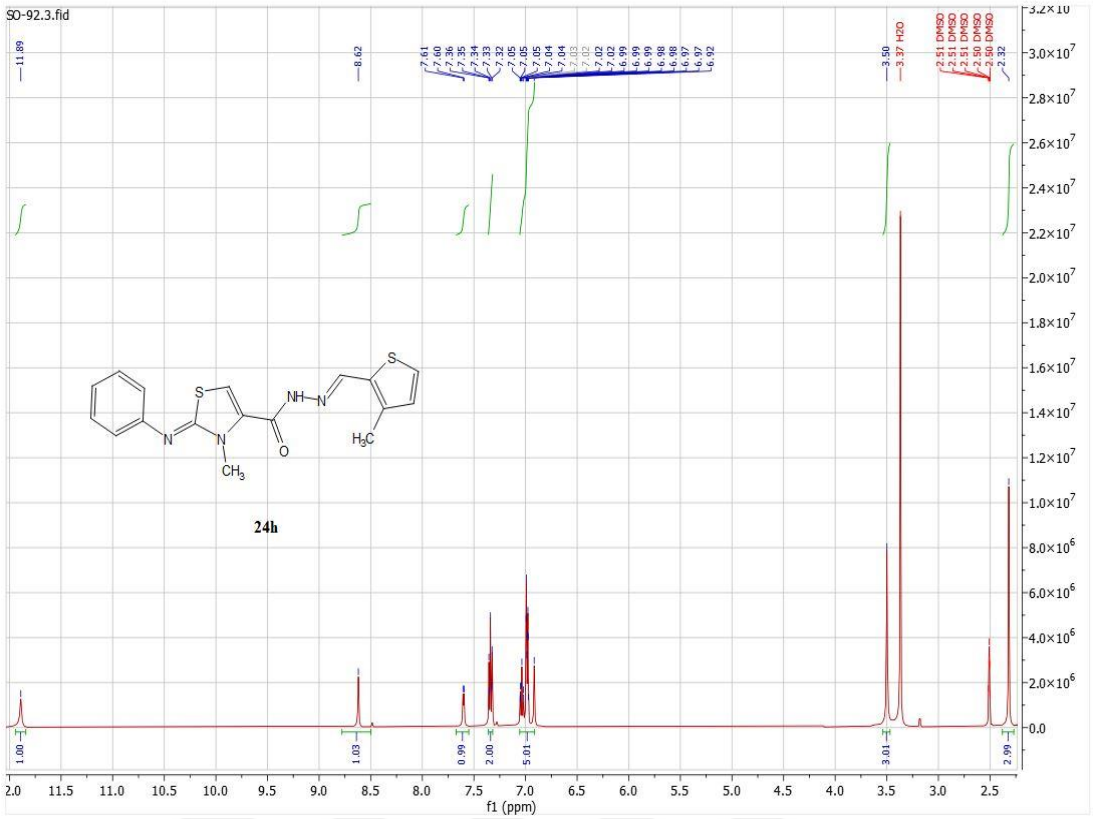

Figure 4.59 ^{1}H NMR of **24h**

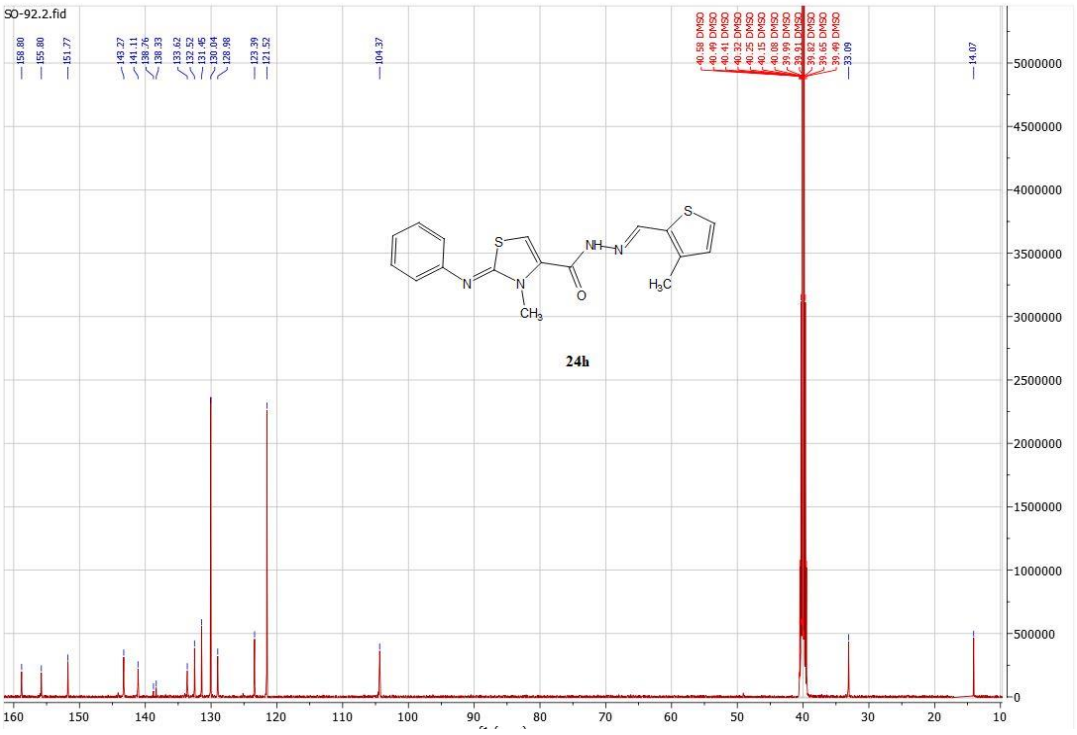

Figure 4.60 ^{13}C NMR of **24h**

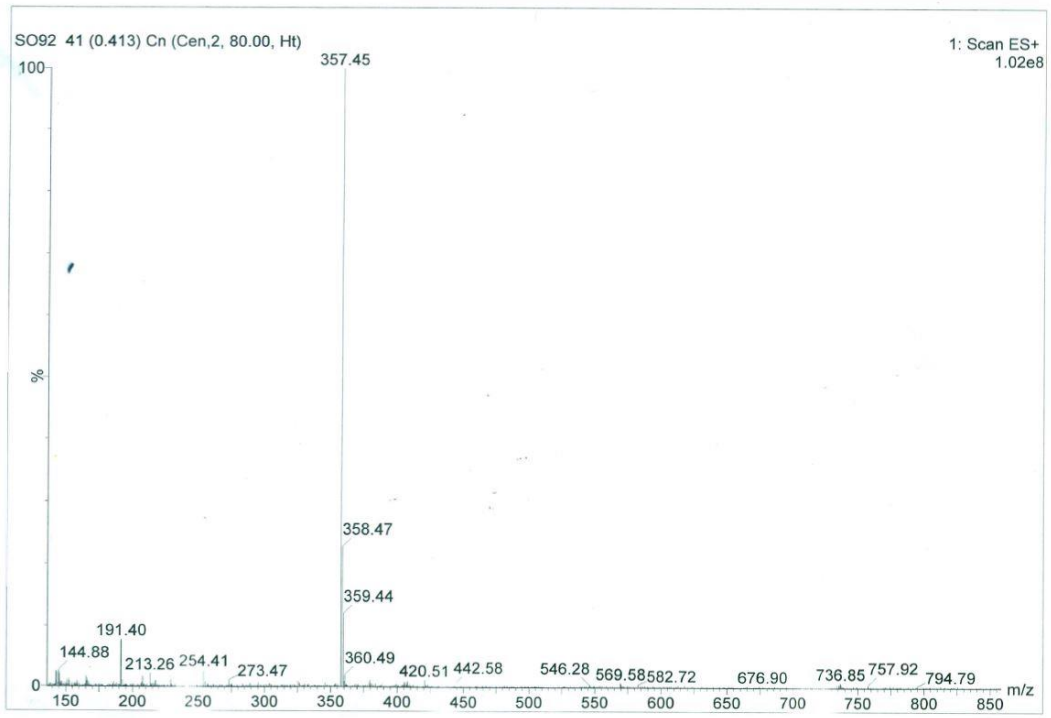

Figure 4.61 LC/MS of **24h**

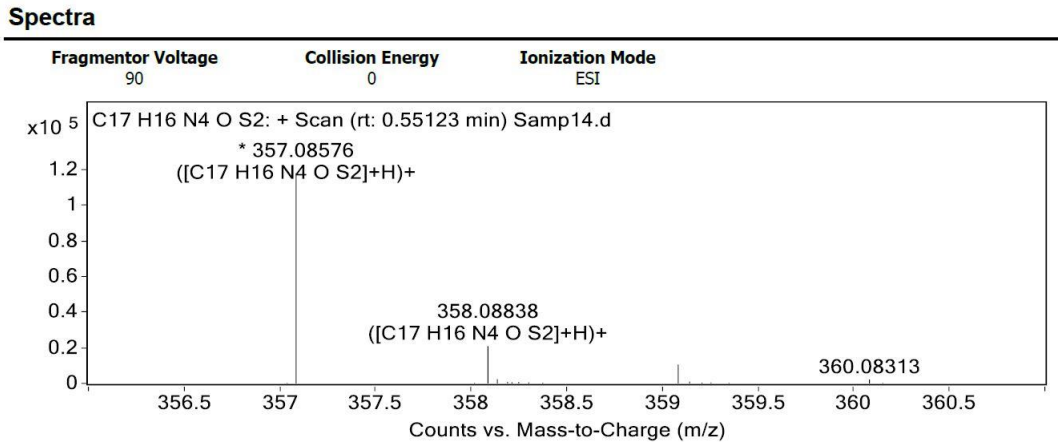

Figure 4.61 LC-QTOF-MS spectrum of compound **24h**

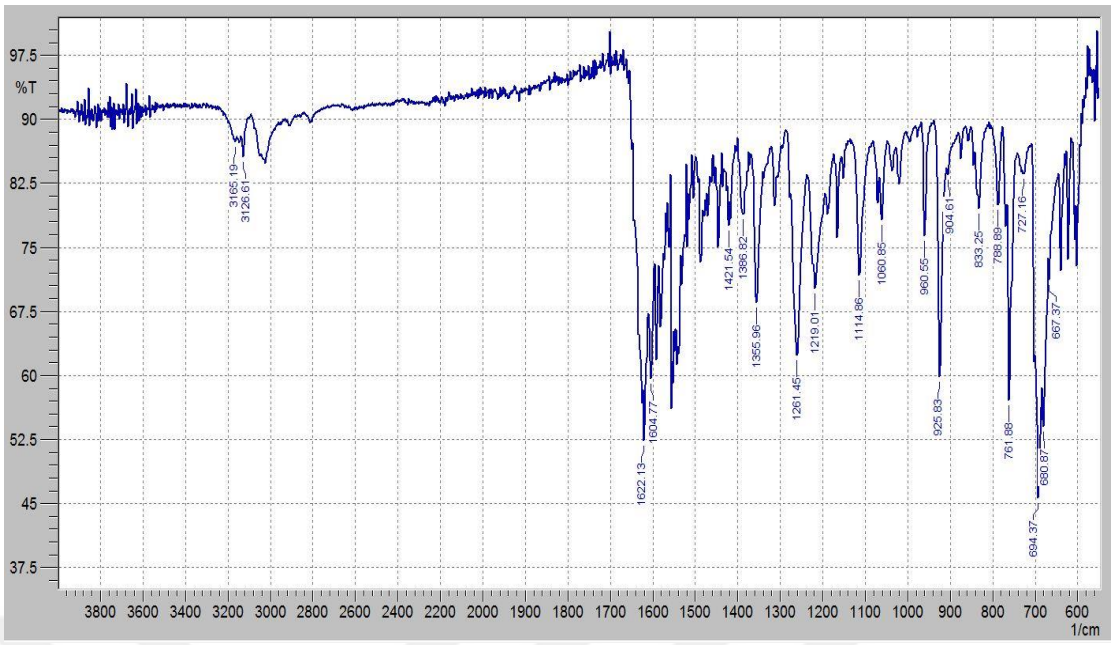

Figure 4.62 FT-IR of **24i**

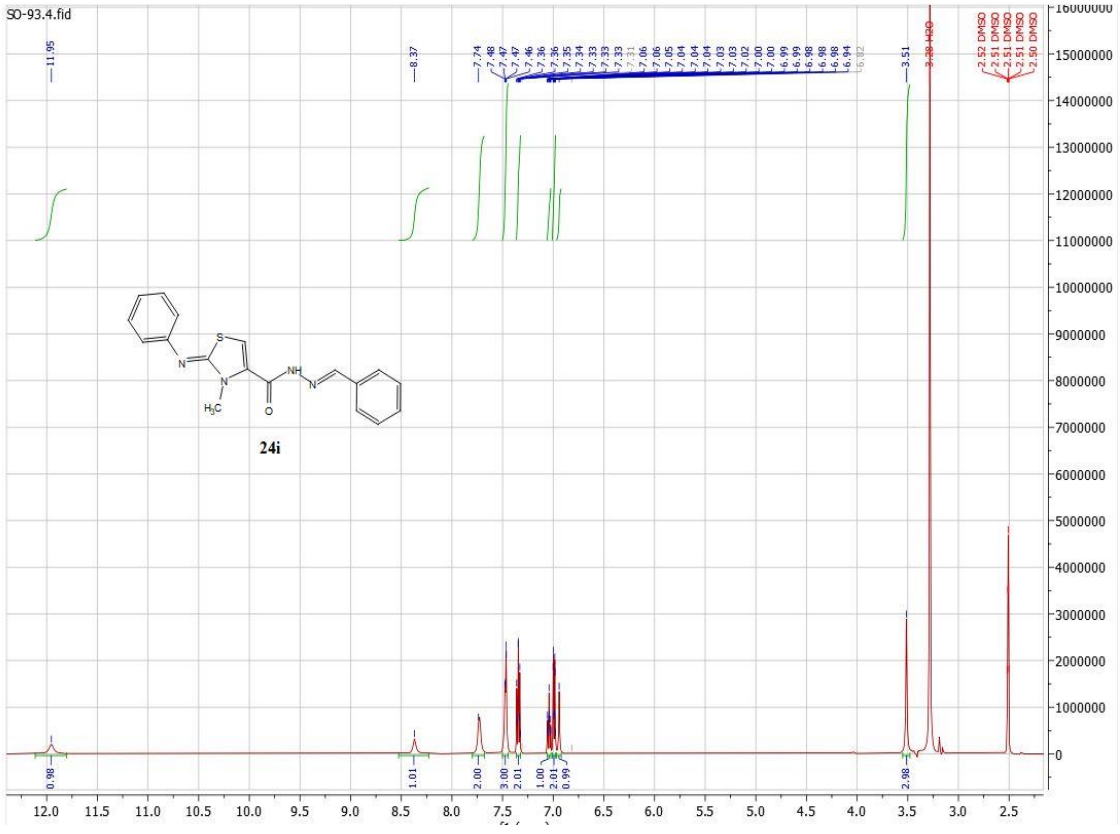

Figure 4.63 ^{1}H NMR of **24i**

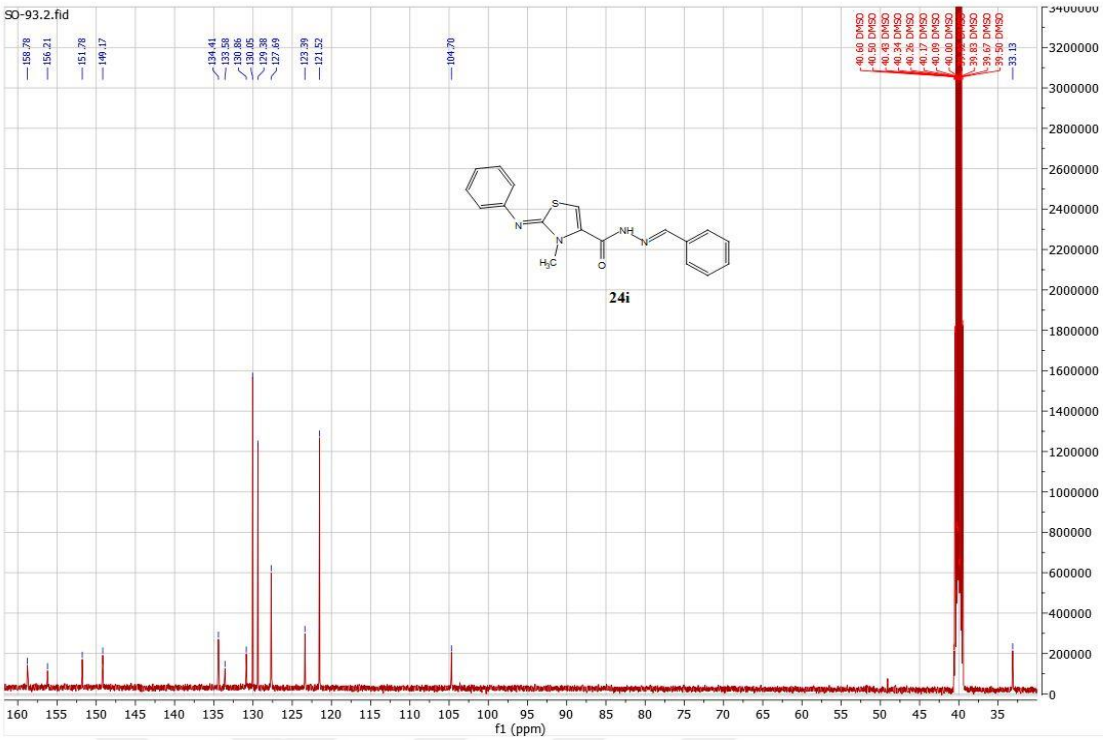

Figure 4.64 ^{13}C NMR of **24i**

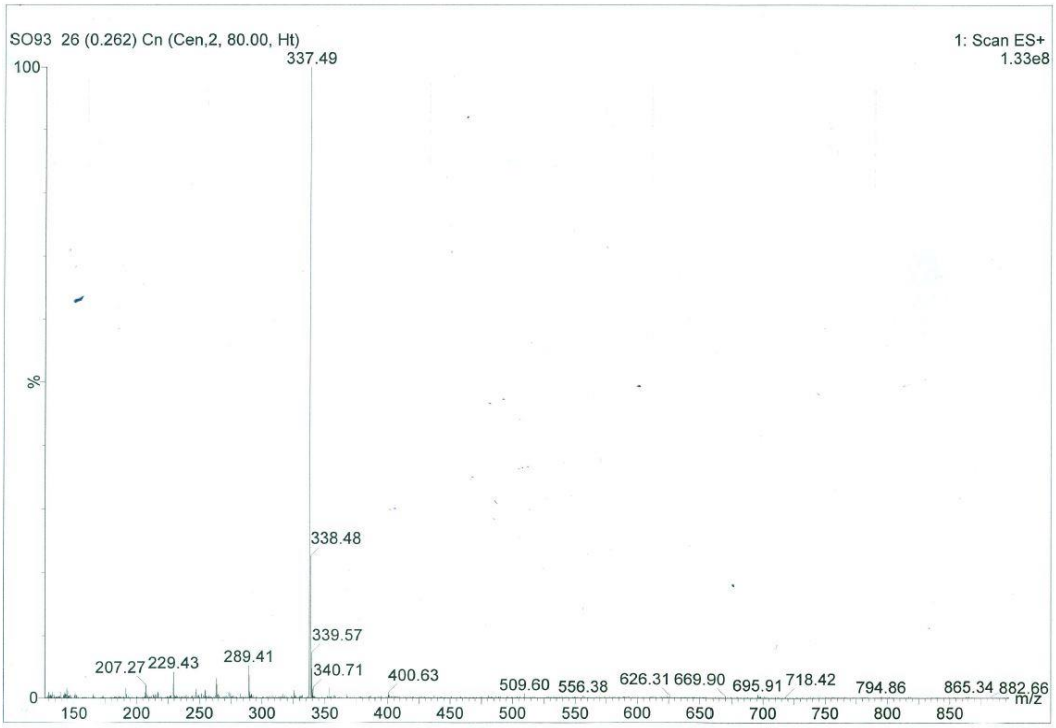

Figure 4.65 LC/MS of **24i**

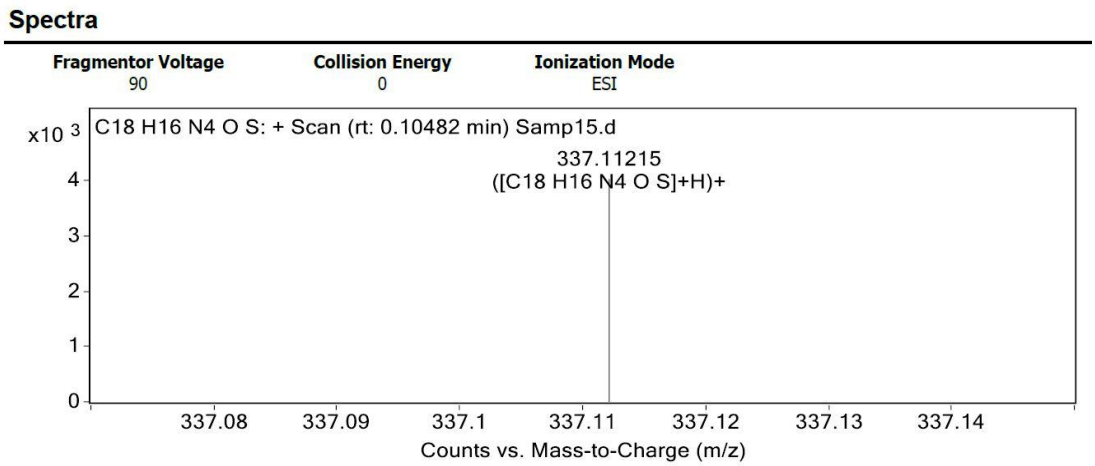

Figure 4.66 LC-QTOF-MS spectrum of compound **24i**

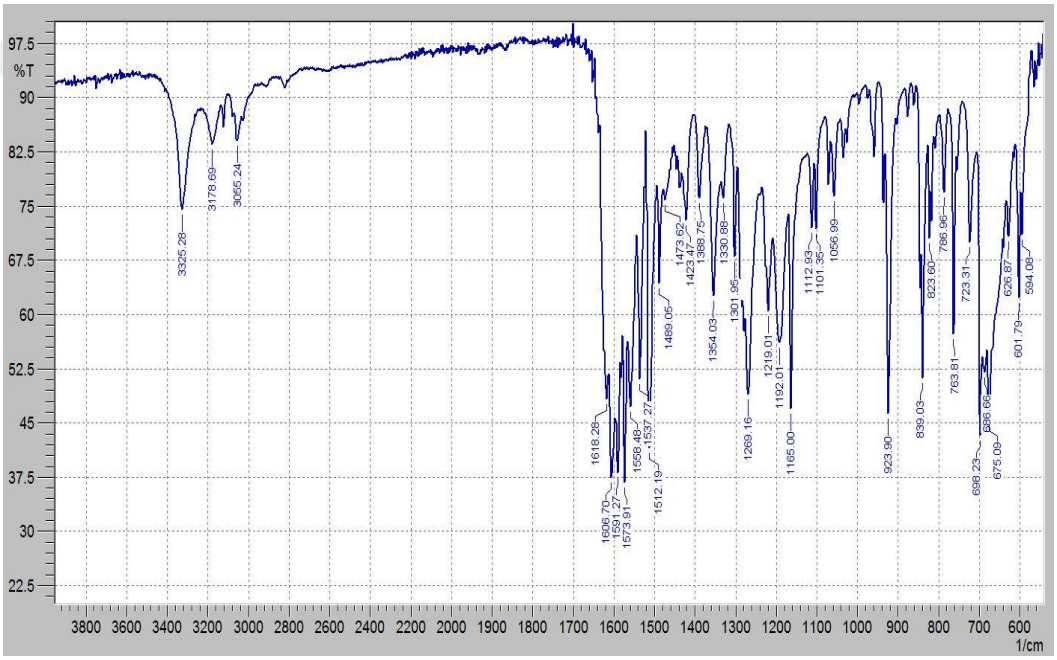

Figure 4.67 FT-IR of **24j**

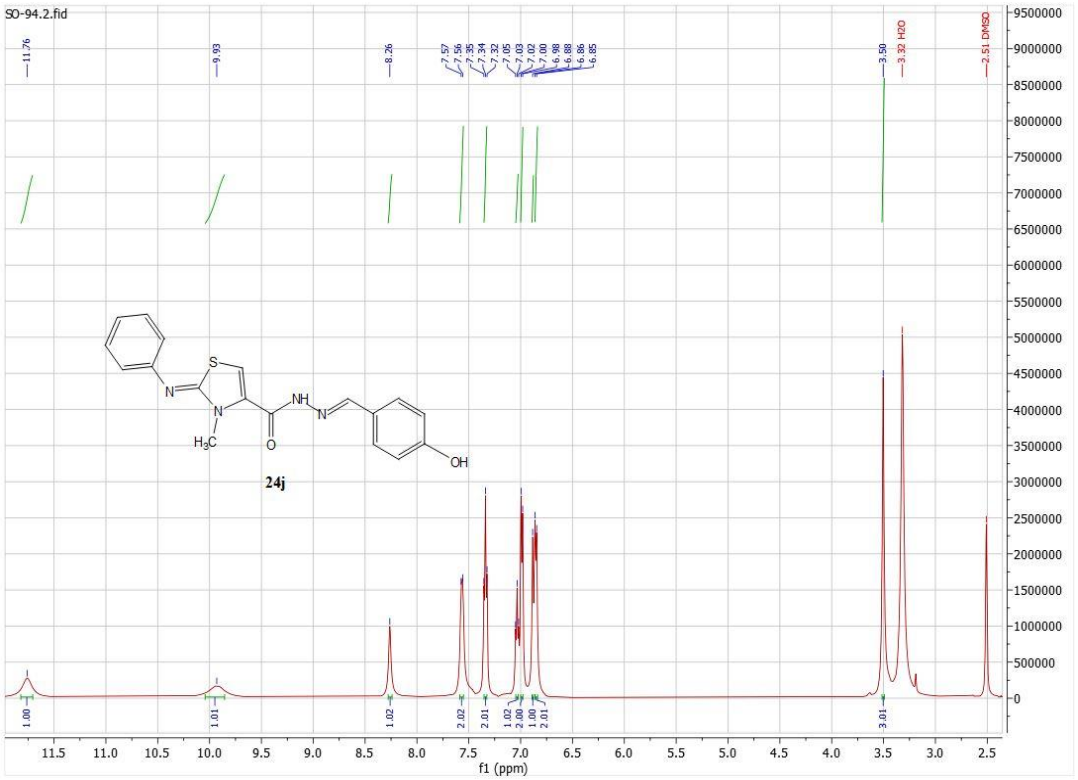

Figure 4.68 ^{1}H NMR of **24j**

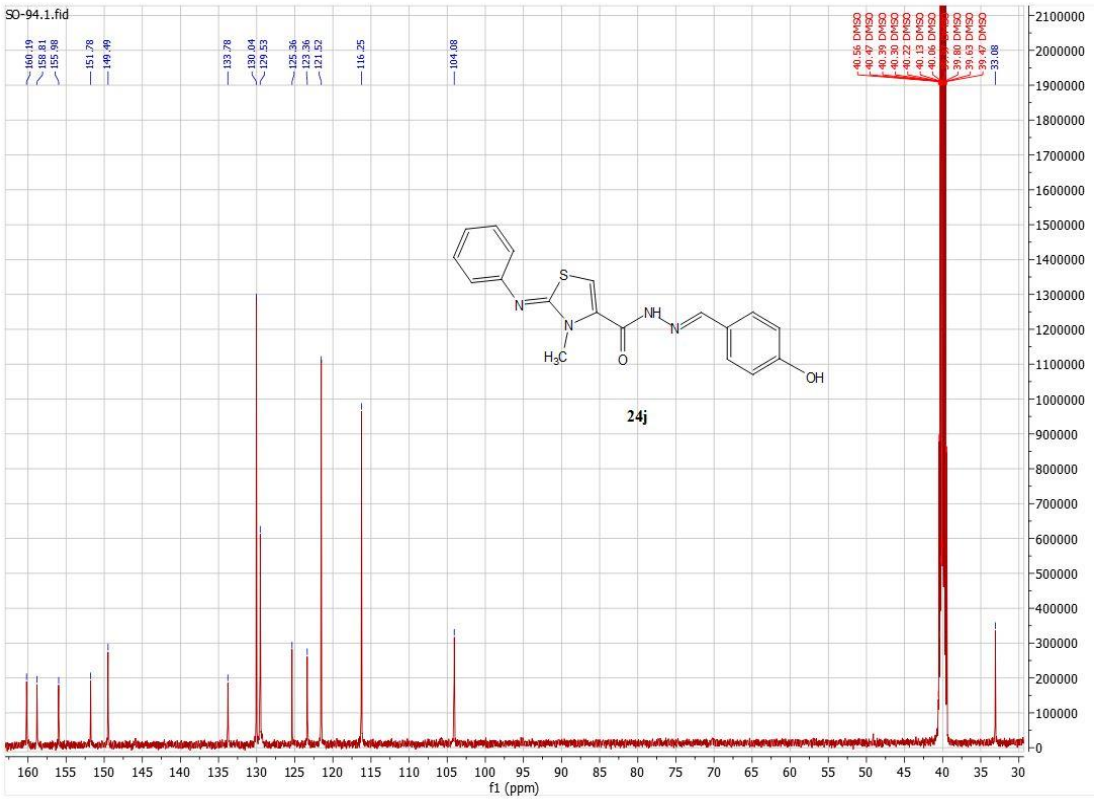

Figure 4.69 ^{13}C NMR of **24j**

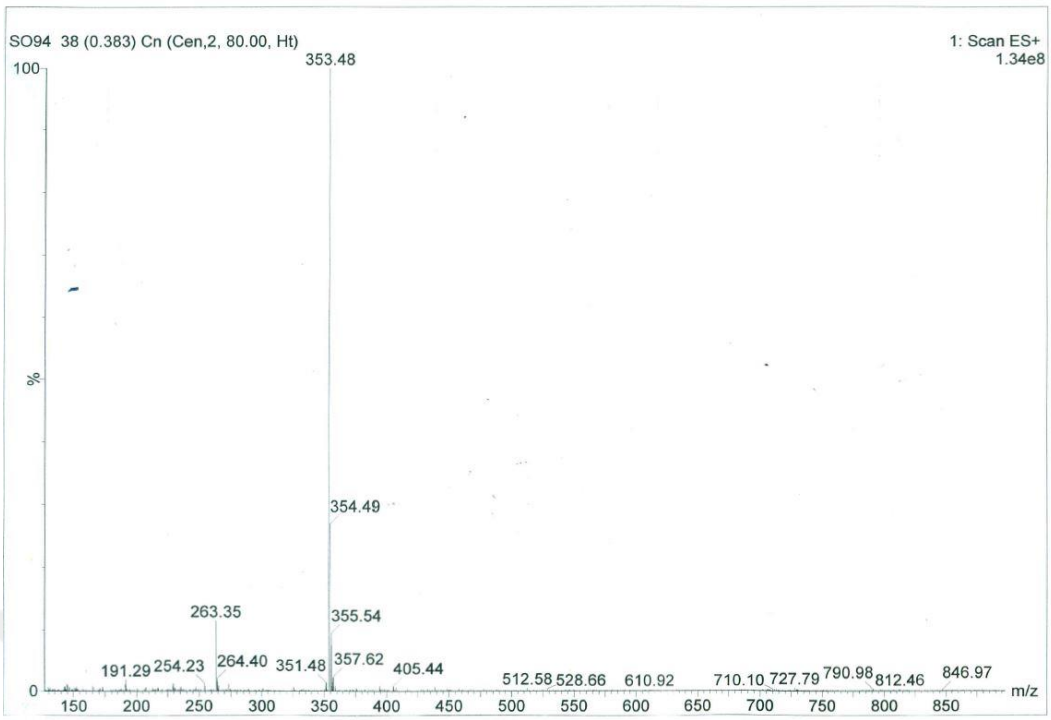

Figure 4.70 LC/MS of **24j**

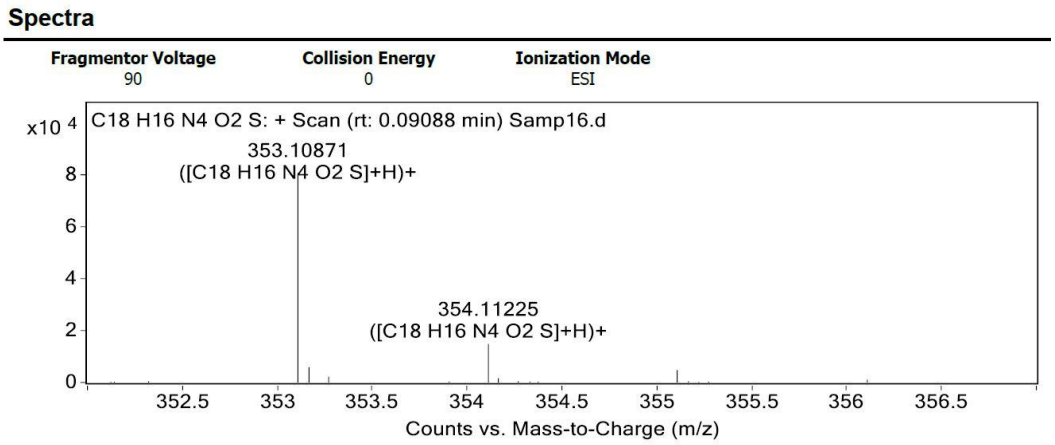

Figure 4.71 LC-QTOF-MS spectrum of compound **24j**